



1506  
UNIVERSITÀ  
DEGLI STUDI  
DI URBINO  
CARLO BO

DIPARTIMENTO DI SCIENZE PURE E APPLICATE

Corso di dottorato di ricerca in: SCIENZE DI BASE E APPLICAZIONI

Curriculum: SCIENZE CHIMICHE E SCIENZE FARMACEUTICHE

XXXI CICLO

# **Medicinal Chemistry Approaches to Widen Therapeutic Potential for Melatonin and Temozolomide Derivatives**

SSD: CHIM/08

RELATORE

Chiar.mo Prof. Gilberto Spadoni

DOTTORANDO

Dott.ssa Lucia Furiassi

Anno Accademico 2017/2018

# Table of Contents

Preface.....	4
<b>Section I: Medicinal Chemistry Approaches to Widen Therapeutic Potential for Melatonin Derivatives .....</b>	<b>5</b>
<b>1.1 General Introduction .....</b>	<b>6</b>
<b>1.2 Design and Synthesis of New Tetrahydroquinoline Melatonin Receptor Ligands .....</b>	<b>12</b>
<b>1.2.1 Introduction and Aim of the Work .....</b>	<b>13</b>
<b>1.2.2 Results and Discussion.....</b>	<b>17</b>
<b>1.2.3 Conclusions.....</b>	<b>34</b>
<b>1.2.4 Experimental Section.....</b>	<b>35</b>
<b>1.2.4.1 Materials and Methods.....</b>	<b>35</b>
<b>1.2.4.2 Reagents.....</b>	<b>35</b>
<b>1.2.4.3 Synthesis and Physicochemical Characterization of THQ MLT Receptor Ligands .....</b>	<b>36</b>
<b>1.3 Dual-acting Melatoninergetic Derivatives: Design, Synthesis and Pharmacological Investigations.....</b>	<b>46</b>
<b>1.3.1 Introduction and Aim of the Work .....</b>	<b>47</b>
<b>1.3.2 Results and Discussion.....</b>	<b>56</b>
<b>1.3.2.1. Chemistry .....</b>	<b>56</b>
<b>1.3.2.2. <i>In vitro</i> Pharmacological Studies and SARs .....</b>	<b>59</b>
<b>1.3.2.3. <i>In vivo</i> Intraocular Pressure (IOP) Lowering Effects.....</b>	<b>62</b>
<b>1.3.3 Conclusions.....</b>	<b>64</b>
<b>1.3.4 Experimental Section.....</b>	<b>65</b>
<b>1.3.4.1 Materials and Methods.....</b>	<b>65</b>
<b>1.3.4.2 Reagents.....</b>	<b>65</b>
<b>1.3.4.3 Synthesis and Physicochemical Characterization of Dual-acting Compounds .....</b>	<b>66</b>
<b>Section II: C8-Substituted Temozolomide Derivatives: SAR Studies and Effects on Stability .....</b>	<b>83</b>
<b>2.1 Introduction and Aim of the Work .....</b>	<b>84</b>
<b>2.1.1 General Introduction.....</b>	<b>84</b>
<b>2.1.2 Summary of Known SAR on Imidazotetrazines Derivatives.....</b>	<b>87</b>

2.1.3 Aim of the Work .....	89
2.2 Result and Discussions.....	91
2.3 Conclusions.....	103
2.4 Experimental Section.....	104
2.4.1 Materials and Methods.....	104
2.4.2 Synthesis and Physicochemical Characterization of C8-Temozolomide Derivatives	104
List of Abbreviations .....	115
Acknowledgements .....	118
References.....	119

## Preface

The work described in this thesis was primarily focused on the design, synthesis, physicochemical characterization and biological evaluation of small molecules of pharmaceutical interest.

The thesis consists of two sections, one concerning the development of new melatonin derivatives and the other regarding the expansion of the structure-activity relationships of the anticancer agent temozolomide.

Specifically, part of the melatonergic work has been dedicated to the design and synthesis of different MLT receptor ligands structurally characterized by a tetrahydroquinoline scaffold. The semi rigid THQ ring was found to be a good synthetically accessible template for the design of potent MLT ligands with different topology.

- Rivara, S.; Scalvini, L.; Lodola, A.; Mor, M.; Caignard, D-H.; Delagrang, P.; Collina, S.; Lucini, V.; Scaglione, F.; Furiassi, L.; Mari, M.; Lucarini, S.; Bedini, A.; Spadoni, G. *J. Med. Chem.*, **2018**, 61, 3726.

In the second part of this first section, new dual-acting compounds have been designed and synthesized by combining the interesting properties of melatonin derivatives with other, potentially synergistic, pharmacological activities. The new dual-acting compounds have showed a promising antiglaucoma activity.

- Spadoni, G.; Bedini, A.; Furiassi, L.; Mari, M.; Mor, M.; Scalvini, L.; Lodola, A.; Ghidini, A.; Lucini, V.; Dugnani, S.; Scaglione, F.; Piomelli, D.; Jung, K-M.; Supuran, C. T.; Lucarini, L.; Durante, M.; Sgambellone, S.; Masini, E.; Rivara, S. *J. Med. Chem.*, **2018**, 61, 7902.

The second section of the thesis, conducted during my visiting period at University of Illinois at Urbana-Champaign, has been carried out in a different research field concerning the anticancer agent temozolomide. To understand the relationship between its structure, hydrolytic stability and anticancer activity, new imidazotetrazines derivatives bearing previously unexplored functionalities at the C8 position have been synthesized and tested against a panel of human GBM cell lines showing interesting anticancer activities.

- Svec, L. R.; Furiassi, L.; Skibinski, C. G.; Fan, T. M.; Riggins, G. J.; Hergenrother, P. J. *ACS Chem. Bio.*, **2018**, 13, 3206.



1506  
UNIVERSITÀ  
DEGLI STUDI  
DI URBINO  
CARLO BO

## **Section I: Medicinal Chemistry Approaches to Widen Therapeutic Potential for Melatonin Derivatives**

## 1.1 General Introduction

Melatonin (*N*-acetyl-5-methoxytryptamine, MLT, **1** in Figure 1), first isolated from bovine pineal gland in 1958,<sup>1</sup> is a tryptophan derivative widely distributed in nature ranging from the plant to animal kingdom. In all vertebrates and humans, the biosynthesis of MLT takes place primarily in the pineal gland<sup>2</sup> and occurs via rate limiting *N*-acetylation of serotonin and subsequent *O*-methylation. Characteristically, pineal MLT is synthesized and secreted in a circadian rhythmic fashion with the highest levels, in all species, during the night dark phase. This rhythmicity is controlled by an endogenous circadian clock in the suprachiasmatic nucleus (SCN) of the hypothalamus, through a neuronal pathway linking the SCN and the pineal gland, and whose activity is synchronized to the 24 h period by the light/dark cycle.<sup>3</sup> Evidence has accumulated that MLT is also produced in extrapineal organs and tissues, such as retina, skin, gastrointestinal tract, bone marrow, immune and hematopoietic cells, some reproductive organs and endocrine glands. However, while pineal MLT diffuses out into the bloodstream and CSF, rapidly reaching all tissues, the extrapineal produced MLT is thought to act only locally. Circulating MLT is preferentially metabolized by cytochrome P-450 to 6-OH-MLT and subsequent conjugated with sulfuric or glucuronic acid. Especially in non-hepatic tissues and under the influence of reactive oxygen species, a substantial fraction of MLT can be metabolized to *N*1-acetyl-*N*2-formyl-5-methoxykynuramine by oxidative pyrrole ring cleavage.

Since MLT isolation,<sup>1</sup> considerable progress has been made towards understanding the molecular biology, pharmacology and medicinal chemistry of the melatonergic system. The circadian pattern of MLT secretion, coupled with the localization of specific MLT binding sites in the brain region associated with the “biological clock” has led to considerable interest in its potential in treating disordered circadian rhythms that occur in jet-lag, shift work, some blind subjects and in delayed/advanced sleep phase syndromes,<sup>4</sup> as well as a sleep-promoting agent. Besides the above cited sleep-inducing and chronobiotic properties, many studies have also indicated the MLT involvement in most of the main physiological functions of the body, including the activity of the immune system, the homeostasis of the cardiovascular system, control of mood and behavior, hormone secretion and pain perception.<sup>5</sup> Other effects of MLT described in the literature include its neuroprotective, anti-inflammatory, retinal, antioxidant and anticancer properties.<sup>6</sup> However, after four-five decades of investigation, the scientific evidence supporting the potential benefits of MLT assumption in humans remains controversial. A major obstacle for the use of MLT for many possible treatment purposes, results from its low absolute bioavailability after exogenous administration (from 1% to 37%), due to first pass metabolism,<sup>7</sup> and its short half-life (40-50 min).<sup>8</sup>

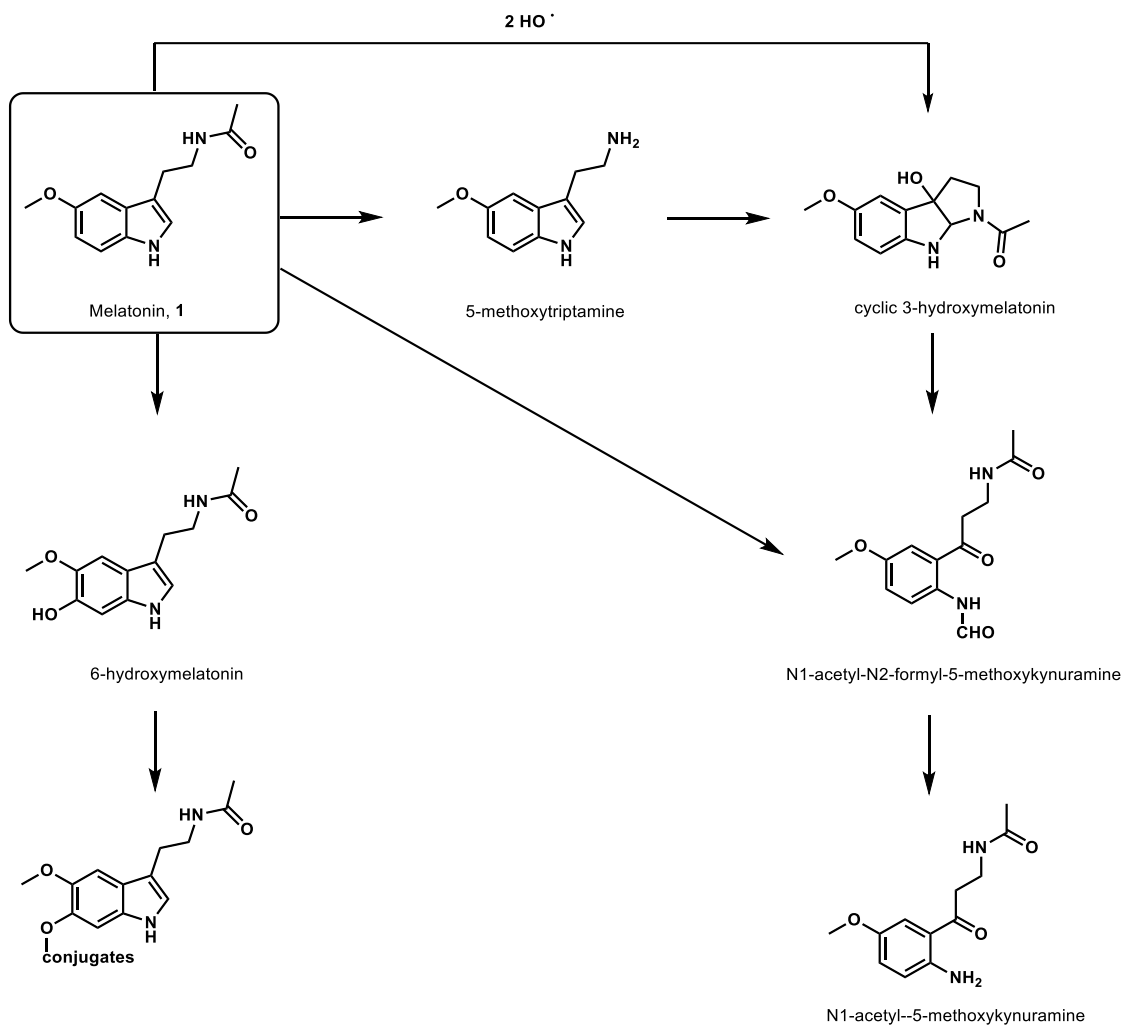


Figure 1 Metabolism of melatonin by human cytochromes p450

A feature that characterizes MLT is the variety of mechanisms it employs to modulate the cell physiology. MLT displays antioxidant effects,<sup>9</sup> and interacts with different intracellular mediators,<sup>10</sup> such as calmodulin or the transcription factor Nrf2, but the majority of its actions are due to the interaction with two G protein-coupled receptors (GPCR), named MT<sub>1</sub> and MT<sub>2</sub>.<sup>11</sup> In addition to these high affinity MLT receptors, another low-affinity MLT binding site, termed MT<sub>3</sub>, has been characterized as a melatonin-sensitive form of the human enzyme quinone reductase 2.<sup>12</sup>

Human MT<sub>1</sub> and MT<sub>2</sub> receptors are 350 and 362 amino acids long respectively, with molecular weights of 39–40 kDa and 55% amino acid homology overall (70% within the transmembrane domains),<sup>13</sup> they exhibit subnanomolar binding affinity for MLT and are negatively coupled to adenylyl cyclase, even if they can also interact with other intracellular signaling pathways. These receptors are mainly expressed in the central nervous system, particularly in the SCN, cerebellum, thalamus, hippocampus, but have also been detected in peripheral organs and tissues.<sup>14</sup> Although great efforts have been devoted in the last few decades, assessing the pharmacology and function of each melatonin receptor subtype remains challenging. This is primarily due to the fact that their native binding site densities in animal tissues are low or undetectable, the tissue-specificity expression might vary depending on the species, and different expression patterns were observed during development, aging and in some pathological conditions.<sup>15</sup> The complexity of MLT receptor signaling and activity is further increased by their ability to homo- and heterodimerize with different G-proteins; receptor oligomerization can alter receptor function (*i.e.* increase or decrease function) depending on the oligomerization partner and which signal transduction processes are being affected.

Efforts to define the physiological role of MLT through the activation of MT<sub>1</sub> and MT<sub>2</sub> receptors have led, over the years, to the design and synthesis of several high affinity melatonin receptor ligands. These derivatives, which activities span from full agonist, to partial agonist, antagonist and inverse agonist, belong to structurally different classes that range from simple indole derivatives and its bioisosteres to ring opened derivatives and conformationally restricted ligands.<sup>16</sup>

Some of these MLT ligands are available on the market (Figure 2); in particular the nonselective MT<sub>1</sub>/MT<sub>2</sub> agonists ramelteon (Rozerem, **2**) and tasimelteon (Hetlioz, **3**), have obtained marketing authorization for the treatment of insomnia and non-24-h sleep–wake disorder respectively.<sup>17,18</sup> The naphthalene MLT bioisostere agomelatine (Valdoxan/Thymanax, **4**), endowed with MT<sub>1</sub>/MT<sub>2</sub> agonist and 5-HT<sub>2C</sub> antagonist activities, is prescribed for the treatment of major depression.<sup>19</sup> These early studies also allowed to obtain information on the structural elements required for high binding affinity. The pharmacophore structure that can be found in almost all MLT receptor agonists is composed by an amide group connected, by a linker chain, to an aromatic nucleus carrying a methoxy group or one of its bioisosteres, such as bromine.



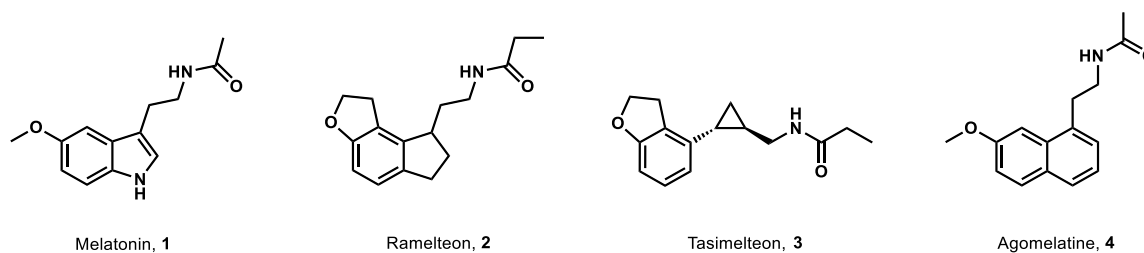


*Figure 2 Melatonin and market approved melatonineric drugs*

Unfortunately, none of the most clinically advanced MLT ligands discriminates between MT<sub>1</sub> and MT<sub>2</sub> subtypes. Therefore, in recent years, much work has been undertaken to identify or develop new candidates more metabolically stable than MLT, exhibiting higher affinity to the MT<sub>1</sub> and MT<sub>2</sub> receptors, and most importantly, showing selectivity towards individual receptor subtype. Subtype-selective MLT receptor agonists and antagonists could be used as valuable experimental tools in understanding the role of this enigmatic neurohormone in health and disease, and opening new therapeutic perspectives by targeting a specific receptor. In the last few decades, MLT receptor subtype selectivity has registered some important advances leading to the identification of a number of selective compounds. The first encouraging results in this area refer to the development of MT<sub>2</sub>-antagonists or partial agonists.

These compounds comprise benzofuran (**7a-c**) and tetrahydronaphthalenic derivatives (**8a-b**), 6,7-dihydro-5*H*-benzo[*c*]azepino[2,1-*a*]indoles (**11**), 2-*N*-acylaminoalkylindoles (**6**), tetrahydroisoquinoline (**9a-b**), 10,11-dihydrodibenzocycloheptene (**12**) and anilinoethylamido derivatives (**13a-c**) (Figure 3), and display various degrees of binding affinity and selectivity. The main feature identified in these MT<sub>2</sub>-selective antagonists or partial agonists is the presence of a flexible bulky hydrophobic substituent in a position topologically equivalent to C2 or N1 of melatonin.

From a comparison of the results obtained from structure-activity relationship studies at the two receptor subtypes, it seems that the MT<sub>2</sub> subtype is characterized by a higher steric tolerance in the region of space surrounding the N1-C2 binding region of MLT. This hydrophobic pocket is positioned out-of-plane of the indole nucleus of MLT and its occupation has been proposed as a key feature to confer MT<sub>2</sub>-selectivity and reduction of intrinsic activity. Docking experiments within three-dimensional homology models of the MT<sub>1</sub> and MT<sub>2</sub> receptors provided a possible explanation for the observed MT<sub>2</sub> selectivity and low intrinsic activity.<sup>16</sup>

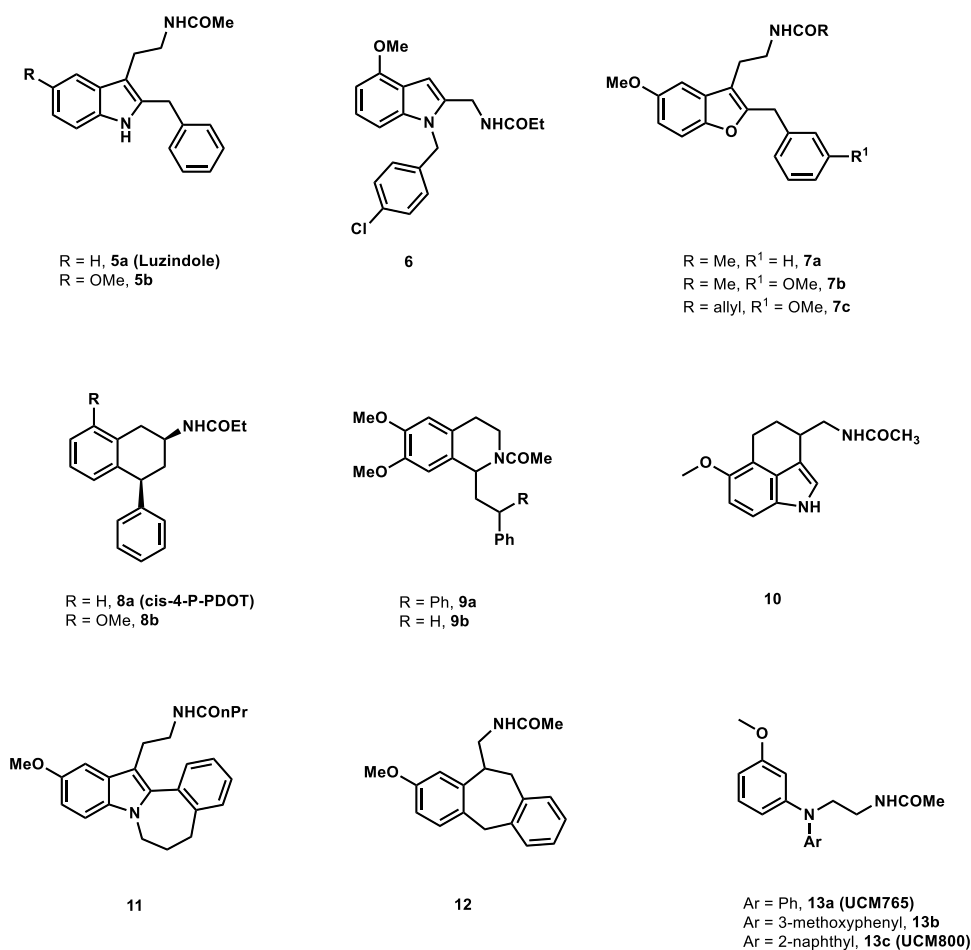


Figure 3 Structures of representative MT<sub>2</sub> selective ligands

Research on new MLT ligands has expanded to also identify selective compounds for the MT<sub>1</sub> receptor subtype. Unfortunately, these attempts have not yet borne good fruit, making it difficult to ascertain the physiological role of this receptor subtype. The first approach used to develop MT<sub>1</sub> selective ligands was the preparation of symmetric dimers, by coupling two moieties deriving from known ligands through an appropriate spacer. Binding affinity, intrinsic activity and subtype selectivity of these dimers depend on the position of the junction and on the length of the linker. Among MT<sub>1</sub>-selective dimers, two of the most interesting ligands are compounds **14**<sup>20</sup> and **15a**<sup>21</sup> (Figure 4), respectively obtained by linking two agomelatine units, or two molecules of the monomer ligand based on the 3-methoxyanilino skeleton, through their methoxy substituent by a three methylene linker. Another strategy used to design MT<sub>1</sub> selective ligands involves the introduction of a bulky hydrophobic substituent in a position topologically equivalent to the 5-methoxy group of MLT. For instance, compounds endowed with good binding affinity and MT<sub>1</sub> moderate selectivity (approximately 20-40 fold) were obtained by introducing a 4-phenylbutyl group at the C-2 position of a bicyclic scaffold benzofuran, benzoxazole or dihydrobenzofuran, mimicking the methoxyphenyl fragment of MLT, as exemplified by compounds **16**, **17**, **18** in Figure 4. Using a similar approach the *N*-acetyltryptamine (**19a**) and the *N*-anilinoethylamide derivative (**20**),<sup>22,23</sup> bearing a phenylbutoxy substituent, were

synthesized and they displayed about 10-70 fold preference toward MT<sub>1</sub> receptors. Taken together, all these results have led to the hypothesis that MT<sub>1</sub>-selectivity is favoured by replacement of the 5-methoxy group by a larger substituent. As proposed in a 3D homology model of the MT<sub>1</sub> receptor, the phenylbutyloxy group, and in general a bulkier lipophilic substituent, could be accommodated in a lipophilic region, mainly defined by the transmembrane helices TM3 and TM4, characterized by the presence of some amino acids smaller than those present in the analogue MT<sub>2</sub> binding site region.<sup>24</sup>

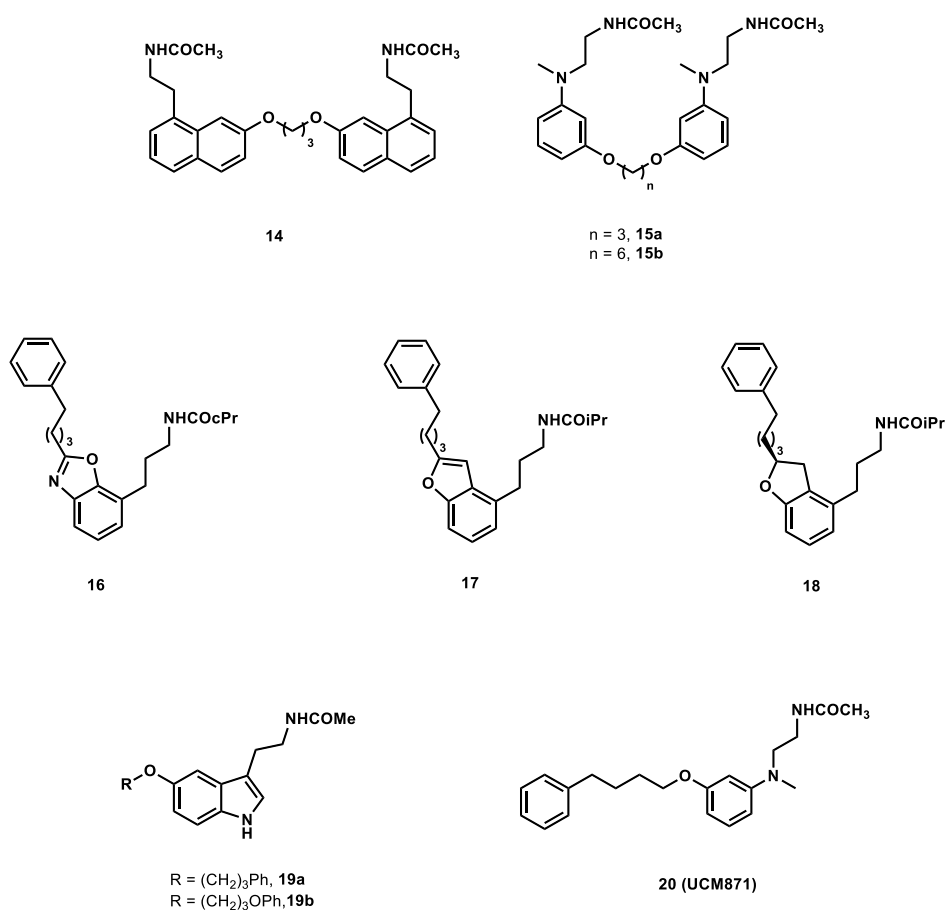


Figure 4 Structures of representative MT<sub>1</sub> selective melatonin ligands

## **1.2 Design and Synthesis of New Tetrahydroquinoline Melatonin Receptor Ligands**

## 1.2.1 Introduction and Aim of the Work

Despite the efforts already undertaken, the research for new melatonin selective ligands remains a scientific and medical challenge. New candidates should be novel to be patented, must be characterized by high potency and selectivity, and must have good biopharmaceutical and PK properties. Among the previously reported MLT receptor ligands, the class of anilinoethylamides (**13a-c** in Figure 3) has proven to be one of the most interesting and versatile. These compounds show a general good affinity for MLT receptors and, particularly, the possibility to be chemically modified, giving predictable modulations of selectivity and intrinsic activity. A problem with anilinoethylamides SAR profile is the existence of a parallelism between MT<sub>2</sub> selectivity and lowering of intrinsic activity, so it seemed hard to get MT<sub>2</sub>-selective full agonists within this class. In an attempt to satisfy this need, the research team, where I spent most of my PhD course, has recently developed a new class of tetrahydroquinoline (THQ) derivatives carrying an acylaminomethyl side chain in position 2 (Figure 5).<sup>25</sup> Specifically, starting from the structure of *N*-anilinoethylamides ligands, the flexible ethylamide side chain was constrained in a six-membered ring to reproduce the putative bioactive conformation of the endogenous hormone, previously identified and validated by studying potent conformationally constrained ligands such as the tricyclic 1,3,4,5-tetrahydrobenzo[*cd*]indole agonist **21**. SAR optimization, based on superposition models with known melatonergic ligands, resulted in *N*-1-benzyl-5-methoxyquinolin-2-yl)methyl]propionamide (UCM1014, **22** in Figure 5), which is the most potent and selective MT<sub>2</sub> full agonist reported to date ( $K_{iMT_2} = 0.001$  nM, more than 10000-fold selectivity over the MT<sub>1</sub> receptor).<sup>25</sup>

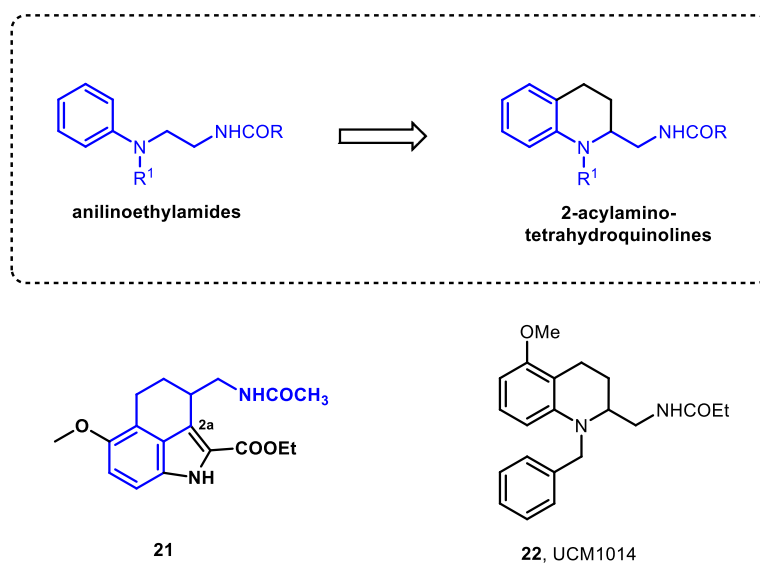


Figure 5

As highlighted in Figure 6 the tetrahydroquinoline ring, in which the heterocyclic nitrogen can replace the carbon *2a* of the tricyclic derivative **21**, could represent an excellent scaffold to favour the proper arrangement of pharmacophoric groups, providing potent and selective MLT ligands.

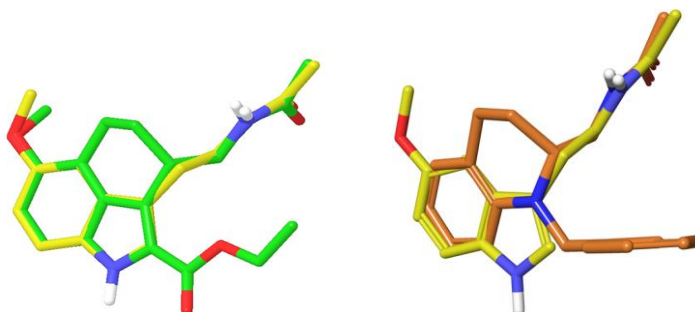


Figure 6 (left): superposition of compound **21** (green carbons) to the putative bioactive conformation of MLT (yellow carbons); (right): superposition of the tetrahydroquinoline UCM1014 (orange carbons) to the putative bioactive conformation of MLT (yellow carbons)

Indeed, the tetrahydroquinoline system is a very common structural motif found in several biologically active natural products and pharmacologically relevant therapeutic agents (Figure 7).<sup>26</sup> For example, the potent antiviral agent virantmycin and the antibiotic helquinoline isolated, respectively from a strain of *Streptomyces* or *Janibacter limosus*, belong to the wide variety of 1,2,3,4-tetrahydroquinoline-based natural products. Tetrahydroquinoline compounds with interesting biological activities also include quinfamide, a luminal amebicide used to treat chronic and subacute amebiasis, and nicainoprol, a calcium channel antagonist used as antiarrhythmic agent. Some of other compounds containing tetrahydroquinoline scaffold interact with neurotransmitter receptors and other membrane receptor, such as the glycine site at NMDA receptor antagonist (**23**), the 5-HT<sub>3</sub> receptor antagonist (**24**) or the  $\beta_3$ -adrenergic agonist (**25**). The tetrahydroquinoline system is also the key structural fragment of compounds acting on steroid hormone receptors (*i.e.* the ER $\beta$  estrogen receptor agonist (**26**) and the inhibitor of cholesteryl ester transfer protein torcetrapib, used in clinical trials as anti hypercholesterolemic drug), or of inhibitors of therapeutically relevant enzymes such as the commercial antithrombotic drug argatroban, acting as a thrombin inhibitor. The above cited biologically active compounds, widely support the idea to consider the tetrahydroquinoline ring a “privileged structure”, a term first coined by Ben Evans<sup>27</sup> and more recently refined by Klaus Mueller,<sup>28</sup> to define “small, non-planar structures with robust conformations that provide interesting 3D exit vectors for substitution, with drug-like properties and ideally readily accessible synthetically”.

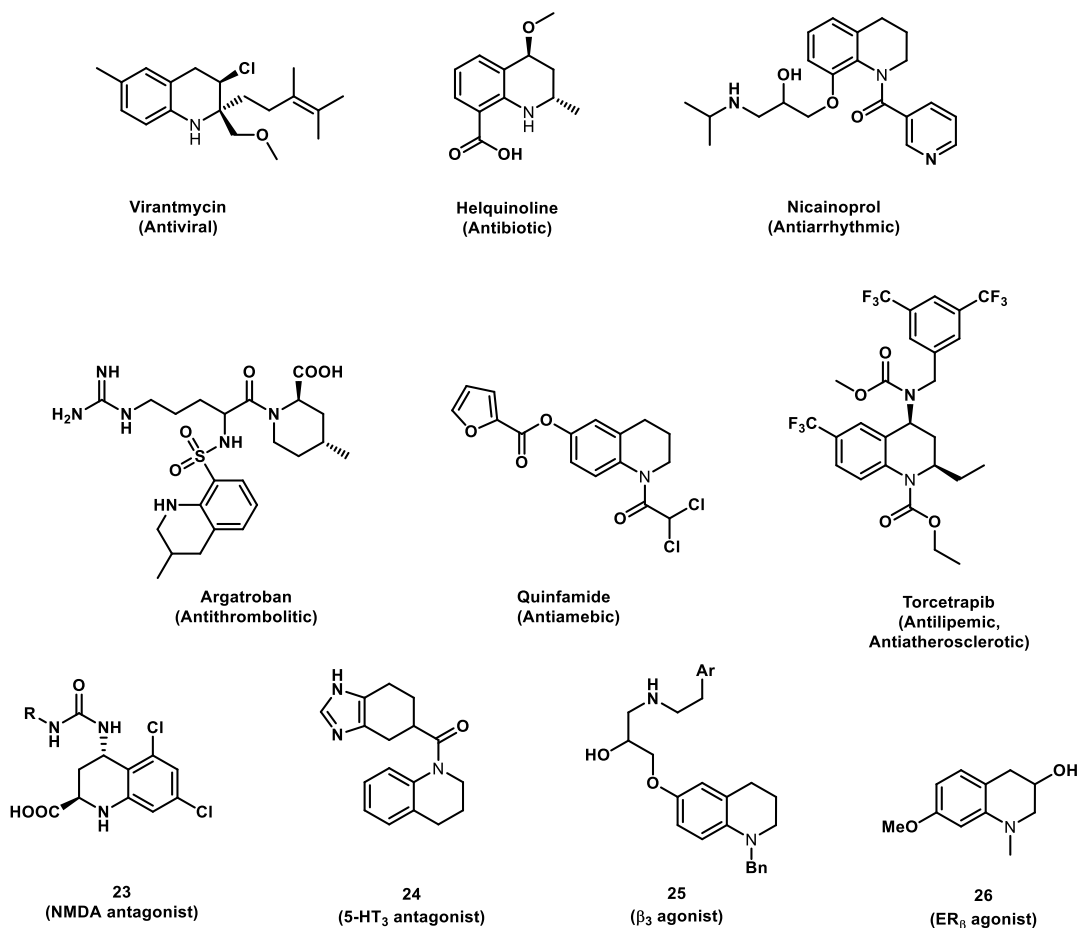


Figure 7 Examples of Pharmacologically Relevant Tetrahydroquinolines

The semi-rigid THQ scaffold seems to possess geometries suitable for decoration with different side chains, and can be considered a good template for chemical diversification to discover novel MLT receptor ligands. Given the peculiar geometries of the THQ ring and the previous excellent results obtained for 2-acylaminomethyl-THQs, one of the main purposes of my PhD work was to test the possibility to get new MLT receptor ligands with different patterns of substitution on the THQ scaffold.

In particular, we i) designed two different classes of THQs with an amide side chain in position 1 or 3 and different substituents on the THQ ring (Figure 8), and ii) compared the behavior of THQs with that of the corresponding tetralin analogues to evaluate if the THQ scaffold can be considered as a valuable bioisostere of the tetralin ring present in some of the best known and most characterized MT<sub>1</sub>/MT<sub>2</sub> ligands (e.g., 4-P-PDOT, **8a** in Figure 3).

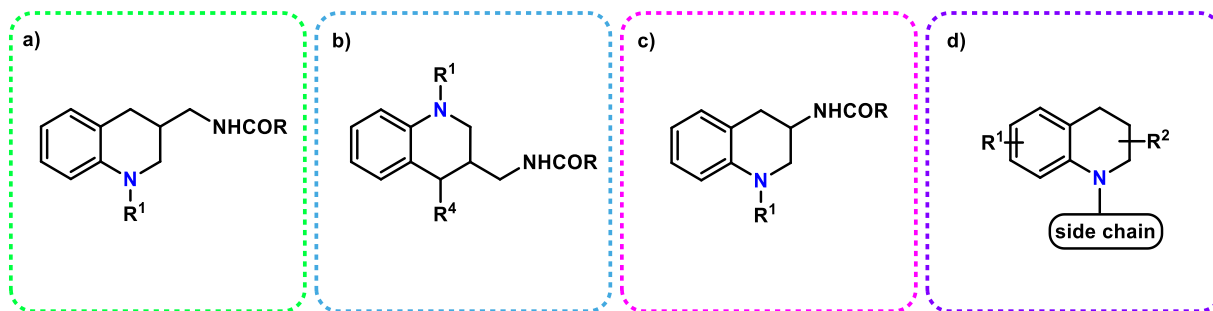


Figure 8 Schematic representation of new designed tetrahydroquinoline melatonin receptor ligands

The synthesis and pharmacological characterization of these new compounds could allow to expand the chemical space of MLT receptor ligands, and to obtain new interesting lead candidates with potential therapeutic perspectives in melatonergic diseases.



## 1.2.2 Results and Discussion

Taking into account previous structure-activity relationships for the melatonergic ligands, and considering that previously developed pharmacophoric models seem to indicate that the tetrahydroquinoline ring is not involved in polar interactions with the amino acids present in the receptor binding site, we started our exploration by testing the possibility to shift the THQ nitrogen, in the 2-acylaminomethyl-THQ series, to the opposite site of the heterocycle (Figure 9).

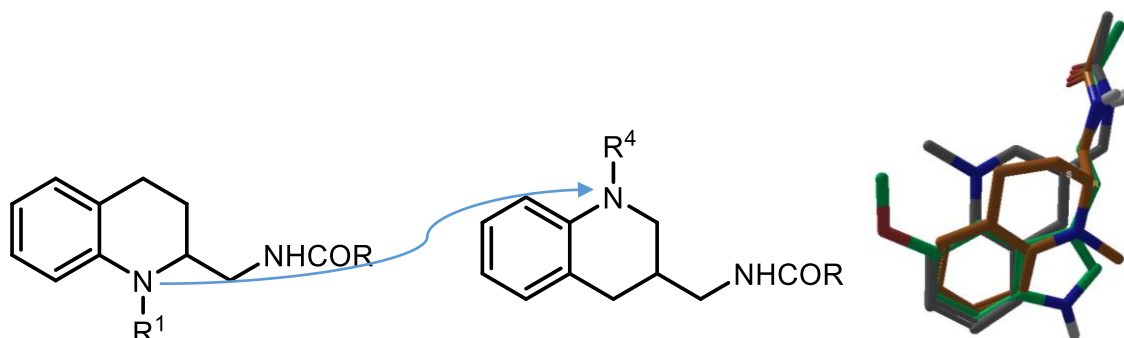
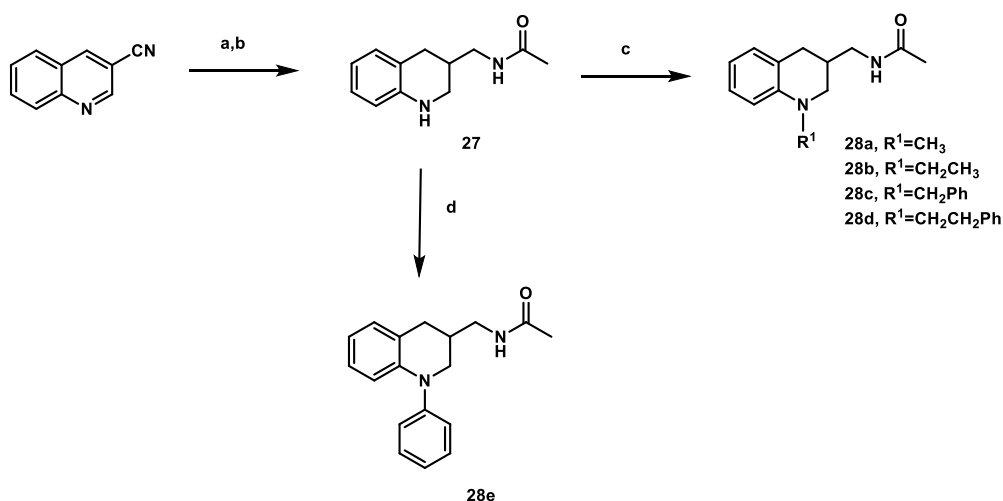


Figure 9. Nitrogen shift to the opposite site of the heterocycle and superposition of a 2-acylaminomethylTHQs prototype (UCM934:  $R^1=Me$ ,  $R=Et$ : orange), MLT (green) and the 3-acetylaminomethyl-THQ **28a** (blue)

We therefore prepared the new 3-acetylaminomethyl-THQ **27**, and its derivatives **28a-e** in which we investigated the influence on receptor activity of the size and shape of the substituent on the THQ nitrogen atom. The synthetic procedures used to synthesize these compounds are depicted in Scheme 1. Briefly, hydrogenation (4 atm, 60 °C) of the commercially available 3-cyanoquinoline in the presence of Raney-Ni and ammonia (a simultaneous reduction of the nitrile and pyridine ring occurs), followed by *N*-acetylation of the intermediate primary methanamine, provided the desired 3-methanamidotetrahydroquinoline **27**. *N*1-substituted 3-methanamido derivatives **28a-e** were prepared by *N*1-alkylation of **27** with the suitable alkyl halide (**28a-d**) or by palladium-catalyzed *N*1-arylation (**28e**) using bromobenzene, palladium (II) acetate, and ( $\pm$ )-BINAP.



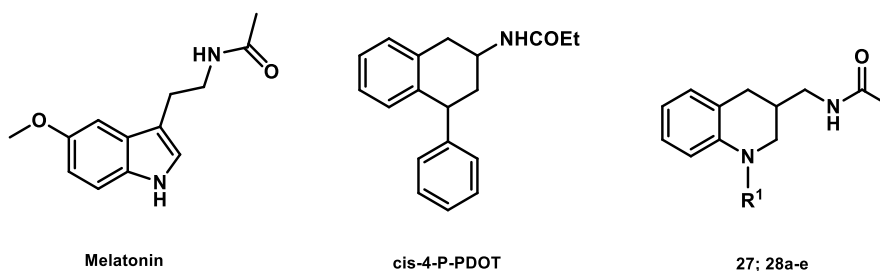
*Scheme 1* Synthesis of 3-acetylaminoethyl-THQs. Reagents and conditions: (a) H<sub>2</sub> (4 atm), Raney-Ni, 2 M NH<sub>3</sub> in EtOH, THF, 60 °C, 16 h; (b) Ac<sub>2</sub>O, Et<sub>3</sub>N, THF, rt, 1 h, two steps (a, b) yield 70%; (c) R-X, Et<sub>3</sub>N, toluene, Δ, 1–16 h, yield 46–85%; (d) bromobenzene, Pd(OAc)<sub>2</sub>, (±)-BINAP, *t*-BuOK, toluene, 100 °C, 24 h, yield 29%.

The new synthesized tetrahydroquinoline derivatives were evaluated for their binding affinity and intrinsic activity at human MT<sub>1</sub> and MT<sub>2</sub> receptors stably transfected in Chinese hamster ovarian (CHO) cells using 2-[<sup>125</sup>I]iodomelatonin as radioligand. The *h*MT<sub>1</sub> and *h*MT<sub>2</sub> binding affinity and intrinsic activity values of the new THQs derivatives **27** and **28a-e** are reported in Table 1, together with those of the reference compounds melatonin and cis-4-P-PDOT.

Compound **28e**, having a phenyl group on the tetrahydroquinoline nitrogen, showed MT<sub>1</sub> and MT<sub>2</sub> binding affinities in the same range as MLT and 4-P-PDOT and it behaved as an antagonist with slight MT<sub>2</sub> selectivity (10 fold). These data confirm THQ as a versatile and efficient scaffold to derive MLT receptor ligands and a valuable bioisostere of the tetraline ring.

Binding affinities of these compounds are quite correlated with the size of the substituent on the nitrogen atom. The *N*-unsubstituted compound (**27**) is the one with lower receptor binding affinity and increased potency is observed moving from *N*-methyl (**28a**) to *N*-ethyl (**27b**) and *N*-phenyl (**28e**). The *N*-benzyl derivative **28c** showed the highest MT<sub>2</sub>-selectivity (59 fold), consistently with what previously observed for compounds with out-of-plane substituents.

Table 1 Binding affinity and intrinsic activity of 3-acylaminomethyl tetrahydroquinoline derivatives at human MT<sub>1</sub> and MT<sub>2</sub> melatonin receptors



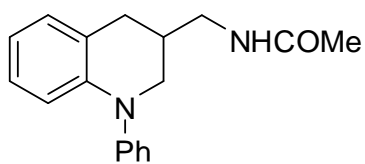
Compound <sup>a</sup>	R <sup>1</sup>	MT <sub>1</sub>			MT <sub>2</sub>		
		K <sub>i</sub> (nM)	EC <sub>50</sub> (nM)	E <sub>max</sub> (%)	K <sub>i</sub> (nM)	EC <sub>50</sub> (nM)	E <sub>max</sub> (%)
<b>1</b> (MLT) <sup>b</sup>		0.23	1.7	123 ± 13	0.52	0.4	76 ± 6
<b>Cis-4-P-PDOT</b> <sup>c</sup>		76		23 ± 6	0.69		46 ± 2
<b>27</b>	H	430			110		
<b>28a</b>	Me	83	>10000		15	10	32 ± 3
<b>28b</b>	Et	20	>10000		1	7	59 ± 8
<b>28c</b>	Bn	59			1	3	28 ± 4
<b>28d</b>	C <sub>6</sub> H <sub>5</sub> CH <sub>2</sub> CH <sub>2</sub>	246			47	80	47 ± 5
<b>(+/-)-28e</b>	Ph	2.4	>10000	27 ± 9	1.2	>10000	10 ± 1
<b>(-)-28e</b>	Ph	3.02		30 ± 8	1.38		29 ± 2
<b>(+)-28e</b>	Ph	1.58		25 ± 9	0.78		5 ± 3

K<sub>i</sub> and EC<sub>50</sub> (nM) values are geometric mean values of at least two separate experiments performed in duplicate. E<sub>max</sub> values are arithmetic mean values ± SEM. <sup>a</sup>Chiral compounds were tested as racemates. <sup>b</sup>Taken from ref 29. <sup>c</sup>Taken from ref 30.

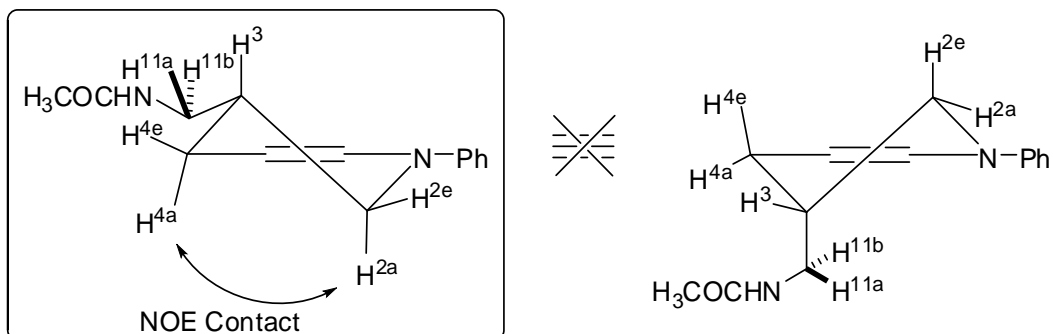
NMR conformational studies of the most potent compound **28e** (Table 2) revealed a high prevalence of half-chair conformation for the tetrahydroquinoline ring wherein the C3 acylaminomethyl side chain has an equatorial arrangement.

In details, <sup>1</sup>H-<sup>1</sup>H vicinal coupling constant analysis in DMSO-*d*<sub>6</sub> showed *J* values = 10.0 and 4.5 Hz for H<sub>3</sub> with H<sub>2a</sub> and H<sub>2e</sub> respectively, indicative of an anti-arrangement of H<sub>3</sub> with H<sub>2a</sub>, and with H<sub>3</sub> gauche to H<sub>2e</sub>; this is consistent with an equatorial arrangement of the C3-side chain. Additionally, the NOE contact between H<sub>2a</sub> and H<sub>4a</sub> is in line with the suggested equatorial arrangement of the side chain. Similar NMR patterns, supporting equatorial conformations of the amide side chain, were recorded for the other 3-acylaminomethyl-THQs **27** and **28b-d**.

Table 2. Chemical shifts, Geminal and Vicinal Coupling Constant Values Observed by NMR Spectroscopy (400 MHz) for compound **28e** in DMSO-*d*<sub>6</sub>.



**28e** (S + R)



Proton	$\delta$ (ppm)	Protons	J (Hz)
H <sup>2a</sup>	2.52	<sup>3</sup> J <sub>2a-3</sub> <sup>2</sup> J <sub>2a-2e</sub>	10.0 16.0
H <sup>2e</sup>	2.84	<sup>4</sup> J <sub>2e-4e</sub> <sup>3</sup> J <sub>2e-3</sub> <sup>2</sup> J <sub>2e-2a</sub>	1.5 <sup>a</sup> (long range W coupling) 4.5 16.0
H <sup>3</sup>	2.13	<sup>3</sup> J <sub>3-4e</sub> <sup>3</sup> J <sub>3-2e</sub> <sup>3</sup> J <sub>3-2a</sub> <sup>3</sup> J <sub>3-11a</sub> <sup>3</sup> J <sub>3-11b</sub> <sup>3</sup> J <sub>3-4a</sub>	3.5 4.5 10.0 6.0 6.0 9.0
H <sup>4a</sup>	3.25	<sup>3</sup> J <sub>4a-3</sub> <sup>2</sup> J <sub>4a-4e</sub>	9.0 11.5
H <sup>4e</sup>	3.63	<sup>4</sup> J <sub>4-2e</sub> <sup>3</sup> J <sub>4e-3</sub> <sup>2</sup> J <sub>4e-4a</sub>	1.5 <sup>a</sup> (long range W coupling) 3.5 11.5
H <sup>11a</sup>	3.06	<sup>3</sup> J <sub>11a-3</sub> <sup>2</sup> J <sub>11a-11b</sub>	6.0 13.5
H <sup>11b</sup>	3.13	<sup>3</sup> J <sub>11b-3</sub> <sup>2</sup> J <sub>11b-11a</sub>	6.0 13.5

<sup>a</sup> The H<sup>2e</sup> signal is a broad dd in the 400MHz <sup>1</sup>H NMR spectrum, the long range coupling constant is clearly visible in the H<sup>4e</sup> signal and in the corresponding COSY cross peaks.

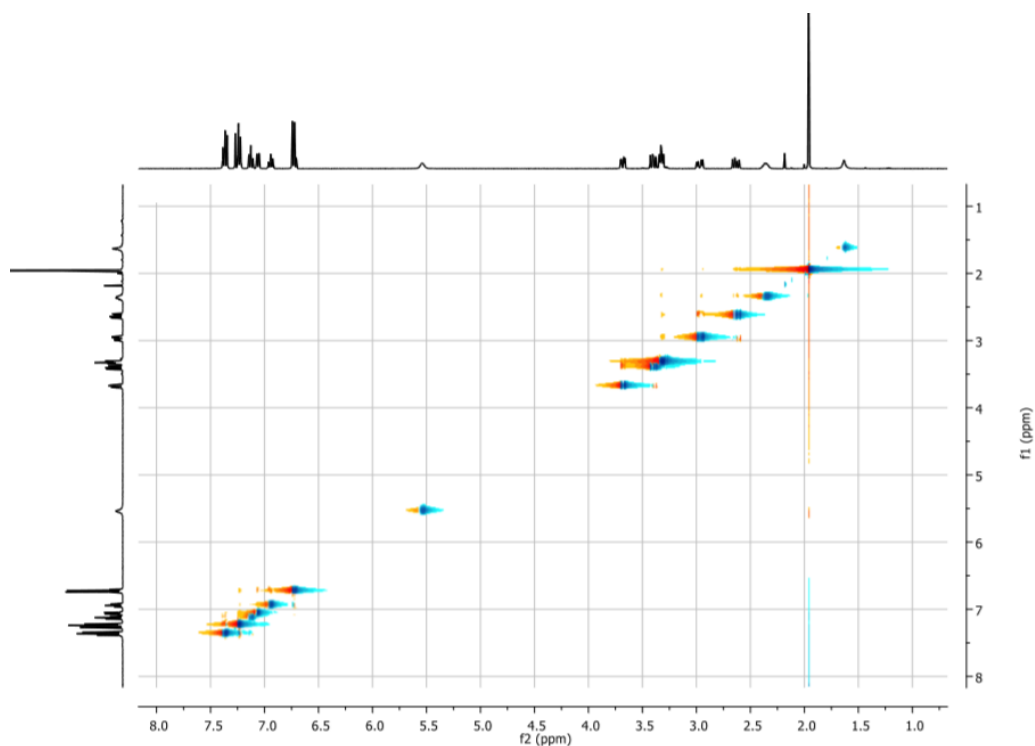


Figure 10 NOESY spectrum for compound **28e**. The spectrum was recorded at 298 K on a 400 MHz using a 0,036 mM solution of **28e** in CDCl<sub>3</sub>. Mixing time 300 ms.

Interestingly, the equatorial arrangement of the C3-actylaminomethyl side chain allows a good superposition with the putative bioactive conformation of MLT as shown in Figure 11.

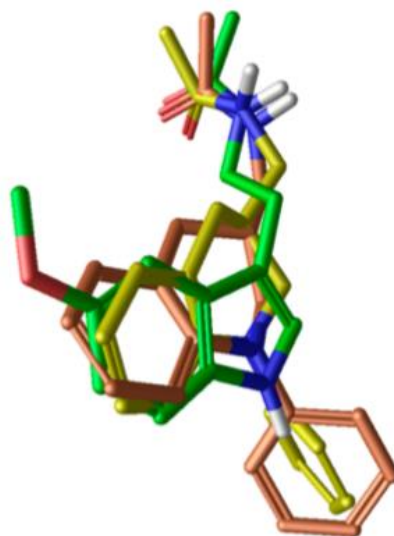
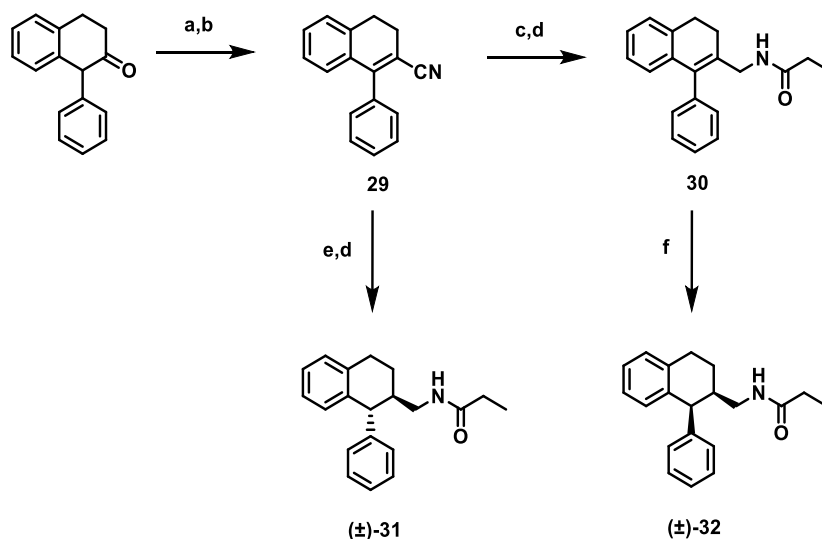


Figure 11 Superposition of melatonin (green carbons) and the enantiomers of compound **28e**

Separation of the two enantiomers of the compound **28e** by semi preparative chiral HPLC allowed us to investigate the influence of chirality on their interaction with melatonin receptors. The enantiomers displayed similar binding affinities and intrinsic activities at both receptors, likely due to the equatorial arrangement of the acetylaminoethyl side chain, which allows good superposition of each enantiomer to the putative bioactive conformation of MLT (see Figure 11).

To further validate the CH/N isosterism in the field of MLT ligands we prepared and tested the two *trans*- and *cis*-1-phenyl-2-acetylaminoethyl-tetralin diastereoisomers **31** and **32** (Scheme 2), in which the THQ nitrogen is replaced by a CH group.

The synthetic route adopted for the preparation of tetralin derivatives **31–32** is depicted in Scheme 2. The first step involved the reaction of 1-phenyl-3,4-dihydronaphthalen-2(1*H*)-one,<sup>31</sup> with trimethylsilyl cyanide and ZnI<sub>2</sub> followed by treatment with phosphorus oxychloride in pyridine to give the intermediate nitrile **29**, which was converted into the dihydronaphthalene derivative **30** by reduction with LiAlH<sub>4</sub>/AlCl<sub>3</sub> and subsequent *N*-acylation of the crude intermediate amine with propionic anhydride. The *trans*-(**31**) and *cis*-(**32**) tetralin target compounds were respectively obtained by reduction of the unsaturated nitrile **29** with LiAlH<sub>4</sub> followed by *N*-acylation with propionic anhydride or by Pd-catalyzed hydrogenation of **30**.

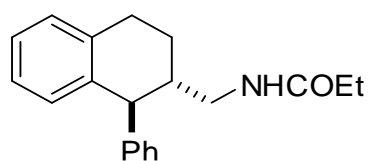


Scheme 2 Synthesis of 3-acylaminoethyl tetralines. Reagents and conditions: (a) trimethylsilyl cyanide,  $ZnI_2$ , toluene, rt, 18 h; (b)  $POCl_3$ ,  $Py$ , reflux, 1 h, two steps (a, b) yield 65%; (c)  $LiAlH_4/AlCl_3$ , dry THF, rt, 1 h; (d) propionic anhydride,  $Et_3N$ , THF, rt, 16 h, two steps (c, d) yield 37%; (e)  $LiAlH_4$ , THF, reflux, 2 h, two steps (e, d) yield 30%; (f)  $H_2$  (4 atm), 10% Pd-C, MeOH, 60 °C, 6 h, yield 47%.

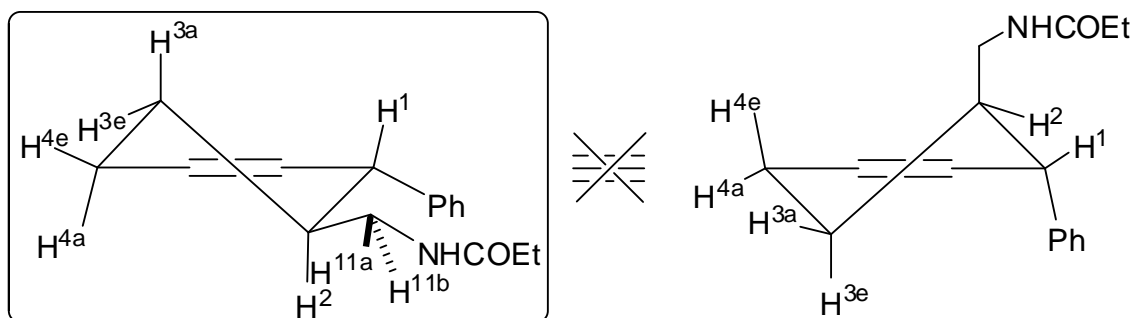
To obtain information about their preferred conformational states, the tetraline derivatives **31** and **32** were submitted to suitable NMR studies.  $^1H$  NMR spectrum of the *trans*-tetralin derivative (**31**) showed vicinal coupling constants between  $H_2$  and the two distinct  $H_3$  protons ( $J_{2-3e} \approx 3.0$ ;  $J_{2-3a} \approx 9.0$ ), which is consistent with an axial arrangement for the  $H_2$ ; these data together with a  $^3J_{1-2}$  value of  $\approx 8$  Hz confirm the diequatorial arrangement of both amido side chain and phenyl substituent (Table 3).

On the contrary, the NMR spectrum of the *cis*-tetralin derivative (**32**) revealed an equilibrium between the equatorial and the axial arrangement of its side chain. In fact, the observed coupling constants values between  $H^2$  and the two  $H^3$  protons ( $J_{2-3a} = 6.5$  Hz and  $J_{2-3e} = 3.5$  Hz (Table 4)) derives respectively, from the combination of a gauche and an anti-arrangement of the two protons, and from two gauche arrangements.

Table 3 *J* coupling constant for compound 31



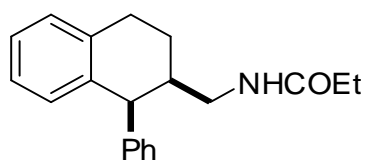
*trans*-31



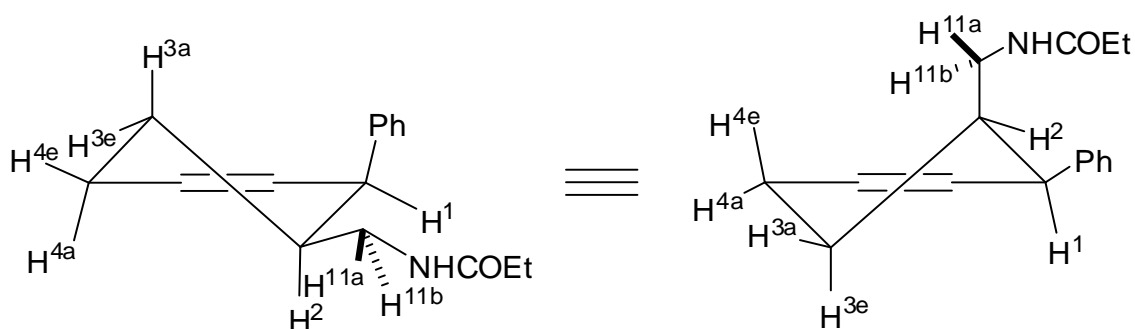
Proton	$\delta$ (ppm) <i>CD</i> <sub>3</sub> <i>OD</i>	<i>J</i> (Hz) <i>CD</i> <sub>3</sub> <i>OD</i>
H <sup>1</sup>	3.84	<sup>3</sup> <i>J</i> <sub>1-2</sub> = 8.0
H <sup>2</sup>	2.14	<sup>3</sup> <i>J</i> <sub>2-3e</sub> = 3.0
		<sup>3</sup> <i>J</i> <sub>2-11a</sub> = 5.5
		<sup>3</sup> <i>J</i> <sub>2-1</sub> = 8.0
		<sup>3</sup> <i>J</i> <sub>2-11b</sub> = 8.0
H <sup>3a</sup>	1.57	<sup>3</sup> <i>J</i> <sub>2-3a</sub> = 9.0
		<sup>3</sup> <i>J</i> <sub>3a-4e</sub> = 6.5
		<sup>3</sup> <i>J</i> <sub>3a-4a</sub> = 8.5
		<sup>3</sup> <i>J</i> <sub>3a-2</sub> = 9.0
H <sup>3e</sup>	2.03	<sup>2</sup> <i>J</i> <sub>3a-3e</sub> = 13.5
		<sup>3</sup> <i>J</i> <sub>3e-2</sub> = 3.0
		<sup>3</sup> <i>J</i> <sub>3e-4a</sub> = 5.5
		<sup>3</sup> <i>J</i> <sub>3e-4e</sub> = 5.5
H <sup>11a</sup>	3.14	<sup>2</sup> <i>J</i> <sub>3e-3a</sub> = 13.5
		<sup>3</sup> <i>J</i> <sub>11a-2</sub> = 5.5
H <sup>11b</sup>	3.19	<sup>3</sup> <i>J</i> <sub>11b-2</sub> = 8.0
		<sup>2</sup> <i>J</i> <sub>11b-11a</sub> = 13.5



Table 4 J coupling constant for compound 32



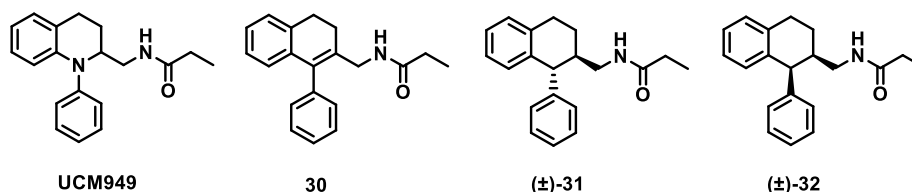
*cis*-32



Proton	$\delta$ (ppm) DMSO- $d_6$	$J$ (Hz) DMSO- $d_6$
H <sup>3a</sup>	1.51	${}^3J_{3a-4e} = 6.0$
		${}^3J_{3a-2} = 6.5$
		${}^3J_{3a-4a} = 11.5$
		${}^2J_{3a-3e} = 13.5$
H <sup>3e</sup>	1.68	${}^3J_{3e-4e} = 1.5$
		${}^3J_{3e-2} = 3.5$
		${}^3J_{3e-4a} = 6.5$
		${}^2J_{3e-3a} = 13.5$
H <sup>4a</sup>	2.82	${}^3J_{4a-3e} = 6.5$
		${}^3J_{4a-3a} = 11.5$
		${}^2J_{4a-4e} = 18.0$
H <sup>4e</sup>	3.00	${}^3J_{4e-3e} = 1.5$
		${}^3J_{4e-3a} = 6.0$
		${}^2J_{4e-4a} = 18.0$
H <sup>11a</sup>	2.54	${}^3J_{11a-NH} = 6.0$
		${}^3J_{11a-2} = 6.0$
		${}^2J_{11a-11b} = 13.0$
H <sup>11b</sup>	2.93	${}^3J_{11b-NH} = 5.5$
		${}^3J_{11b-2} = 5.5$
		${}^2J_{11b-11a} = 13.0$

Both compounds display good receptor binding affinity (Table 5); in particular the *trans* isomer **31** in its diequatorial conformation is a potent and selective (~300 times) MT<sub>2</sub> partial agonist (MT<sub>1</sub> K<sub>i</sub> = 62 nM, E<sub>max</sub> = 61%; MT<sub>2</sub> K<sub>i</sub> = 0.23 nM, E<sub>max</sub> = 78%), in analogy to what observed for the 2-acylaminomethyl-THQ bioisostere UCM949.

Table 5 Binding affinity and intrinsic of tetraline derivatives at human MT<sub>1</sub> and MT<sub>2</sub> melatonin receptors



Compound <sup>a</sup>	MT <sub>1</sub>		MT <sub>2</sub>	
	K <sub>i</sub> (nM)	E <sub>max</sub> (%)	K <sub>i</sub> (nM)	E <sub>max</sub> (%)
<b>1</b> (MLT) <sup>b</sup>	0.23	123 ± 13	0.52	76 ± 6
<i>UCM949</i> <sup>c</sup>	1.6	69 ± 12	0.06	90 ± 0.5
<b>30</b>	28	16 ± 8	3.81	30 ± 6
<b>31</b>	62	61 ± 4	0.23	78 ± 9
<b>32</b>	3.5	56 ± 8	0.22	75 ± 3

K<sub>i</sub> and EC<sub>50</sub> (nM) values are geometric mean values of at least two separate experiments performed in duplicate. E<sub>max</sub> values are arithmetic mean values ± SEM. <sup>a</sup>Chiral compounds were tested as racemates. <sup>b</sup>Taken from ref 29. <sup>c</sup>Taken from ref 25.

Molecular superposition models provide an explanation of the observed high affinity and MT<sub>2</sub> selectivity for compound **31**. As shown in Figure 12a, the *trans*-isomer **31**, in its diequatorial conformation, can be closely superposed to the bioactive conformation of melatonin, and placing the phenyl substituent in the out-of-plane region conferring MT<sub>2</sub> selectivity.

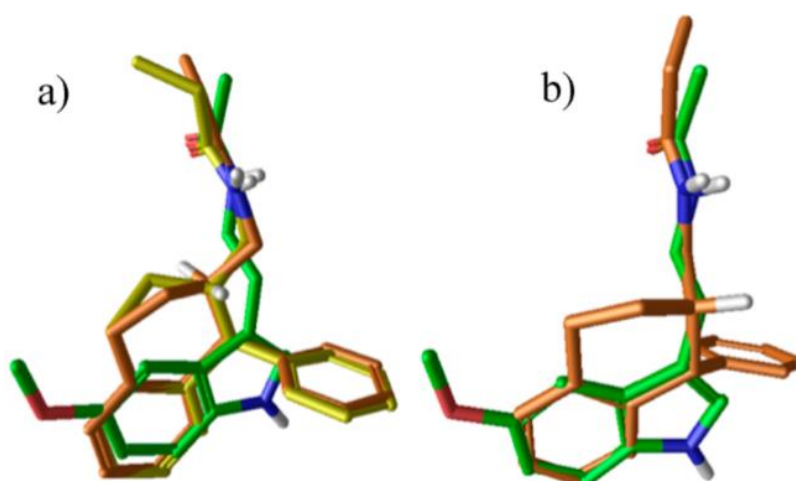


Figure 12 (a) Superposition of the bioactive conformation of melatonin (green carbons) with compound **31** (yellow carbons) and compound **32** (orange carbons) with equatorial arrangement of its side chain. (b) Superposition of melatonin and compound **32** with axial arrangement of its side chain.

All these results clearly demonstrated that THQ derivatives can mimic the SARs observed for tetraline analogs and viceversa.

The THQ scaffold could also be arranged in a different way to the alignment proposed in Figure 9 and 13 (left), especially in the absence of bulky *N*-substituent. An alternative arrangement is proposed in Figure 13 (right) in which the aromatic portion of the THQ ring is positioned in the same region as the benzene of the indole of MLT, and to point the amide groups in the same direction, the tetrahydropyridine ring is superposed to the fused six-membered ring of the tricyclic 1,3,4,5-tetrahydrobenzo[*cd*]indole agonist **21**, (Figure 13 on the right), in analogy to what previously proposed for the series of 2-acylaminomethylTHQs.<sup>25</sup>

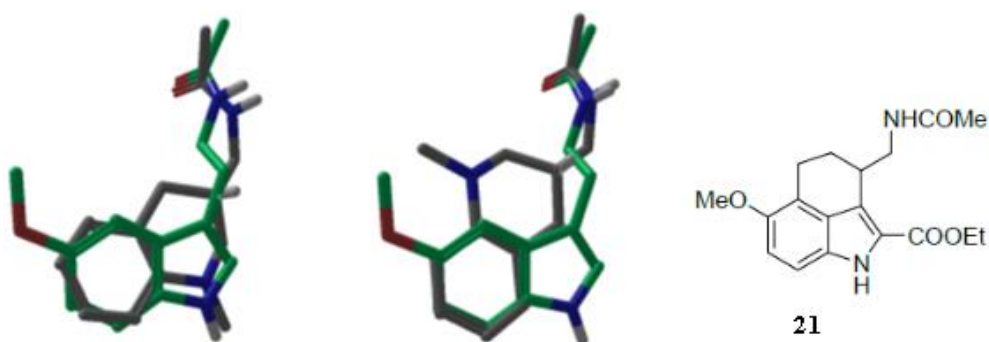


Figure 13 Classical superposition of **28a** to the bioactive conformation of MLT (left) and alternative superposition (right)

If this alternative orientation is possible, 3-acylaminomethyl-THQs should allow substitution at C4 with groups that in general can be accommodated in allowed regions of the MT<sub>1</sub> and, particularly, MT<sub>2</sub> binding sites.

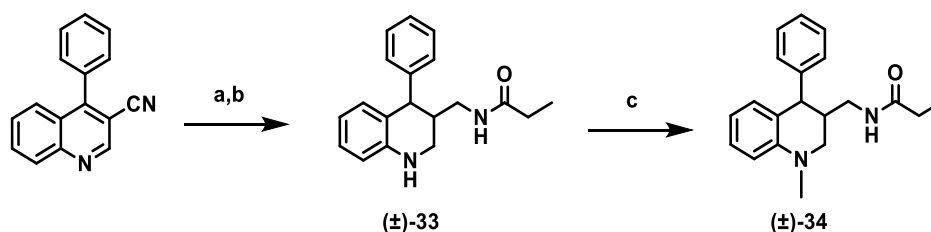
In order to confirm this “alternative spatial arrangement” we synthesized and tested the tetrahydroquinoline derivative (**34**, Scheme 3) having the propionylaminomethyl side chain in position 3, a methyl group on the nitrogen and a phenyl ring in position 4.

This compound **34** can be considered a new application of the design of melatonin ligands based on the THQ scaffold, in which the bulkier substituent, generally involved in the modulation of binding affinity and MT<sub>1</sub>/MT<sub>2</sub> subtype selectivity, is linked at the C4 position instead of the THQ nitrogen. **34** can be also considered a bioisostere of the 1-phenyl-2-acylaminomethylTHQ (UCM949) by applying the classical isosteric CH/N replacement at the atom opposite to the THQ nitrogen.

Compound (+/-)-*cis*-**34** was prepared following the steps outlined in Scheme 3. Hydrogenation of 4-phenylquinoline-3-carbonitrile<sup>32</sup> in the presence of Raney-Ni and ammonia, and subsequent *N*-acylation of the intermediate primary methanamine with propionic anhydride provided the 4-phenyl-

tetrahydroquinoline derivative **33**, which was then converted to the desired *N*-methyl derivative **34** by reductive amination using 37% HCHO and NaBH<sub>3</sub>CN.

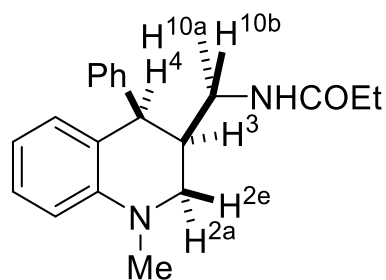
<sup>1</sup>H NMR analysis ( $J_{4,3} \approx 5.0$  Hz) confirmed that the applied synthetic procedure makes it possible to obtain only a racemic mixture of the *cis*-**34** isomers.



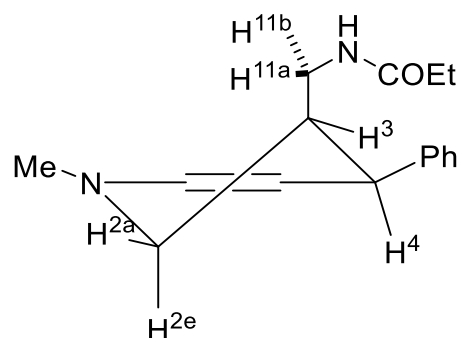
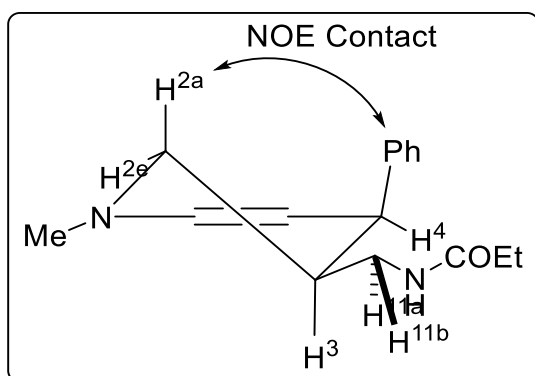
Scheme 3 Synthesis of 4-substituted 3-acylaminoethylTHQ. Reagents and conditions: (a) H<sub>2</sub> (4 atm), Raney-Ni, 2 M NH<sub>3</sub> in EtOH, THF, 40 °C, 12 h; (b) propionic anhydride, Et<sub>3</sub>N, THF, rt, 1 h, two steps (a, b) yield 46%; (c) 37% HCHO, NaBH<sub>3</sub>CN, MeOH/AcOH, 40 °C, 3 h, yield 72%.

The THQ derivative *cis*-**34** showed MT<sub>1</sub> and MT<sub>2</sub> binding affinities (MT<sub>1</sub> K<sub>i</sub> = 3.4 nM; MT<sub>2</sub> K<sub>i</sub> = 0.48 nM) in the same range as the *N*-phenyl derivative **28e** with a partial agonist behaviour and only minimal selectivity (7 fold) for the MT<sub>2</sub> subtype. NMR conformational studies revealed that the amide side chain has equatorial arrangement as confirmed from the large coupling constant  $J_{2a-3}$  (~11.5 Hz) and the small one  $J_{2e-3}$  (~4.0 Hz), and the phenyl ring is in pseudo-axial position ( $J_{3-4} \sim 5$  Hz and long-range W coupling  ${}^4J_{2e-4} \approx 1.0$  Hz) (Table 6). The pseudo-axial arrangement of the phenyl substituent was further confirmed by 2D-NOESY experiments showing a cross peak between proton 2a and the hydrogens of the phenyl ring.

Table 6 J coupling constant for compound 34



34



Proton	Chemical shift (ppm)	Coupling constant (Hz)
H <sup>2a</sup>	2.93	<sup>3</sup> J <sub>2a-3</sub> = 11.5 <sup>2</sup> J <sub>2a-2e</sub> = 11.5
H <sup>2e</sup>	3.10	<sup>4</sup> J <sub>2e-4</sub> = 1.0 (long range W coupling) <sup>a</sup> <sup>3</sup> J <sub>2e-3</sub> = 4.0 <sup>2</sup> J <sub>2a-2e</sub> = 11.5
H <sup>3</sup>	2.28	<sup>3</sup> J <sub>3-4</sub> = 4.5 <sup>3</sup> J <sub>3-11b</sub> = 5.0 <sup>3</sup> J <sub>3-2e</sub> = 4.0 <sup>3</sup> J <sub>3-11a</sub> = 9.0 <sup>3</sup> J <sub>3-2a</sub> = 11.5
H <sup>4</sup>	4.13	<sup>4</sup> J <sub>4-2e</sub> = 1.0 (long range W coupling) <sup>a</sup> <sup>3</sup> J <sub>4-3</sub> = 4.5
H <sup>11a</sup>	2.52	<sup>3</sup> J <sub>11a-3</sub> = 9.0 <sup>2</sup> J <sub>11a-11b</sub> = n.c. <sup>b</sup>
H <sup>11b</sup>	2.96	<sup>3</sup> J <sub>11b-3</sub> = 5.5 <sup>2</sup> J <sub>11b-11a</sub> = n.c. <sup>c</sup>

<sup>a</sup>The H<sup>4</sup> signal is a broad doublet in the 400MHz <sup>1</sup>H NMR spectra, the long range coupling constant is clearly visible in the H<sup>2e</sup> signal and corresponding COSY cross peaks. <sup>b</sup> Not computable, the signal is partially covered by DMSO-d<sub>6</sub> signal. <sup>c</sup> Not computable, the signal is partially covered by NMe signal.

The axial arrangement of the phenyl substituent seems to indicate that the preferential accommodation of *cis*-**34** within the MT<sub>1</sub> binding site is that outlined in Figure 14b, since in the 14a orientation the phenyl substituent would be placed in a region considered forbidden at MT<sub>1</sub> receptor.

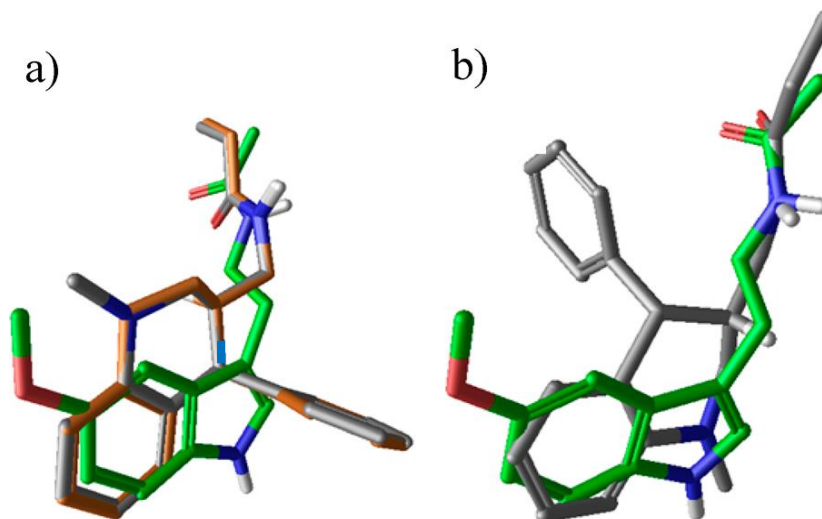
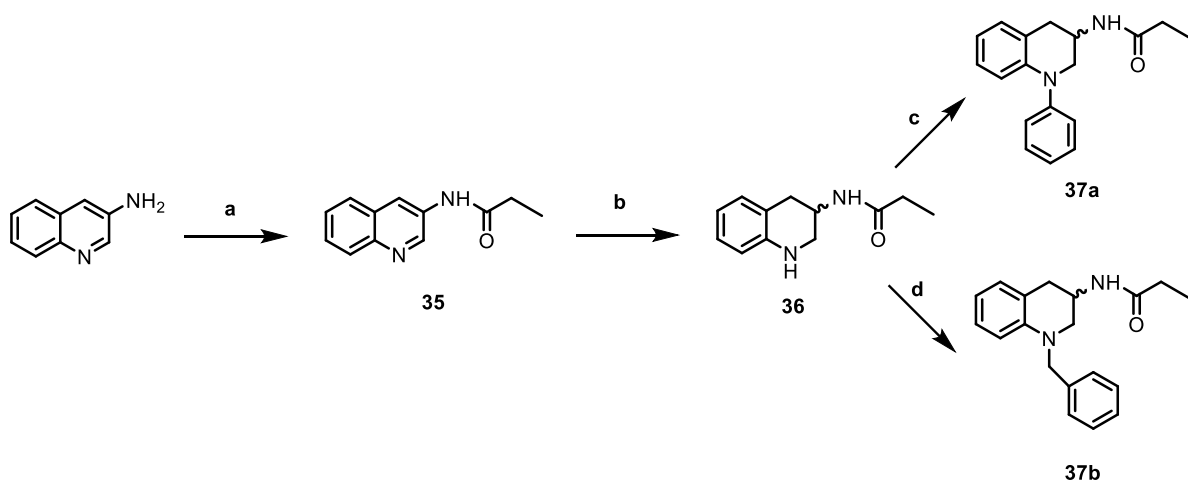


Figure 14 Alternative accommodations of *cis*-**34** within the MT<sub>1</sub> binding site

To further explore the versatility of the THQ ring as a good template for the design of new MLT receptor ligands, we evaluated the possibility of eliminating the methylene spacer of the side chain, by directly linking the amide group to position 3, in agreement to what already reported for tetraline bioisosteres, such as 4-P-PDOT or its analogs.

The new 3-propionylaminoTHQ derivatives **37a-b** were prepared according to the synthetic steps illustrated in Scheme 4.

A key intermediate for their synthesis was 3-propionamidotetrahydroquinoline (**36**)<sup>33</sup> which was obtained by *N*-acylation of the commercially available 3-aminoquinoline with propionic anhydride and subsequent reduction of the pyridine ring with NaBH<sub>3</sub>CN/ AcOH. The *N*-phenyl (**37a**) and *N*-benzyl (**37b**) desired compounds were respectively prepared by palladium catalyzed *N*-arylation or *N*-benzylation of **36**.



Scheme 4 Synthesis of 3-propionylaminoTHQ derivatives **37a-b**. Reagents and conditions: (a) propionic anhydride,  $Et_3N$ , THF, reflux, 3 h, yield 81%; (b)  $NaBH_3CN$ , AcOH, 50 °C to rt, 20 h, yield 40%; (c) bromobenzene,  $Pd(OAc)_2$ , ( $\pm$ )-BINAP,  $t-BuOK$ , toluene, 100 °C, 6 h, yield 46%; (d) benzyl bromide,  $Et_3N$ , toluene, reflux, 1 h, yield 61%.

The results of binding studies with the new THQ derivatives **37a-b** are shown in Table 7. **37a** showed nanomolar affinity and it behaved as a partial agonist ( $MT_1 K_i = 22$  nM,  $EC_{50} = 20$  nM;  $MT_2 K_i = 2$  nM,  $EC_{50} = 1$  nM). Compared to *cis*-4-P-PDOT, its formal CH/N isostere, the *N*-phenyl-THQ **37a** displayed the same  $MT_1$  receptor affinity and a similar partial agonist, behavior but it resulted less potent at  $MT_2$  receptor and thus less  $MT_2$ -selective (11 fold). Replacing the *N*-phenyl substituent with a benzyl group restored  $MT_2$  selectivity and shifted intrinsic activity toward antagonism ( $MT_1 K_i = 892$  nM;  $MT_2 K_i = 6$  nM,  $EC_{50} = >10000$  nM). This is consistent to the greater hindrance of the benzyl group, which can occupy the previously proposed accessory out of plane binding site region conferring  $MT_2$  selectivity.<sup>34</sup> The pharmacological results for the 3-propionamido THQs confirm, once again, the bioisosterism between the tetralin and THQ rings.

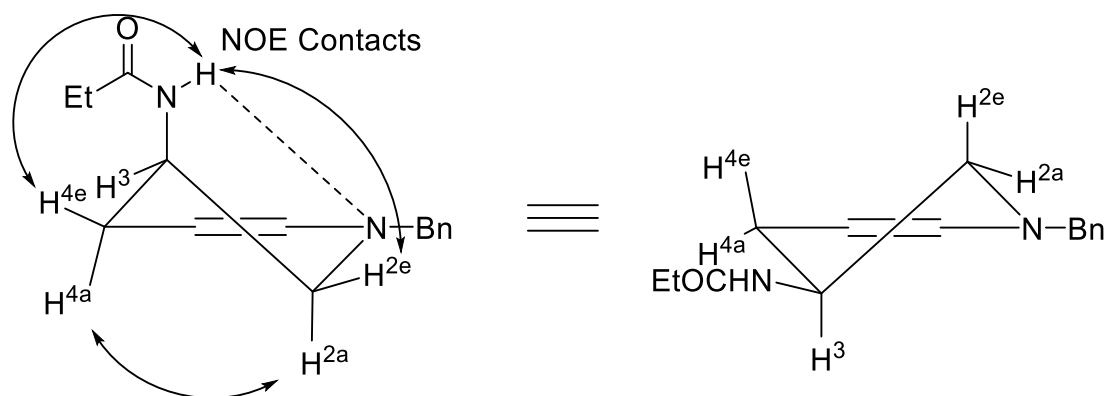
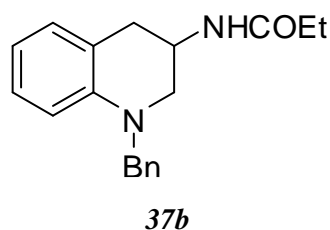
Table 7 Binding affinity and intrinsic of **37a-b** at human  $MT_1$  and  $MT_2$  melatonin receptors

Compound <sup>a</sup>	R <sup>1</sup>	MT <sub>1</sub>			MT <sub>2</sub>		
		K <sub>i</sub> (nM)	EC <sub>50</sub> (nM)	E <sub>max</sub> (%)	K <sub>i</sub> (nM)	EC <sub>50</sub> (nM)	E <sub>max</sub> (%)
<b>1</b> (MLT) <sup>b</sup>		0.23	1.7	123 ± 13	0.52	0.4	76 ± 6
<b>Cis-4-P-PDOT</b> <sup>c</sup>		76		23 ± 6	0.69		46 ± 2
<b>37a</b>	Ph	22	20	29 ± 3	2	1	41 ± 3
<b>37b</b>	Bn	892			6	>10000	

K<sub>i</sub> and EC<sub>50</sub> (nM) values are geometric mean values of at least two separate experiments performed in duplicate. E<sub>max</sub> values are arithmetic mean values ± SEM. <sup>a</sup>Chiral compounds were tested as racemates. <sup>b</sup>Taken from ref 29 <sup>c</sup>Taken from ref 30

NMR conformational investigations of **37b** pointed out that such compound does not assume a fixed arrangement of the THQ nucleus, as shown from the conflicting *J* values registered in CDCl<sub>3</sub> and DMSO-*d*<sub>6</sub> (Table 8).

Table 8 J coupling constant for compound 37b



Main conformation in  $CDCl_3$

Main conformation in  $DMSO-d_6$

Proton	$\delta$ (ppm) $CDCl_3$	J (Hz) $CDCl_3$	$\delta$ (ppm) $DMSO-d_6$	J (Hz) $DMSO-d_6$
H <sup>4e</sup>	2.77	<sup>4</sup> J <sub>4e-2e</sub> = 2.5 (long range W coupling) <sup>3</sup> J <sub>4e-3</sub> = 3.0 <sup>2</sup> J <sub>4e-4a</sub> = 16.5	2.69	<sup>3</sup> J <sub>4e-3</sub> = 9.0 <sup>2</sup> J <sub>4e-4a</sub> = 15.5
H <sup>4a</sup>	3.16	<sup>3</sup> J <sub>4a-3</sub> = 4.5 <sup>2</sup> J <sub>4a-4e</sub> = 16.5	2.93	<sup>4</sup> J <sub>4a-2a</sub> = 1.5 (long range W coupling) <sup>a</sup> <sup>3</sup> J <sub>4a-3</sub> = 4.5 <sup>2</sup> J <sub>4a-4e</sub> = 15.5
H <sup>2e</sup>	3.29	<sup>4</sup> J <sub>2e-4e</sub> = 2.5 (long range W coupling) <sup>3</sup> J <sub>2e-3</sub> = 4.0 <sup>2</sup> J <sub>2e-2a</sub> = 11.5	3.17	<sup>3</sup> J <sub>2e-3</sub> = 8.5 <sup>2</sup> J <sub>2e-2a</sub> = 11.0
H <sup>2a</sup>	3.54	<sup>3</sup> J <sub>2a-3</sub> = 2.5 <sup>2</sup> J <sub>2a-2e</sub> = 11.5	3.40	<sup>4</sup> J <sub>2a-4a</sub> = 1.5 (long range W coupling) <sup>3</sup> J <sub>2a-3</sub> = 4.0 <sup>2</sup> J <sub>2a-2e</sub> = 11.0
H <sup>3</sup>	4.54	<sup>3</sup> J <sub>3-2a</sub> = 2.5 <sup>3</sup> J <sub>3-4e</sub> = 3.0 <sup>3</sup> J <sub>3-2e</sub> = 4.0 <sup>3</sup> J <sub>3-4a</sub> = 4.5	4.13	<sup>3</sup> J <sub>3-2a</sub> = 4.0 <sup>3</sup> J <sub>3-4a</sub> = 4.5 <sup>3</sup> J <sub>3-2e</sub> = 8.5 <sup>3</sup> J <sub>3-4e</sub> = 9.0

<sup>a</sup> The H<sup>4a</sup> signal is a broad dd in the 400MHz <sup>1</sup>H NMR spectra, the long range coupling constant is clearly visible in the H<sup>2a</sup>.



To further extend chemical space of THQ ligands for melatonin receptors, we finally consider the possibility to move the side chain to the *N*-1 THQ position. A new series of THQ melatonin analogues, bearing the amido side chain attached at the *N*-1 position of the THQ nucleus, were synthesized and tested for their affinity for the melatonin receptors. Optimization of the C-2, C-8 substituent and of the side chain led to interesting compounds with different pharmacological profiles in term of affinity, subtype selectivity and functional selectivity. Further details will be omitted, because the obtained results are being evaluated for a possible patent application.

### 1.2.3 Conclusions

In conclusion, three new series of tetrahydroquinoline derivatives were synthesized and tested to extend the chemical space of melatonin receptor ligands. Different ligand-based techniques, such as pharmacophore models, SAR studies and classical isosteric CH/N replacement, were applied to design these new compounds. Thanks to alternative accommodations of the ligands within the binding site, all new synthesized THQs fulfill the pharmacophore requirements for proper receptor binding, with the possibility of modulating, at least partially, both  $MT_2/MT_1$  selectivity and intrinsic activity, through appropriate substitutions on the tetrahydroquinoline ring. The obtained results reinforce our initial hypothesis that the semi-rigid THQ ring possess geometries suitable for decoration with different side chains and it can be considered a good synthetically accessible template for the design of potent MLT receptor ligands with different topology.

## 1.2.4 Experimental Section

### 1.2.4.1 Materials and Methods

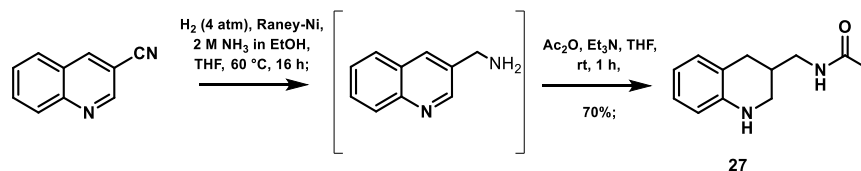
Melting points were determined on a Buchi B-540 capillary melting point apparatus and are uncorrected.  $^1\text{H}$  NMR and  $^{13}\text{C}$  NMR spectra were recorded on a Bruker AVANCE 200 or 400 instrument. Chemical shifts ( $\delta$  scale) are reported in parts per million (ppm) relative to the central peak of the solvent. Coupling constants ( $J$ ) are given in hertz (Hz).  $^1\text{H}$  and  $^{13}\text{C}$  signals were unambiguously assigned by COSY, NOESY, DEPT135, HMQC, and HMBC experiments. EI MS spectra (70 eV) were taken on a Fisons Trio 1000 instrument; only molecular ions ( $\text{M}^+$ ) and base peaks are given. ESI MS spectra were taken on a Waters Micromass ZQ instrument; only molecular ions ( $\text{M}+1$ ) $^+$  or ( $\text{M}-1$ ) $^-$  are given. High-resolution mass spectroscopy was performed on a Micro mass Q-ToF Micromass spectrometer (Micromass, Manchester, UK) using an ESI source. The purity of tested compounds, determined by high performance liquid chromatography (HPLC), was greater than 95%. These analyses were performed on a Waters HPLC/UV/MS system (separation module Alliance HT2795, Photo Diode Array Detector 2996, mass detector Micromass ZQ; software: MassLynx 4.1). Column chromatography purifications were performed under “flash” conditions using Merck 230–400 mesh silica gel. Analytical thin-layer chromatography (TLC) was carried out on Merck silica gel 60 F<sub>254</sub> plates. Chiral HPLC runs were conducted on a Jasco (Cremella, LC, Italy) HPLC system equipped with a Jasco AS-2055 plus autosampler, a PU2089 plus quaternary gradient pump, and an MD-2010 plus multiwavelength detector. Experimental data were acquired and processed by Jasco Borwin PDA and Borwin Chromatograph Software. Solvents used for chiral chromatography were HPLC grade and supplied by Carlo Erba (Milan, Italy). Optical rotation values were measured on a Jasco (Cremella, LC, Italy) photoelectric polarimeter DIP 1000 with a 0.2 dm cell at the sodium D line ( $\lambda = 589$  nm); sample concentration values ( $c$ ) are given in  $10^{-2}$  g mL $^{-1}$ .

### 1.2.4.2 Reagents

3-Quinolinecarbonitrile and 3-aminoquinoline were purchased from commercial suppliers and used without further purification.

### 1.2.4.3 Synthesis and Physicochemical Characterization of THQ MLT Receptor Ligands

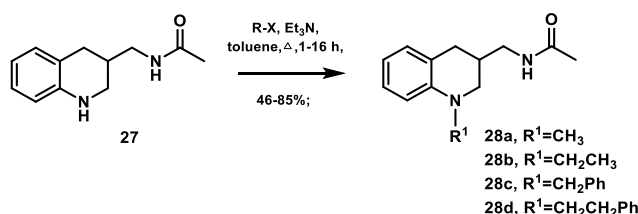
#### (±)-*N*-[(1,2,3,4-Tetrahydroquinolin-3-yl)methyl]acetamide (**27**)



To prepare this compound, quinoline-3-carbonitrile (0.154 g, 1 mmol) was submitted to catalytic hydrogenation (Raney-Ni,  $\text{H}_2$  4 atm, 60 °C, 16 h). The catalyst was filtered on Celite, the filtrate was concentrated *in vacuo*, and the residue was partitioned between EtOAc and water. The organic phase was washed with brine, dried ( $\text{Na}_2\text{SO}_4$ ), and evaporated under reduced pressure to give the corresponding crude oily amine, which was used without any further purification.  $\text{Et}_3\text{N}$  (0.14 mL, 1 mmol) and propionic anhydride (0.13 mL, 1 mmol) were added to a cold solution of the above crude amine in THF (6 mL), and the resulting mixture was stirred at room temperature for 1 h. The solvent was removed by distillation under reduced pressure, and the residue was taken up in EtOAc and washed with a saturated aqueous solution of  $\text{NaHCO}_3$  and then with brine. After drying over  $\text{Na}_2\text{SO}_4$ , the solvent was removed by distillation *in vacuo* to give a crude product that was purified by silica gel flash chromatography (EtOAc–MeOH 95:5 as eluent) and crystallization. White solid, mp 126–7 °C (diethyl ether–petroleum ether), 70% yield.

$^1\text{H}$  NMR (200 MHz,  $\text{CDCl}_3$ ):  $\delta$  6.94–7.02 (m, 2H), 6.63 (dd, 1H,  $J^1 = 1.0$ ,  $J^2 = 7.5$  Hz), 6.49 (d, 1H,  $J = 7.5$  Hz), 5.68 (br s, 1H), 3.83 (br s, 1H), 3.17–3.43 (m, 3H), 3.05 (dd, 1H,  $J^1 = 8.0$ ,  $J^2 = 11.0$  Hz), 2.86 (dd, 1H,  $J^1 = 5.0$ ,  $J^2 = 11.0$  Hz), 2.53 (dd, 1H,  $J^1 = 8.0$ ,  $J^2 = 16.0$  Hz), 2.18–2.23 (m, 1H), 1.98 (s, 3H).  $^{13}\text{C}$  NMR (100 MHz,  $\text{CDCl}_3$ ):  $\delta$  170.4, 144.0, 129.7, 126.9, 120.0, 117.6, 114.3, 44.7, 42.3, 32.5, 30.7, 23.3. EI MS ( $m/z$ ): 204 ( $\text{M}^+$ ), 130 (100). HR MS (ESI):  $m/z$  calculated for  $\text{C}_{12}\text{H}_{16}\text{N}_2\text{O}$ , [ $\text{M} + \text{H}$ ] $^+$ : 205.1341, found: 205.1341.

#### General Procedure for *N*1-Alkylation of *N*-[(1,2,3,4-tetrahydroquinolin-3-yl)methyl]acetamide (**27**): Preparation of compounds **28a-d**



A solution of *N*-[(1,2,3,4-tetrahydroquinolin-3-yl)methyl]acetamide **27** (0.204 g, 1 mmol),  $\text{Et}_3\text{N}$  (0.8 mL, 5.7 mmol), and the suitable alkyl halide (5 mmol) in dry toluene (6 mL) was heated for 1–24 h.

After cooling to room temperature, the reaction mixture was poured into water and extracted with EtOAc (4×), and the combined organic phases were washed with brine and dried (Na<sub>2</sub>SO<sub>4</sub>). The solvent was removed by distillation *in vacuo*, and the residue was purified by silica gel flash chromatography and/or crystallization.

**(±)-N-[(1-Methyl-1,2,3,4-tetrahydroquinolin-3-yl)methyl]acetamide (28a)**

Methyl iodide as alkylating reagent; 70 °C in a sealed vessel for 16 h. Purification by silica gel flash chromatography (EtOAc–cyclohexane 8:2 as eluent) and crystallization. Beige solid, mp 109–10 °C (diethyl ether–petroleum ether), 68% yield.

<sup>1</sup>H NMR (200 MHz, CDCl<sub>3</sub>): δ 7.09 (dd, 1H, *J*<sup>1</sup> = 1.0, *J*<sup>2</sup> = 7.5 Hz), 6.96 (d, 1H, *J* = 7.5 Hz), 6.58–6.66 (m, 2H), 5.63 (br s, 1H), 3.16–3.49 (m, 3H), 2.98 (dd, 1H, *J*<sup>1</sup> = 8.0, *J*<sup>2</sup> = 11.0 Hz), 2.88 (s, 3H), 2.85 (dd, 1H, *J*<sup>1</sup> = 5.0, *J*<sup>2</sup> = 11.0 Hz), 2.54 (dd, 1H, *J*<sup>1</sup> = 8.5, *J*<sup>2</sup> = 16.0 Hz), 2.18–2.34 (m, 1H), 1.99 (s, 3H). <sup>13</sup>C NMR (100 MHz, CDCl<sub>3</sub>): δ 170.3, 145.7, 129.2, 127.3, 121.6, 117.3, 111.6, 54.3, 42.5, 39.5, 32.7, 31.4, 23.3. ESI MS (*m/z*): 219 (M+H)<sup>+</sup>. HR MS (ESI):*m/z* calculated for C<sub>13</sub>H<sub>18</sub>N<sub>2</sub>O, [M + H]<sup>+</sup>: 219.1497, found: 219.1497.

**(±)-N-[(1-Ethyl-1,2,3,4-tetrahydroquinolin-3-yl)methyl]acetamide (28b)**

Ethyl iodide as alkylating reagent; 100 °C in a sealed vessel for 16 h. Purification by silica gel flash chromatography (EtOAc–cyclohexane 8:2 as eluent) and crystallization. Beige solid, mp 84–5 °C (diethyl ether–petroleum ether), 81% yield.

<sup>1</sup>H NMR (200 MHz, CDCl<sub>3</sub>): δ 7.06 (dd, 1H, *J*<sup>1</sup> = 1.5, *J*<sup>2</sup> = 7.5 Hz), 6.96 (d, 1H, *J* = 7.5 Hz), 6.53–6.62 (m, 2H), 5.65 (br s, 1H), 3.13–3.49 (m, 5H), 3.02 (dd, 1H, *J*<sup>1</sup> = 8.0, *J*<sup>2</sup> = 11.0 Hz), 2.83 (dd, 1H, *J*<sup>1</sup> = 5.0, *J*<sup>2</sup> = 16.0 Hz), 2.52 (dd, 1H, *J*<sup>1</sup> = 8.5, *J*<sup>2</sup> = 16.0 Hz), 2.13–2.32 (m, 1H), 1.99 (s, 3H), 1.12 (t, 3H, *J* = 7.0 Hz). <sup>13</sup>C NMR (100 MHz, CDCl<sub>3</sub>): δ 170.4, 144.3, 129.6, 127.3, 120.9, 116.1, 110.8, 51.3, 45.5, 42.5, 32.5, 31.8, 23.3, 10.6. EI MS (*m/z*): 232 (M<sup>+</sup>), 130 (100). HR MS (ESI): *m/z* calculated for C<sub>14</sub>H<sub>20</sub>N<sub>2</sub>O, [M + H]<sup>+</sup>: 233.1654, found: 233.1654.

**(±)-N-[(1-Benzyl-1,2,3,4-tetrahydroquinolin-3-yl)methyl]acetamide (28c)**

Benzyl bromide as alkylating reagent; 1 h under reflux. Purification by silica gel flash chromatography (EtOAc as eluent) and crystallization. White solid, mp 97–8 °C (diethyl ether–petroleum ether); 85% yield.

<sup>1</sup>H NMR (200 MHz, CDCl<sub>3</sub>): δ 7.22–7.37 (m, 5H), 6.97–7.05 (m, 2H), 6.54–6.65 (m, 2H), 5.41 (br s, 1H), 4.56 (d, 1H, *J* = 16.5 Hz), 4.36 (d, 1H, *J* = 16.5 Hz), 3.34 (ddd, 1H, *J*<sup>1</sup> = 1.5, *J*<sup>2</sup> = 3.5, *J*<sup>3</sup> = 11.5 Hz), 3.22–3.30 (m, 2H), 3.12 (ddd, 1H, *J*<sup>1</sup> = 1.0, *J*<sup>2</sup> = 7.5, *J*<sup>3</sup> = 11.0 Hz), 2.92 (dd, 1H, *J*<sup>1</sup> = 5.0, *J*<sup>2</sup> = 15.0 Hz), 2.57 (dd, 1H, *J*<sup>1</sup> = 8.5, *J*<sup>2</sup> = 16.0 Hz), 2.21–2.34 (m, 1H), 1.91 (s, 3H). <sup>13</sup>C NMR (100 MHz,

$CDCl_3$ ):  $\delta$  170.3, 145.1, 138.7, 129.6, 128.7, 127.4, 127.1, 126.9, 120.5, 116.6, 111.2, 55.1, 51.9, 42.1, 32.4, 31.7, 23.3. EI MS (m/z): 294 ( $M^+$ ), 144 (100). HR MS (ESI): m/z calculated for  $C_{19}H_{22}N_2O$ ,  $[M + H]^+$ : 295.1810, found: 295.1810.

**( $\pm$ )-*N*-[(1-Phenylethyl-1,2,3,4-tetrahydroquinolin-3-yl)methyl]acetamide (28d)**

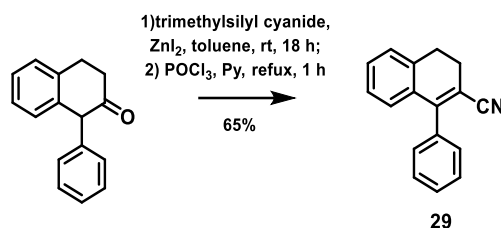
2-Phenylethyl bromide as alkylating reagent; 16 h under reflux. Purification by silica gel flash chromatography (EtOAc as eluent) and crystallization. White solid, mp 123–4 °C ( $CH_2Cl_2$ –petroleum ether); 46% yield.  $^1H$  NMR (200 MHz,  $CDCl_3$ ):  $\delta$  7.19–7.37 (m, 5H), 7.07–7.15 (m, 1H), 6.97 (dd, 1H,  $J^1 = 1.0$ ,  $J^2 = 7.5$  Hz), 6.57–6.70 (m, 2H), 5.22 (br s, 1H), 3.46–3.56 (m, 2H), 3.08–3.18 (m, 3H), 2.77–2.96 (m, 4H), 2.49 (dd, 1H,  $J^1 = 8.0$ ,  $J^2 = 16.0$  Hz), 2.02–2.20 (m, 1H), 1.92 (s, 3H).  $^{13}C$  NMR (100 MHz,  $CDCl_3$ ):  $\delta$  170.2, 144.5, 140.0, 129.6, 129.0, 128.5, 127.3, 126.2, 120.6, 116.1, 110.4, 53.3, 52.6, 42.2, 32.8, 32.3, 31.7, 23.3. ESI MS (m/z): 309 ( $M + H$ ) $^+$ . HR MS (ESI): m/z calculated for  $C_{20}H_{24}N_2O$ ,  $[M + H]^+$ : 309.1967, found: 309.2012.

**( $\pm$ )-*N*-[(1-Phenyl-1,2,3,4-tetrahydroquinolin-3-yl)methyl]acetamide (28e)**

A Schlenk flask was charged with  $Pd(OAc)_2$  (22 mg, 0.1 mmol), ( $\pm$ )-BINAP (60 mg, 0.1 mmol), *t*-BuOK (0.26 g, 2.32 mmol), and **27** (0.204 g, 1 mmol) in dry toluene (2 mL) under nitrogen atmosphere. Bromobenzene (0.2 mL, 2 mmol) was added dropwise via syringe, and the resulting mixture was stirred at 100 °C for 6 h. After cooling to room temperature, the reaction mixture was quenched with water and then extracted twice with  $CH_2Cl_2$ . The combined organic phases were dried over  $Na_2SO_4$  and concentrated by distillation under reduced pressure to yield a crude residue that was purified by silica gel flash chromatography (cyclohexane–EtOAc 3:7 as eluent) and crystallization. White solid, mp 144–5 °C (diethyl ether–petroleum ether); 29% yield.

$^1H$  NMR (400 MHz,  $DMSO-d_6$ ):  $\delta$  7.95 (br t, 1H), 7.01–7.40 (m, 6H), 6.88 (dddd, 1H,  $J^1 = J^2 = 1.5$ ,  $J^3 = J^4 = 8.0$  Hz), 6.65 (dddd, 1H,  $J^1 = J^2 = 1.0$ ,  $J^3 = J^4 = 7.5$  Hz), 6.56 (dd, 1H,  $J^1 = 1.0$ ,  $J^2 = 8.0$  Hz), 3.63 (ddd, 1H,  $J^1 = 1.5$ ,  $J^2 = 3.5$ ,  $J^3 = 11.5$  Hz), 3.25 (dd, 1H,  $J^1 = 9.0$ ,  $J^2 = 11.5$  Hz), 3.13 (dd, 1H,  $J^1 = 6.0$ ,  $J^2 = 13.5$  Hz), 3.06 (dd, 1H,  $J^1 = 6.0$ ,  $J^2 = 13.5$  Hz), 2.84 (ddd, 1H,  $J^1 = 1.5$ ,  $J^2 = 4.5$ ,  $J^3 = 16.0$  Hz), 2.52 (dd, 1H,  $J^1 = 10.0$ ,  $J^2 = 16.0$  Hz), 2.13 (dddddd, 1H,  $J^1 = 3.5$ ,  $J^2 = 4.5$ ,  $J^3 = J^4 = 6.0$ ,  $J^5 = 9.0$ ,  $J^6 = 10.0$  Hz), 1.81 (s, 3H).  $^{13}C$  NMR (100 MHz,  $CDCl_3$ ):  $\delta$  170.3 (CO), 147.9 (C9), 143.8 (C10), 129.8 (C5), 129.5, 126.5 (C7), 124.7, 124.0, 122.4, 118.6 (C6), 115.4 (C8), 53.5 (C4), 42.2 (C11), 33.1 (C3), 31.5 (C2), 23.3 ( $CH_3$ ). EI MS (m/z): 280 ( $M^+$ ), 208 (100). HR MS (ESI): m/z calculated for  $C_{18}H_{20}N_2O$ ,  $[M + H]^+$ : 281.1654, found: 281.1692.

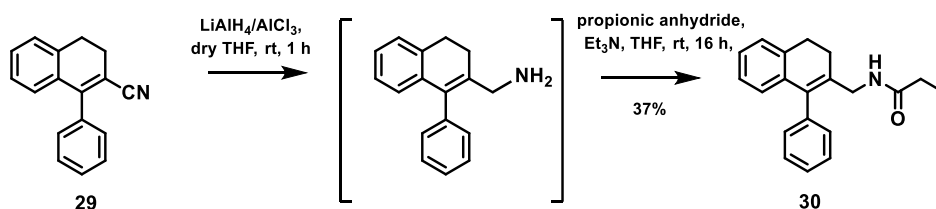
### 1-Phenyl-3,4-dihydronaphthalene-2-carbonitrile (**29**)



A solution of 1-phenyl-3,4-dihydronaphthalen-2(1H)-one (**17**) (1 g, 4.5 mmol), trimethylsilyl cyanide (0.8 mL, 6 mmol), and ZnI<sub>2</sub> (0.038 g, 0.11 mmol) in dry toluene (3.5 mL) was stirred at room temperature for 18 h. Pyridine (6 mL) and afterward POCl<sub>3</sub> (1.3 mL, 14 mmol) were added to the above solution, and the resulting mixture was refluxed for 1 h. After cooling to room temperature, the reaction mixture was poured into 5% HCl/ice, and the aqueous phase was extracted with EtOAc. The combined organic extracts were washed with brine, dried (Na<sub>2</sub>SO<sub>4</sub>), and concentrated under reduced pressure to give a crude residue that was purified by flash chromatography (silica gel, cyclohexane–EtOAc 9:1 as eluent) and crystallization. White solid, mp 81–2 °C (diethyl ether–petroleum ether); 65% yield.

<sup>1</sup>H NMR (200 MHz, CDCl<sub>3</sub>): δ 6.86–7.51 (m, 9H), 2.95–2.99 (m, 2H), 2.64–2.73 (m, 2H). ESI MS (m/z): 232 (M + H)<sup>+</sup>.

### N-[(1-Phenyl-3,4-dihydronaphthalen-2-yl)methyl]propionamide (**30**)

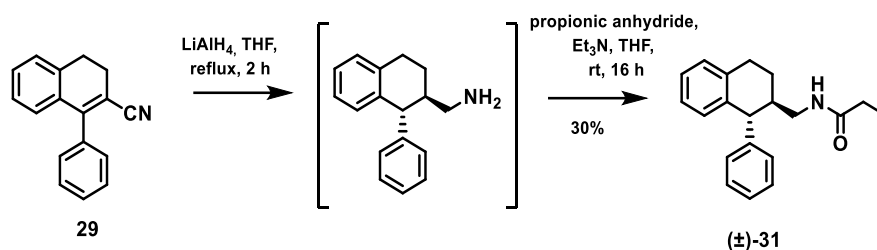


A suspension of aluminum trichloride (0.293 g, 2.2 mmol) in dry THF (2.8 mL) was added to a stirred ice-cooled suspension of LiAlH<sub>4</sub> (0.041 g, 1.1 mmol) in dry THF (1.3 mL) under a nitrogen atmosphere. The mixture was stirred for 10 min, a solution of the nitrile **29** (232 mg, 1.0 mmol) in dry THF (0.9 mL) was then added dropwise, and the resulting mixture was stirred at room temperature for 2 h. Water was carefully added at 0 °C, and the resulting mixture was filtered through a Celite pad. The filtrate was concentrated *in vacuo* and partitioned between water and EtOAc. The combined organic phases were washed with brine, dried (Na<sub>2</sub>SO<sub>4</sub>), and concentrated under reduced pressure to yield the crude desired amine, which was used without any further purification. Et<sub>3</sub>N (0.15 mL, 1.07 mmol) and propionic anhydride (0.136 mL, 1.07 mmol) were added to a stirred solution of the above crude amine in dry THF (12 mL), and the mixture was stirred at room temperature for 16 h. The solvent was evaporated *in vacuo*, and the residue was dissolved in EtOAc. The solution was washed with 2 N NaOH and brine, dried (Na<sub>2</sub>SO<sub>4</sub>), and then concentrated under reduced pressure to give a crude residue that was purified

by flash chromatography (silica gel, cyclohexane–EtOAc 7:3 as eluent) and crystallization. White solid, mp 154–5 °C (EtOAc–petroleum ether); 37% yield.

<sup>1</sup>H NMR (200 MHz, *CDCl*<sub>3</sub>): δ 7.35–7.49 (m, 3H), 7.00–7.19 (m, 5H), 6.61 (dd, 1H, *J*<sup>1</sup> = 1.5, *J*<sup>2</sup> = 7.0 Hz), 5.29 (br t, 1H), 3.91 (d, 2H, *J* = 6.0 Hz), 2.85–2.93 (m, 2H), 2.41–2.49 (m, 2H), 2.19 (q, 2H, *J* = 7.5 Hz), 1.14 (t, 3H, *J* = 7.5 Hz). <sup>13</sup>C NMR (100 MHz, *CDCl*<sub>3</sub>): δ 173.7, 138.5, 136.8, 136.1, 135.3, 133.7, 129.9, 128.6, 127.2, 126.9, 126.2, 126.0, 42.1, 29.8, 28.3, 25.9, 9.9. ESI MS (*m/z*): 292 (*M*+*H*)<sup>+</sup>. HR MS (ESI): *m/z* calculated for C<sub>20</sub>H<sub>21</sub>NO, [*M* + *H*]<sup>+</sup>: 292.1701, found: 292.1715.

**(±)-*trans*-N-[(1-Phenyl-1,2,3,4-tetrahydronaphthalen-2-yl)methyl]propionamide (31)**

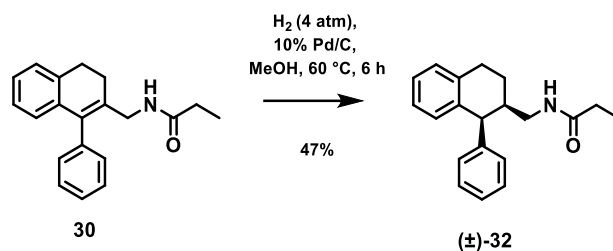


A solution of **29** (0.1 g, 0.43 mmol) in dry THF (1.5 mL) was added dropwise to a stirred ice-cooled suspension of LiAlH<sub>4</sub> (0.035 g, 0.92 mmol) in dry THF (0.5 mL) under nitrogen atmosphere at 0 °C. The reaction mixture was refluxed for 2 h, quenched by water addition at 0 °C, and then filtered on Celite. The filtrate was extracted with EtOAc (3×), and the combined organic phases were dried (Na<sub>2</sub>SO<sub>4</sub>) and concentrated under reduced pressure to give the desired crude corresponding amine. Et<sub>3</sub>N (0.08 mL, 0.57 mmol) and propionic anhydride (0.07 mL, 0.54 mmol) were added to a solution of the above crude amine in THF (5 mL), and the resulting mixture was stirred at room temperature for 16 h. After distillation of the solvent under reduced pressure, the residue was partitioned between EtOAc and 2 N NaOH. The organic layer was washed with brine, dried (Na<sub>2</sub>SO<sub>4</sub>), and concentrated under reduced pressure to give a crude residue which was purified by flash chromatography (silica gel, CH<sub>2</sub>Cl<sub>2</sub>–acetone 95:5 as eluent) and crystallization. White solid, mp 120–1 °C (EtOAc–petroleum ether); 30% yield.

<sup>1</sup>H NMR (400 MHz, *MeOD*): δ 7.27–7.31 (m, 2H), 7.20 (dddd, 1H, *J*<sup>1</sup> = *J*<sup>2</sup> = 1.5, *J*<sup>3</sup> = *J*<sup>4</sup> = 7.5 Hz), 7.06–7.14 (m, 4H), 6.98 (ddd, 1H, *J*<sup>1</sup> = 1.5, *J*<sup>2</sup> = *J*<sup>3</sup> = 8.0 Hz), 6.71 (d, 1H, *J* = 8.0 Hz), 3.84 (d, 1H, *J* = 8.0 Hz), 3.19 (dd, 1H, *J*<sup>1</sup> = 8.0, *J*<sup>2</sup> = 13.5 Hz), 3.14 (dd, 1H, *J*<sup>1</sup> = 5.5, *J*<sup>2</sup> = 13.5 Hz), 2.87–2.99 (m, 2H), 2.17 (q, 2H, *J* = 7.5 Hz), 2.14 (dddd, 1H, *J*<sup>1</sup> = 3.0, *J*<sup>2</sup> = 5.5, *J*<sup>3</sup> = *J*<sup>4</sup> = 8.0, *J*<sup>5</sup> = 9.0 Hz), 2.03 (dddd, 1H, *J*<sup>1</sup> = 3.0, *J*<sup>2</sup> = *J*<sup>3</sup> = 5.5, *J*<sup>4</sup> = 13.5 Hz), 1.57 (dddd, 1H, *J*<sup>1</sup> = 6.5, *J*<sup>2</sup> = 8.5, *J*<sup>3</sup> = 9.0, *J*<sup>4</sup> = 13.5 Hz), 1.11 (t, 3H, *J* = 7.5 Hz). <sup>13</sup>C NMR (100 MHz, *CDCl*<sub>3</sub>): δ 173.8 (CO), 145.8, 139.0, 136.6, 130.2, 129.3, 128.6, 126.5, 125.93, 125.89, 50.7 (C1), 43.7 (C2), 42.8 (C11), 29.6 (C4), 28.8 (CH<sub>2</sub>CH<sub>3</sub>), 26.2 (C3), 9.8 (CH<sub>2</sub>CH<sub>3</sub>). ESI MS (*m/z*): 294 (*M* + 1)<sup>+</sup>. HR MS (ESI): *m/z* calculated for C<sub>20</sub>H<sub>23</sub>NO, [*M* + *H*]<sup>+</sup>: 294.1858, found: 294.1858.



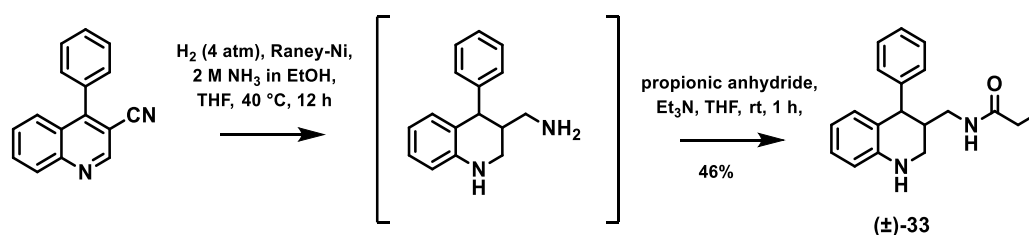
(±)-*cis*-*N*-[(1-Phenyl-1,2,3,4-tetrahydronaphthalen-2-yl)methyl]propionamide (**32**)



A solution of **30** (0.3 g, 1.3 mmol) in MeOH (6 mL) was hydrogenated (4 atm) in the presence of 10% Pd/C for 6 h at 60 °C. The catalyst was removed by filtration on Celite, and the filtrate was evaporated under reduced pressure to afford a crude product that was purified by flash chromatography (silica gel,  $\text{CH}_2\text{Cl}_2$ -acetone 95:5 as eluent) and crystallization. White solid, mp 129–30 °C (diethyl ether–petroleum ether); 47% yield.

$^1\text{H}$  NMR (400 MHz,  $\text{DMSO}-d_6$ ):  $\delta$  7.72 (br t, 1H), 7.15–7.26 (m, 4H), 7.12 (dddd, 1H,  $J^1 = J^2 = 1.5$ ,  $J^3 = J^4 = 7.5$  Hz), 7.03 (dd, 1H,  $J^1 = J^2 = 7.0$  Hz), 6.96–6.98 (m, 2H), 6.85 (d, 1H,  $J = 7.5$  Hz), 4.25 (d, 1H,  $J = 5.0$  Hz), 3.00 (ddd, 1H,  $J^1 = 1.5$ ,  $J^2 = 6.0$ ,  $J^3 = 18.0$  Hz), 2.93 (ddd, 1H,  $J^1 = J^2 = 5.5$ ,  $J^3 = 13.0$  Hz), 2.82 (ddd, 1H,  $J^1 = 6.5$ ,  $J^2 = 11.5$ ,  $J^3 = 18.0$  Hz), 2.54 (ddd, 1H,  $J^1 = J^2 = 6.0$ ,  $J^3 = 13.0$  Hz), 2.05–2.13 (m, 1H), 2.09 (q, 2H,  $J = 7.5$  Hz), 1.68 (dddd, 1H,  $J^1 = 1.5$ ,  $J^2 = 3.5$ ,  $J^3 = 6.5$ ,  $J^4 = 13.5$  Hz), 1.51 (dddd, 1H,  $J^1 = 6.0$ ,  $J^2 = 6.5$ ,  $J^3 = 11.5$ ,  $J^4 = 13.5$  Hz), 0.99 (t, 3H,  $J = 7.5$  Hz).  $^{13}\text{C}$  NMR (100 MHz,  $\text{CDCl}_3$ ):  $\delta$  173.8 (CO), 143.1, 138.8, 136.4, 130.6, 130.0, 128.9, 128.1, 126.5, 126.2, 125.9, 47.9 (C1), 42.8 (C11), 38.8 (C2), 29.7 ( $\text{CH}_2\text{CH}_3$ ), 28.8 (C4), 21.6 (C3), 9.9 ( $\text{CH}_2\text{CH}_3$ ). ESI MS ( $m/z$ ): 294 ( $\text{M} + 1$ )<sup>+</sup>. HR MS (ESI):  $m/z$  calculated for  $\text{C}_{20}\text{H}_{23}\text{NO}$ , [ $\text{M} + \text{H}$ ]<sup>+</sup>: 294.1858, found: 294.1858.

(±)-*N*-[(4-Phenyl-1,2,3,4-tetrahydroquinolin-3-yl)methyl]propionamide (**33**)

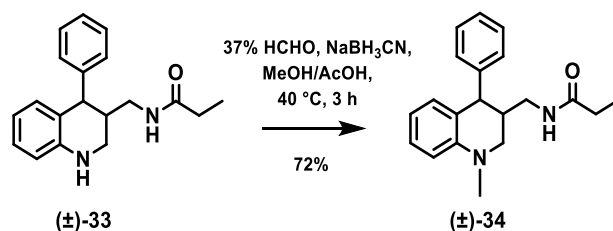


A solution of 4-phenylquinoline-3-carbonitrile (0.230 g, 1 mmol) in THF (5 mL) and 2 M  $\text{NH}_3$  in EtOH (0.6 mL) was hydrogenated (4 atm) over Raney-Ni for 16 h at 60 °C. The catalyst was filtered on Celite, the filtrate was concentrated *in vacuo*, and the residue was partitioned between EtOAc and water. The organic phase was washed with brine, dried ( $\text{Na}_2\text{SO}_4$ ), and evaporated under reduced pressure to give the corresponding crude oily amine, which was used without any further purification.  $\text{Et}_3\text{N}$  (0.14 mL, 1 mmol) and propionic anhydride (0.13 mL, 1 mmol) were added to a cold solution of the above crude amine in THF (6 mL), and the resulting mixture was stirred at room temperature for 1 h. The solvent was removed by distillation under reduced pressure, and the residue was taken up in EtOAc and washed

with a saturated aqueous solution of NaHCO<sub>3</sub> and then with brine. After drying over Na<sub>2</sub>SO<sub>4</sub>, the solvent was removed by distillation *in vacuo* to give a crude product that was purified by silica gel flash chromatography (EtOAc–MeOH 98:2 as eluent) and crystallization. White solid (CHCl<sub>3</sub>–hexane); 46% yield.

<sup>1</sup>H NMR (400 MHz, *acetone-d*<sub>6</sub>): δ 7.25–7.29 (m, 2H), 7.14–7.21 (m, 3H), 7.00 (br s, 1H), 6.93 (ddd, 1H, *J*<sup>1</sup> = 1.5, *J*<sup>2</sup> = *J*<sup>3</sup> = 8.0 Hz), 6.78 (dd, 1H, *J*<sup>1</sup> = 1.0, *J*<sup>2</sup> = 7.5 Hz), 6.63 (dd, 1H, *J*<sup>1</sup> = 1.0, *J*<sup>2</sup> = 8.0 Hz), 5.27 (br s, 1H), 4.16 (d, 1H, *J* = 4.5), 3.29 (dddd, 1H, *J*<sup>1</sup> = 1.0, *J*<sup>2</sup> = *J*<sup>3</sup> = 4.0, *J*<sup>4</sup> = 11.5 Hz), 3.16 (ddd, 1H, *J*<sup>1</sup> = *J*<sup>2</sup> = 5.5, *J*<sup>3</sup> = 14.0 Hz), 3.05 (ddd, 1H, *J*<sup>1</sup> = 3.0, *J*<sup>2</sup> = *J*<sup>3</sup> = 11.5 Hz), 2.71 (ddd, 1H, *J*<sup>1</sup> = 6.0, *J*<sup>2</sup> = 9.0, *J*<sup>3</sup> = 14.0 Hz), 2.28–2.36 (m, 1H), 2.15 (q, 2H, *J* = 7.5 Hz), 1.05 (t, 3H, *J* = 7.5 Hz). ESI MS (*m/z*): 295 (M + H)<sup>+</sup>.

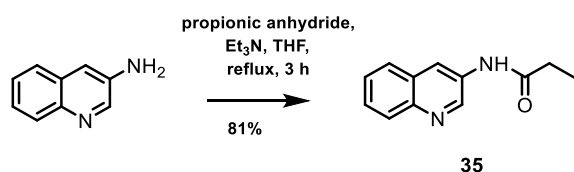
**(±)-*cis*-N-[(1-Methyl-4-phenyl-1,2,3,4-tetrahydroquinolin-3-yl)methyl]propionamide (34)**



Sodium cyanoborohydride (0.1 g, 1.20 mmol) and a 37% aqueous solution of HCHO (0.5 mL) were added to a solution of **33** (0.5 mmol), in MeOH (5 mL) and AcOH (to pH = 5). The resulting mixture was stirred at room temperature for 1 h and then at 40 °C for 3 h. A 30% NaOH aqueous solution was added, and the aqueous phase was extracted with EtOAc. After drying over Na<sub>2</sub>SO<sub>4</sub>, the combined organic layers were concentrated by distillation under reduced pressure to give a crude residue, which was purified by silica gel flash chromatography (cyclohexane–EtOAc 6:4 as eluent) and crystallization. White solid, mp 167–8 °C (EtOAc–petroleum ether); 72% yield.

<sup>1</sup>H NMR (400 MHz, DMSO-*d*<sub>6</sub>): δ 7.76 (br t, 1H), 7.23–7.27 (m, 2H), 7.16–7.19 (m, 1H), 7.05 (ddd, 1H, *J*<sup>1</sup> = 1.5, *J*<sup>2</sup> = 7.5, *J*<sup>3</sup> = 8.0 Hz), 6.98–7.00 (m, 2H), 6.78 (dd, 1H, *J*<sup>1</sup> = 1.5, *J*<sup>2</sup> = 7.5 Hz), 6.70 (d, 1H, *J* = 8.0 Hz), 6.47 (ddd, 1H, *J*<sup>1</sup> = 1.0, *J*<sup>2</sup> = *J*<sup>3</sup> = 7.5 Hz), 4.13 (dd, 1H, *J*<sup>1</sup> = 1.0, *J*<sup>2</sup> = 4.5 Hz), 3.10 (ddd, 1H, *J*<sup>1</sup> = 1.0, *J*<sup>2</sup> = 4.0, *J*<sup>3</sup> = 11.5 Hz), 2.96 (dd, 1H, *J*<sup>1</sup> = 5 Hz, *J*<sup>2</sup> = n.c.), 2.95 (s, 3H), 2.93 (dd, 1H, *J*<sup>1</sup> = *J*<sup>2</sup> = 11.5 Hz), 2.52 (dd, 1H, *J*<sup>1</sup> = 9.0 Hz, *J*<sup>2</sup> = n.c.), 2.28 (dddd, 1H, *J*<sup>1</sup> = 4.0, *J*<sup>2</sup> = 4.5, *J*<sup>3</sup> = 5.0, *J*<sup>4</sup> = 9.0, *J*<sup>5</sup> = 11.5 Hz), 2.09 (q, 2H, *J* = 8.0 Hz), 0.99 (t, 3H, *J* = 8.0 Hz). <sup>13</sup>C NMR (100 MHz, *MeOD*): δ 175.7 (CO), 145.9 (C9), 142.5 (C10), 129.54 (C5), 129.47, 127.5, 127.4 (C7), 126.0, 124.5, 116.0 (C6), 110.6 (C8), 49.4 (C11), 46.2 (C4), 40.5 (C2), 37.8 (NCH<sub>3</sub>), 36.7 (C3), 28.7 (CH<sub>2</sub>CH<sub>3</sub>), 9.1 (CH<sub>2</sub>CH<sub>3</sub>). ESI MS (*m/z*): 309 (M + H)<sup>+</sup>. HR MS (ESI): *m/z* calculated for C<sub>20</sub>H<sub>24</sub>N<sub>2</sub>O, [M + H]<sup>+</sup>: 309.1967, found: 309.1967.

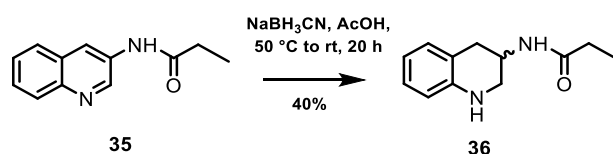
### *N*-(Quinolin-3-yl)propionamide (**35**)



A solution of 3-aminoquinoline (1 g, 7 mmol), Et<sub>3</sub>N (1.53 mL, 11 mmol) and propionic anhydride (0.9 mL, 7 mmol) in THF (30 mL) was heated at reflux for 3 h. After removing the solvent by distillation under reduced pressure, the residue was taken up in CH<sub>2</sub>Cl<sub>2</sub>, washed twice with 2N NaOH, once with brine and dried (Na<sub>2</sub>SO<sub>4</sub>). The solvent was removed under reduced pressure and the crude residue was purified by crystallization. White solid, mp 167–8 °C (CH<sub>2</sub>Cl<sub>2</sub>-petroleum ether); 81% yield.

<sup>1</sup>H NMR (200 MHz, DMSO-*d*<sub>6</sub>): δ 10.57 (s, 1H), 8.92 (s, 1H), 8.70 (s, 1H), 7.86–7.95 (m, 2H), 7.50–7.65 (m, 2H), 2.43 (q, 2H, *J* = 7.5 Hz), 1.12 (t, 3H, *J* = 7.5 Hz). EI MS (*m/z*): 200 (M<sup>+</sup>), 144 (100).

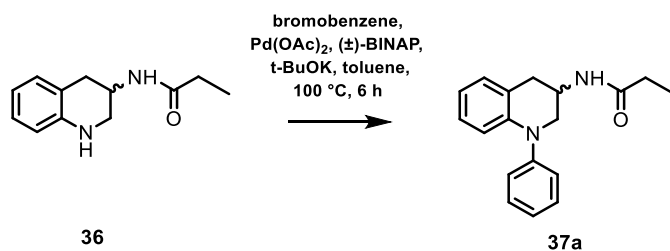
### (±)-*N*-(1,2,3,4-Tetrahydroquinolin-3-yl)propionamide (**36**)<sup>33</sup>



NaBH<sub>3</sub>CN (0.265 g, 4.2 mmol) was added portion wise during 5 min to a solution of *N*-(quinolin-3-yl)propionamide **35** (0.2 g, 1 mmol) in AcOH (3 mL), and the resulting mixture was stirred at room temperature for 1 h, at 50 °C for 1 h, and finally at room temperature for 18 h. The reaction mixture was quenched with water and adjusted to pH 11 by adding 30% NaOH, and the aqueous phase was extracted with CH<sub>2</sub>Cl<sub>2</sub> (3×). The combined organic layers were dried (Na<sub>2</sub>SO<sub>4</sub>) and concentrated under reduced pressure to afford a crude residue, which was purified by silica gel flash chromatography (CH<sub>2</sub>Cl<sub>2</sub>-EtOAc 6:4 as eluent) and crystallization. White solid, mp 90–1 °C (diethyl ether-petroleum ether); 40% yield.

<sup>1</sup>H NMR (200 MHz, CDCl<sub>3</sub>): δ 6.96–7.08, (m, 2H), 6.69 (ddd, 1H, *J*<sup>1</sup> = 1.0, *J*<sup>2</sup> = *J*<sup>3</sup> = 7.5 Hz), 6.55 (dd, 1H, *J*<sup>1</sup> = 1.0, *J*<sup>2</sup> = 8.0 Hz), 5.95 (br s, 1H), 4.44–4.56 (m, 1H), 3.94 (br s, 1H), 3.39 (dd, 1H, *J*<sup>1</sup> = 2.5, *J*<sup>2</sup> = 11.5 Hz), 3.22 (ddd, 1H, *J*<sup>1</sup> = 2.0, *J*<sup>2</sup> = 4.0, *J*<sup>3</sup> = 11.5 Hz), 3.08 (dd, 1H, *J*<sup>1</sup> = 5.0, *J*<sup>2</sup> = 16.5 Hz), 2.74 (ddd, 1H, *J*<sup>1</sup> = 2.0, *J*<sup>2</sup> = 3.5, *J*<sup>3</sup> = 16.5 Hz), 2.17 (q, 2H, *J* = 7.5 Hz), 1.12 (t, 3H, *J* = 7.5 Hz). EI MS (*m/z*): 204 (M<sup>+</sup>), 130 (100).

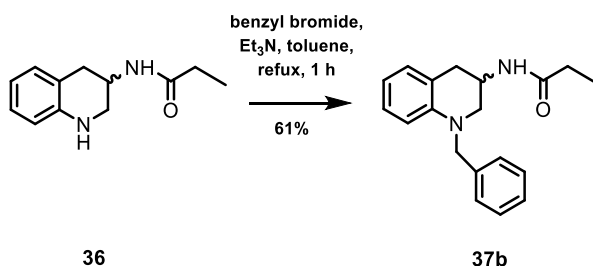
**(±)-N-(1-Phenyl-1,2,3,4-tetrahydroquinolin-3-yl)propionamide (37a)**



A Schlenk flask was charged with Pd(OAc)<sub>2</sub> (22 mg, 0.1 mmol), (±)-BINAP (60 mg, 0.1 mmol), *t*-BuOK (0.26 g, 2.32 mmol), and **36** (0.204 g, 1 mmol) in dry toluene (2 mL) under nitrogen atmosphere. Bromobenzene (0.2 mL, 2 mmol) was added dropwise via syringe, and the resulting mixture was stirred at 100 °C for 6 h. After cooling to room temperature, the reaction mixture was quenched with water and then extracted twice with CH<sub>2</sub>Cl<sub>2</sub>. The combined organic phases were dried over Na<sub>2</sub>SO<sub>4</sub> and concentrated by distillation under reduced pressure to yield a crude residue that was purified by silica gel flash chromatography (cyclohexane–EtOAc 3:7 as eluent) and crystallization. Beige solid, mp 163–4 °C (CH<sub>2</sub>Cl<sub>2</sub>–petroleum ether); 46% yield.

<sup>1</sup>H NMR (200 MHz, CDCl<sub>3</sub>): δ 6.94–7.44 (m, 7H), 6.71–6.80 (m, 2H), 5.79 (br s, 1H), 4.53–4.63 (m, 1H), 3.76 (dd, 1H, *J*<sup>1</sup> = 2.5, *J*<sup>2</sup> = 11.5 Hz), 3.59 (ddd, 1H, *J*<sup>1</sup> = 2.0, *J*<sup>2</sup> = 4.5, *J*<sup>3</sup> = 11.5 Hz), 3.22 (dd, 1H, *J*<sup>1</sup> = 5.5, *J*<sup>2</sup> = 16.5 Hz), 2.83 (ddd, 1H, *J*<sup>1</sup> = 2.0, *J*<sup>2</sup> = 3.5, *J*<sup>3</sup> = 16.5 Hz), 2.14 (q, 2H, *J* = 7.5 Hz), 1.09 (t, 3H, *J* = 7.5 Hz). <sup>13</sup>C NMR (100 MHz, CDCl<sub>3</sub>): δ 173.3, 147.4, 143.9, 130.5, 129.7, 126.9, 125.2, 124.7, 120.3, 118.9, 115.1, 54.0, 42.7, 33.4, 29.7, 9.7. EI MS (*m/z*): 280 (M<sup>+</sup>), 206 (100). HR MS (ESI): *m/z* calculated for C<sub>18</sub>H<sub>20</sub>N<sub>2</sub>O, [M + H]<sup>+</sup>: 281.1654, found: 281.1631.

**(±)-N-(1-Benzyl-1,2,3,4-tetrahydroquinolin-3-yl)propionamide (37b)**



A solution of **36** (0.204 g, 1 mmol), Et<sub>3</sub>N (0.8 mL, 5.7 mmol), and benzyl bromide (5 mmol) in dry toluene (6 mL) was heated for 1 h under reflux. After cooling to room temperature, the reaction mixture was poured into water, extracted with EtOAc (4×), and the combined organic phases were washed with brine and dried (Na<sub>2</sub>SO<sub>4</sub>). The solvent was removed by distillation *in vacuo*, and the residue was purified by silica gel flash chromatography (cyclohexane–EtOAc 3:7 as eluent) and crystallization. Beige solid, mp 132–3 °C (CH<sub>2</sub>Cl<sub>2</sub>–petroleum ether); yield 61%.

$^1\text{H}$  NMR (400 MHz,  $\text{DMSO-}d_6$ ):  $\delta$  7.77 (d, 1H,  $J = 7.5$  Hz), 7.20–7.34 (m, 5H), 6.90–6.95 (m, 2H), 6.50–6.53 (m, 2H), 4.53 (d, 1H,  $J = 17.0$  Hz), 4.43 (d, 1H,  $J = 17.0$  Hz), 4.13 (dddd, 1H,  $J^1 = 4.0$ ,  $J^2 = 4.5$ ,  $J^3 = 8.5$ ,  $J^4 = 9.0$  Hz), 3.40 (ddd, 1H,  $J^1 = 1.5$ ,  $J^2 = 4.0$ ,  $J^3 = 11.0$  Hz), 3.17 (dd, 1H,  $J^1 = 8.5$ ,  $J^2 = 11.0$  Hz), 2.93 (ddd, 1H,  $J^1 = 1.5$ ,  $J^2 = 4.5$ ,  $J^3 = 15.5$  Hz), 2.69 (dd, 1H,  $J^1 = 9.0$ ,  $J^2 = 15.5$  Hz), 2.10 (q, 2H,  $J = 7.5$  Hz), 0.99 (t, 3H,  $J = 7.5$  Hz).  $^{13}\text{C}$  NMR (100 MHz,  $\text{CDCl}_3$ ):  $\delta$  173.4 (CO), 144.6, 138.3, 130.4, 128.7, 127.7, 127.1, 126.8, 118.6, 117.1, 111.5, 54.9 (C3), 53.2 (C2), 41.9 ( $\text{CH}_2\text{Ph}$ ), 33.5 (C4), 29.7 ( $\text{CH}_2\text{CH}_3$ ), 9.7 ( $\text{CH}_2\text{CH}_3$ ). EI MS ( $m/z$ ): 294 ( $\text{M}^+$ ), 220 (100). HRMS (ESI):  $m/z$  calculated for  $\text{C}_{19}\text{H}_{22}\text{N}_2\text{O}$ ,  $[\text{M} + \text{H}]^+$ : 295.1810, found: 295.1810.

## **1.3 Dual-acting Melatoninergetic Derivatives: Design, Synthesis and Pharmacological Investigations**

### 1.3.1 Introduction and Aim of the Work

Multitargeting compounds, able to simultaneously modulate more than a single biological target, have gained remarkable relevance in drug discovery owing to the complexity of multifactorial diseases such as cancer, inflammation, psychiatric and degenerative CNS disorders, or the metabolic syndrome. Indeed, the high therapeutic success of many drugs in clinical use, such as acetyl salicylic acid, paracetamol, metformin or statins, is ascribed to their pleiotropic activities on multiple targets. The emerging field of systems or network biology, which considers the description of the complex interactions between the molecular constituents of a living cell, is further stimulating modern drug discovery to intentionally design small molecule drugs with defined multitarget activity.

Multifunctional molecules may have a number of advantages over a “combination of single-target drugs”, or a “single-pill drug combination”, including better distribution in the target tissue, decreased pharmacokinetic complexity, fewer drug-drug interactions, lower risk of toxicity, improved patient compliance and tolerance and lower risk of target-based drug resistance due to modulation of a few targets. Furthermore, multitarget drug discovery also offers economic advantages because the clinical development of a single multitarget drug requires less clinical trials than multiple specific drugs, and can be also a base of drug repurposing. However, it is not easy to design potent multitargeting compounds and problems arise starting from a proper target selection through affinity balancing to avoid affinity to related off-targets.

Classical approaches to design multi-target agents involve three different ways of combination of two pharmacophores (Figure 15): linkage, fusion, and incorporation.

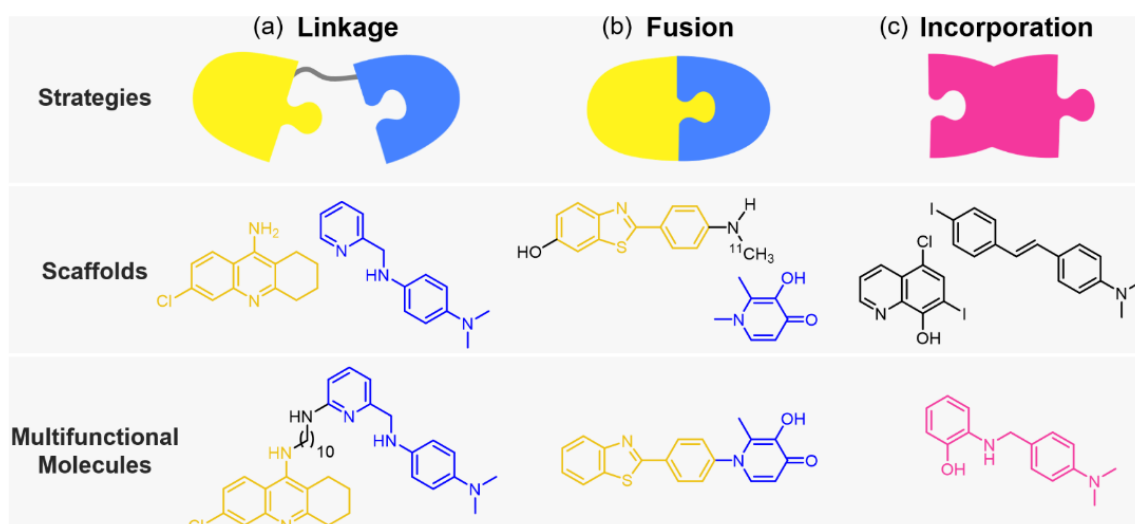


Figure 15 (taken from ref 35) Multitarget agents can arise from linking pharmacophores with stable or biodegradable linkers, fusing of pharmacophores, or merging of pharmacophores for the biological targets of interest

The simplest way to develop this kind of molecules is the pharmacophore connection of two (or more) distinct targets with a stable or biodegradable linker. The length, regiochemistry (site of

attachment), and composition of linkers are crucial optimization tasks to ensure that the original scaffolds retain their activity. For example, the linker cannot join a scaffold at a position that would prevent it from binding to its target. The linker itself may also interact with the target; thus, its chemical properties need to be tailored in order to maximize interactions between the linker and the target.

The fusion approach is basically an extension of the linkage approach with a linker length of zero, such that the two bioactive small molecules addressing two targets are directly joined to one another.

The most elegant way of designing small multifunctional molecules is the incorporation approach, in which the key pharmacophore features required to interact with the targets of interest are combined in one merged pharmacophore. To allow such pharmacophore merging, a certain overlap in the pharmacophores of the individual targets is required. These types of molecules are most favorable in terms of drug-likeness but are the least likely to retain function.

Interesting multifunctional molecules that bind to more than one biological target have recently been described also in the MLT field. A good example is the recently marketed drug agomelatine (Valdoxan/ Thymanax), a potent agonist at melatonin receptors and an antagonist at 5-HT<sub>2C</sub> serotonin receptor, which elicited antidepressant activity with a relatively mild side-effect profile as well as positive effects on sleep.<sup>36</sup> Recently, different series of dual-acting compounds, constituted by melatonin linked to another known neuroprotective agent have been reported as novel potential therapeutic agents for the treatment of neurodegenerative disorders such as Parkinson's and Alzheimer's diseases. Examples of these compounds are shown in Figure 16, including melatonin-tacrine hybrid with potent anticholinesterase and antioxidant activity,<sup>37</sup> melatonin-*N,N*-dibenzyl(*N*-methyl)amine hybrids and melatonin-curcumin dual-acting compound.<sup>38,39</sup>

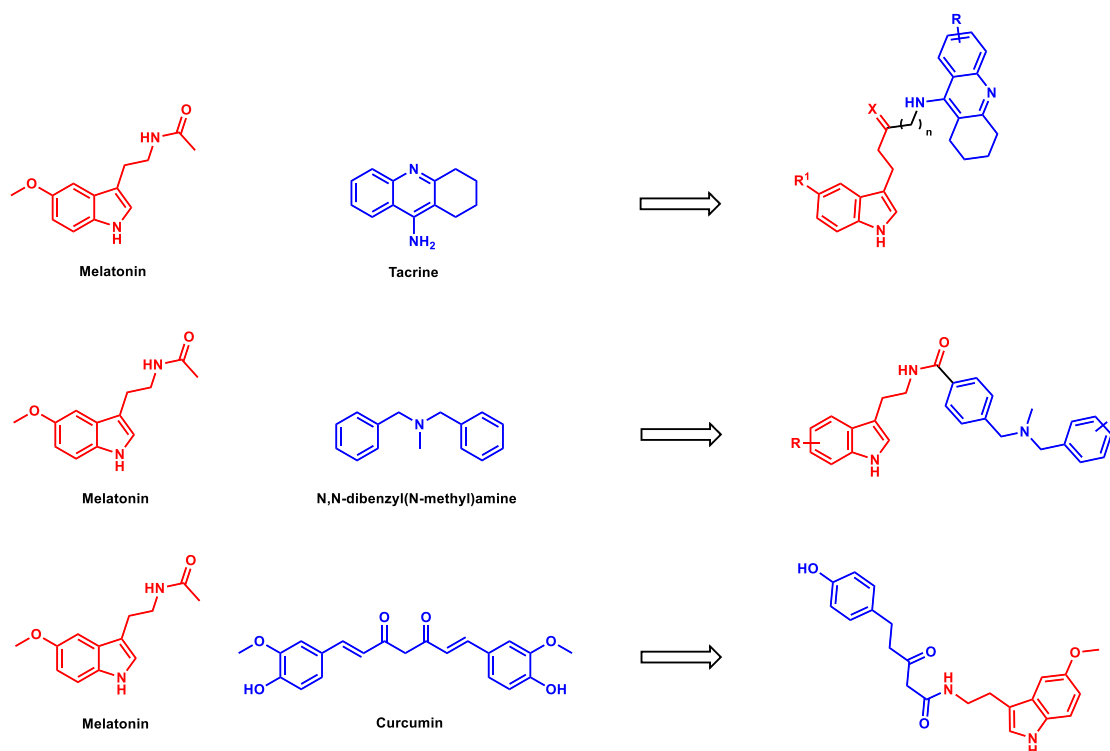




Figure 16 Structures of previously reported melatonin dual-target compounds

To further improve the therapeutic opportunities of MLT derivatives, during my PhD program, I also investigated the possibility to develop multi-target compounds. In particular, we are interested to combine in a single multifunctional agent agonism at the MT<sub>1</sub> melatonin receptor with the ability to enhance endocannabinoid neurotransmission, by inhibiting the activity of the Fatty acid amide hydrolase (FAAH), an integral membrane enzyme involved in the hydrolytic inactivation of the endocannabinoid anandamide (Figure 17).

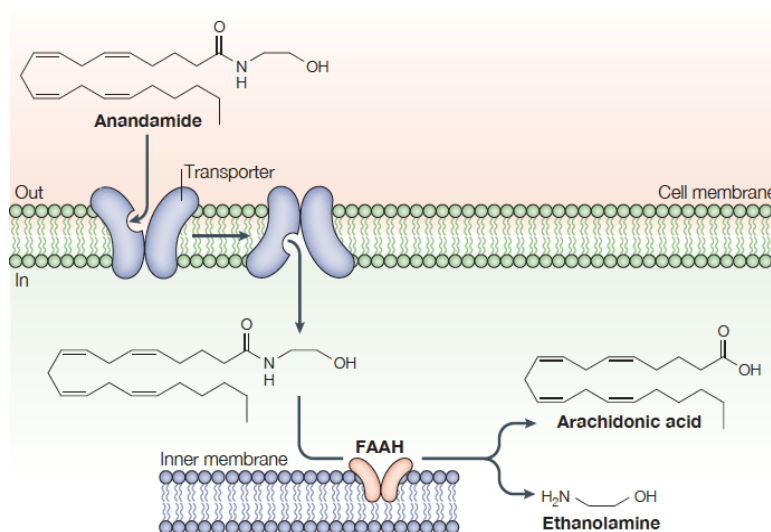


Figure 17 (taken from ref 40)

Activation of MLT receptors and inhibition of FAAH have both shown potential benefits for the treatment of different diseases, such as depression, neurodegenerative CNS disorders, pain and glaucoma.<sup>41,42,43,44</sup>

Glaucoma is a multifactorial disease characterized by progressive optic nerve injury and visual field defects. Elevated intraocular pressure (IOP) is the most widely recognized risk factor for the onset and progression of glaucoma, and IOP-lowering medications represent the primary treatment strategy. Currently, the five most used pharmacologic classes of IOP-lowering drugs are  $\alpha_2$ -adrenergic receptor agonists (e.g. brimonidine),  $\beta$ -adrenergic antagonists (e.g. timolol), carbonic anhydrase inhibitors (e.g. dorzolamide), cholinergic agonists (e.g. pilocarpine, carbachol) and prostaglandin analogs (e.g. latanoprost, travoprost, bimatoprost).

Despite the availability of several active principles and their combinations, the search for new IOP lowering agents is highly active and aims at developing more potent compounds endowed with more persistent action and lower side effects compared to currently available drugs. Currently, the focus of

new glaucoma medical treatments is on novel targets for increasing aqueous humor outflow and/or suppressing aqueous inflow.

In the search of new compounds for the treatment of glaucoma, MLT has been tested as a natural compound with potential ocular hypotensive effects and interesting neuroprotective actions.<sup>9</sup> As aforementioned, MLT is produced not only by the pineal gland, but also by several ocular structures, and its receptors have been identified in different areas, such as in the retina, ciliary body, cornea, lens, and sclera,<sup>45</sup> justifying the hypothesis that MLT may be involved in the regulation of IOP. Indeed, topical and systemic administration of melatonin has been shown to transiently reduce IOP in normotensive and hypertensive/glaucomatous animals, such as mice,<sup>46</sup> rabbits,<sup>47</sup> and monkeys,<sup>48</sup> as well as in humans.<sup>49,50</sup> MLT potentiates the IOP lowering effect exerted by the adrenergic system, as it increases expression of the  $\alpha_2$ - and reduces expression of the  $\beta_2$ -adrenergic receptors that control the synthesis and drainage of aqueous humor in ciliary nonpigmented epithelium.<sup>51</sup> Besides the natural ligand, synthetic MLT receptor agents such as agomelatine,<sup>46</sup> 5-MCA-NAT<sup>52</sup> and IIK7<sup>48</sup> have shown IOP lowering effects.

Reduction of IOP is also a well-known effect observed in cannabis users.<sup>53</sup> The presence of a functional endocannabinoid system in the retina, which includes endogenous cannabinoids, enzymes involved in their synthesis and deactivation, and cannabinoid receptors, supports a role for cannabinoids in retinal circuitry and vision.<sup>54</sup> More recently, reduction of IOP has been observed after administration of endogenous or exogenous cannabinoids, such as  $\Delta^9$ -tetrahydrocannabinol, the main active principle of cannabis, the synthetic cannabinoid CB<sub>1</sub> and CB<sub>2</sub> receptor agonist WIN55212-2, and the endocannabinoid anandamide (AEA) in studies performed in animals and humans.<sup>42</sup>

Collectively, the findings outlined above suggest that both melatonin and endocannabinoid systems might contribute to the regulation of IOP through modulation of specific mechanisms.

One of the main objectives of my PhD thesis was the design and development of novel dual-acting compounds that activate MLT receptors and inhibit FAAH potentially able to exert IOP lowering activity with mutual benefits.

To design these compounds we started from previously developed chemical classes of FAAH inhibitors and MT<sub>1</sub> ligands. Among the previously reported MLT receptor ligands, the class of anilinoethylamides (Figure 18) has proved to be one of the most interesting and versatile.<sup>55</sup> These compounds showed a generally good affinity for MLT receptors and, particularly, the possibility to be derivatized, giving predictable modulation of selectivity and intrinsic activity. In particular, in this class an increase in the size of the substituent on the nitrogen atom shifts the activity from that of a nonselective full agonist (e.g., a methyl group: UCM 793) to an MT<sub>2</sub>-selective partial agonist for the phenyl derivative (UCM765), to a very selective MT<sub>2</sub> antagonist in the case of the naphthyl derivative

(UCM800).<sup>55</sup> Furthermore, the introduction of a bulky lipophilic group on the oxygen atom of the aniline scaffold provided a compound (UCM871) with modest selectivity for the MT<sub>1</sub> receptor.<sup>23</sup>

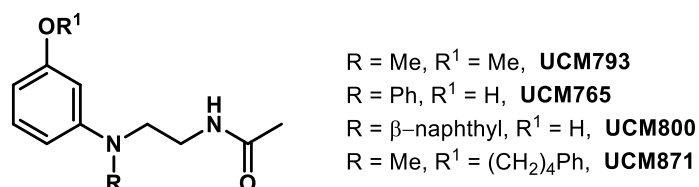


*Figure 18 Anilinoethylamides*

To propose an explanation for the observed MT<sub>1</sub> selectivity shown by UCM871, some years ago Rivara and coll. built a 3D homology model of the MT<sub>1</sub> receptor based on the 3D structure of the active form of the adrenergic β<sub>2</sub> receptor.<sup>24</sup> In the proposed model, within the receptor binding site there is an accessory lipophilic pocket, mainly defined by the transmembrane helices TM3 and TM4, where the phenylbutyloxy group of compound UCM871, and in general a bulky lipophilic substituent, could be accommodated. Selectivity for the MT<sub>1</sub> receptor should come from the fact that the analogue MT<sub>2</sub> binding site region has some bulkier amino acid residues, replacing Val, Leu and Gly in the MT<sub>1</sub> pocket, thus hampering the proper accommodation of the ligand.

Different classes of compounds are known to increase intracellular anandamide levels through FAAH inhibition, including carbamates<sup>56,57,58</sup> and piperidine/ piperazine ureas<sup>59,60,61</sup> that covalently bind to FAAH,<sup>62</sup> and  $\alpha$ - ketoheterocycle derivatives,<sup>63,64,65,66,67</sup> which inhibit FAAH by reversible hemiketal formation with the catalytic serine of the enzyme.<sup>68</sup> Among them, the *N*-alkyl-*O*-arylcarbamates URB597<sup>69</sup> and URB694<sup>70</sup> (Figure 19) have been extensively investigated.<sup>71,72,73,74</sup> URB597 (IC<sub>50</sub> = 4.6 nM) was shown to inhibit FAAH in the nanomolar range and was devoid of activity in a panel of receptors (e.g., CB<sub>1</sub>/CB<sub>2</sub>, NOP1 receptor), ion channels (e.g., Na<sup>+</sup>, K<sup>+</sup>, and Ca<sup>2+</sup> channels), transporters (e.g., AEA transporter), and enzymes (e.g., COX1/2 and MAGL) at 10  $\mu$ M.<sup>75</sup> It has been broadly used preclinically to explore the functions of FAAH, and has been advanced to clinical testing.

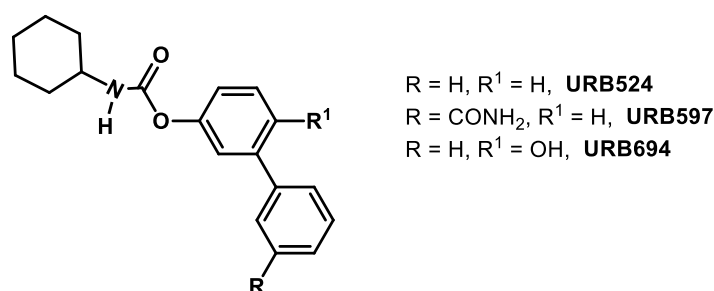


Figure 19 *N*-alkyl-*O*-arylcarbamates

FAAH is an integral membrane-bound enzyme belonging to the serine hydrolase family.<sup>76</sup> Crystal structures of FAAH show that the enzyme is a homodimer in solution, and its active site is characterized by an atypical catalytic triad, consisting of Ser<sup>241</sup>–Ser<sup>217</sup>–Lys<sup>142</sup>. The binding site of FAAH comprises three functional channels: the membrane access channel (MAC), the acyl-chain binding channel (ACB), and the cytosolic port (CP) providing the accommodation of the acyl chain during catalysis, and removing the leaving group after hydrolysis, respectively.<sup>77</sup> Several studies, including computational modeling,<sup>78,79,80,81</sup> supported by the resolution of the crystal structure of humanized rat FAAH in complex with URB597,<sup>82</sup> indicate that *O*-arylcarbamates bind covalently to FAAH and cause its irreversible inhibition. In particular, it has been seen that Ser<sup>241</sup> attacks the carbonyl group of these compounds, leading to the formation of carbamoylated, catalytically inactive FAAH and releasing the *O*-biphenyl moiety as the leaving group (Figure 20).

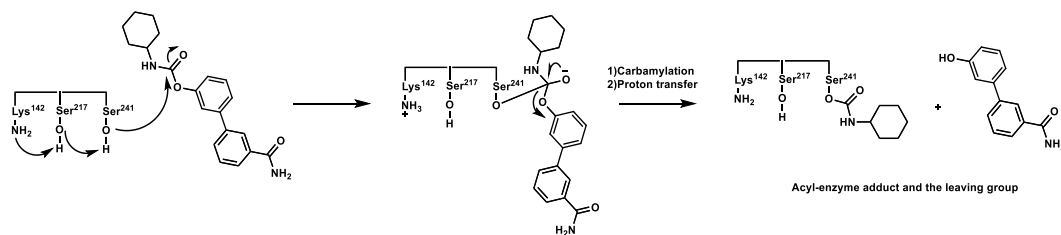


Figure 20 FAAH inhibition mechanism operated by *O*-arylcarbamates

Docking studies performed using URB597 crystal structure and rat FAAH illustrated that the rotatable *N*-cyclohexyl ring occupied the ACB channel. Adjacent to the cyclohexyl group, the carbamate group was confirmed to form a covalent bond with Ser<sup>241</sup>, while the hydroxybiphenyl moiety, which serves as a leaving group, was located in the cytoplasmic access channel and oriented to the other monomer.

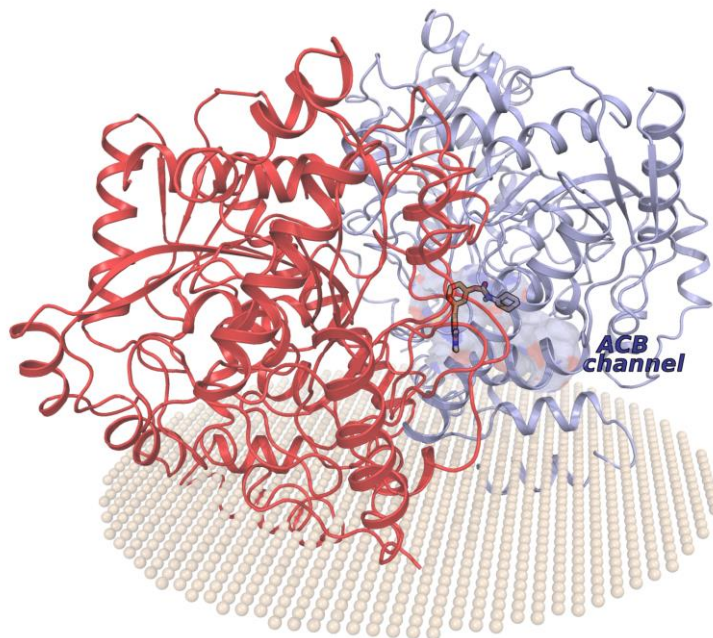


Fig. 21 Docking studies of rat FAAH bound to an irreversible inhibitor

All the above cited observations suggest that both in the MT<sub>1</sub> receptor and in the active site of FAAH there are zones of steric tolerance, allowing the inclusion of pharmacophore elements for both FAAH inhibition and melatonin receptor binding. Therefore, we consider the possibility to join the pharmacophores of anilinoethylamide and *N*-alkyl-*O*-arylcarbamates through an appropriate linker.

We devised therefore two new series of *N*-anilinoethylamide derivatives carrying on the aniline ring an alkoxy linker bound to a carbamoyl portion, intended to exert FAAH inhibition (Figure 22). In one series, the *N*-cyclohexyl-*O*-phenylcarbamate portion was joined to the aniline *O*-alkyl side chain through a second bridging oxygen atom, while in the second one, the cyclohexyl substituent of URB597 was replaced by the aniline *O*-alkyl chain, as known structure–activity relationships for *O*-aryl-*N*-alkyl carbamates had evidenced that a linear alkyl chain is tolerated without significantly affecting FAAH inhibitory potency.<sup>57</sup> In an attempt to improve the potency and obtain compounds with similar activity on the two targets, we also evaluated the effects of the length of the spacer, of the introduction of smaller polar group at the 3' position of the biphenyl nucleus or the replacement of the acetylamino group with a propionylamino one at the melatonineric portion. Indeed, increases in the FAAH inhibitory potency and melatonin binding affinity have been observed by introducing hydrophilic residues (e.g., carbamoyl

and hydroxyl groups) at the 3'-position of the biphenyl nucleus<sup>57</sup> and increasing the length of the alkyl substituent attached to the amide carbonyl group from CH<sub>3</sub> to C<sub>3</sub>H<sub>7</sub>,<sup>16</sup> respectively.

We also explored the possibility to replace the *N*-anilinoethylamide portion with the original indole structure of MLT.

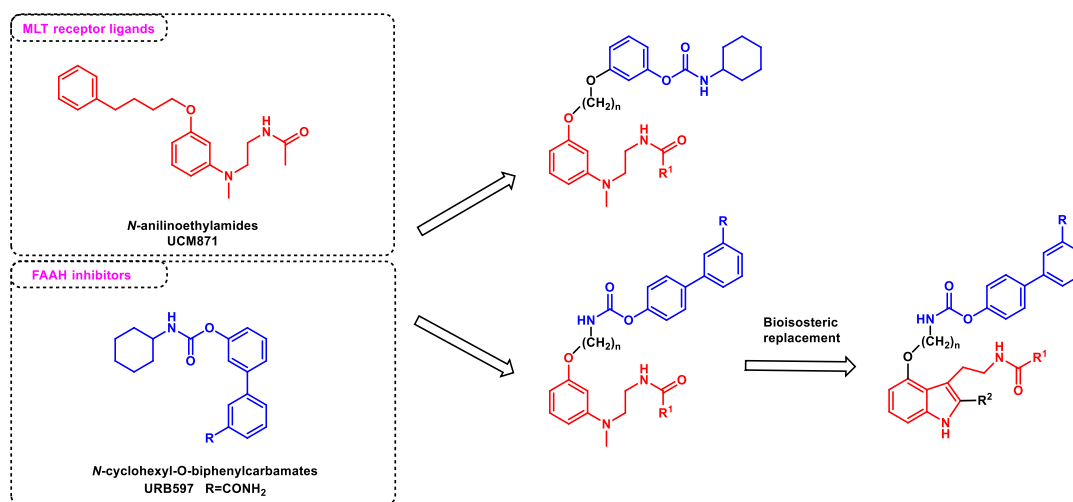


Figure 22 Dual-acting (MLT-FAAH) Designed compounds

The design of these compounds, including the length and the site of attachment of the alkyl spacer, was supported by docking studies within both MT<sub>1</sub> receptor model and the crystal structure of FAAH. The binding pose into the MT<sub>1</sub> receptor obtained for the putative dual-acting compound **55e** is depicted in Figure 23 (left). The melatonergic fragment can undertake polar interactions with typical amino acids in the transmembrane helix 7 (in particular, a hydrogen bond between Tyr<sup>285</sup> and the amide oxygen), and with Tyrosine 187 at the beginning of the transmembrane helix 5 (hydrogen bond with the alkoxy oxygen); instead the diphenyl carbamate alkyl portion could occupy the MT<sub>1</sub> accessory lipophilic pocket and it is oriented toward the extracellular loop, where it could undertake polar interactions, provided that at least four-methylene long spacers were inserted.

The same dual compound could be accommodated also in the FAAH binding site (Figure 23, right): like URB597, the carbamate is positioned in the catalytic site and the biphenyl substituent in the so-called “cytoplasmic access.” channel. The melatonergic portion occupies the ACB channel and forms a hydrogen bond with Tyrosine 335.

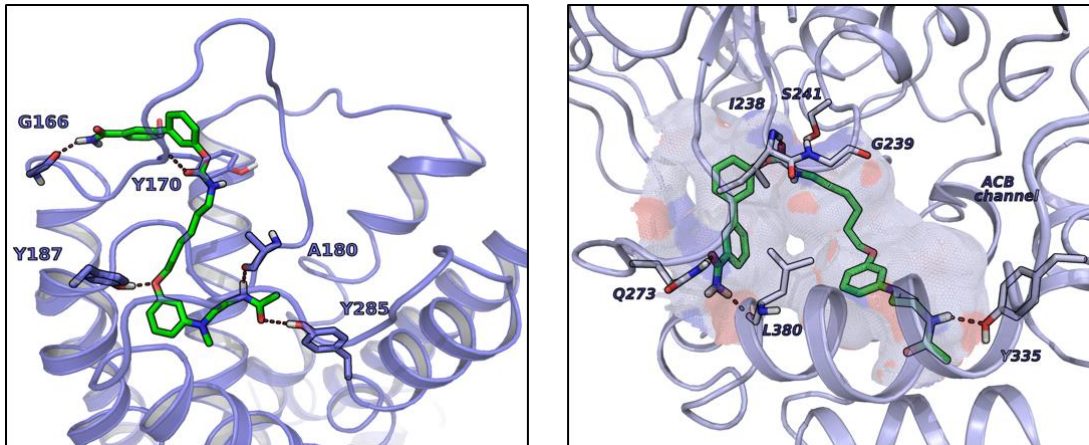
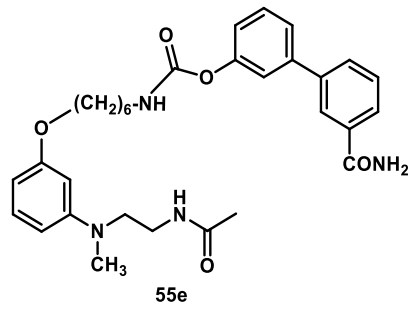
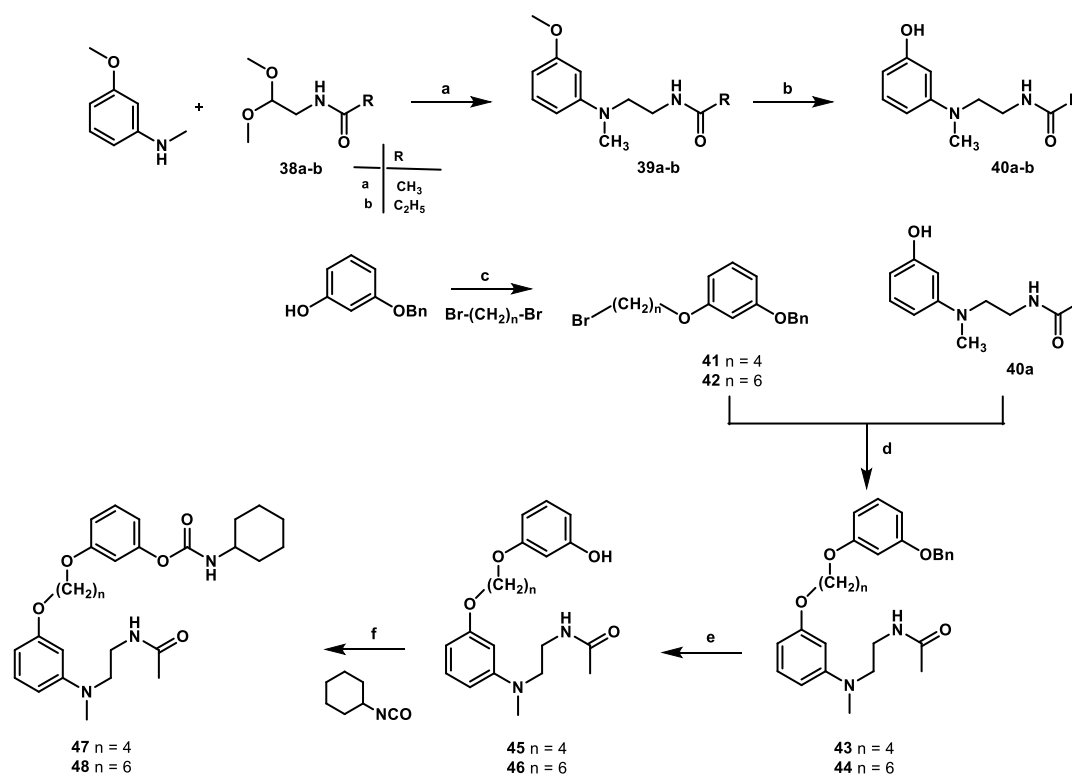


Figure 23 Induced-fit docking solution obtained for compound 55e into the homology model of the MT<sub>1</sub> receptor (left) and FAAH substrate binding site (right)

## 1.3.2 Results and Discussion

### 1.3.2.1. Chemistry

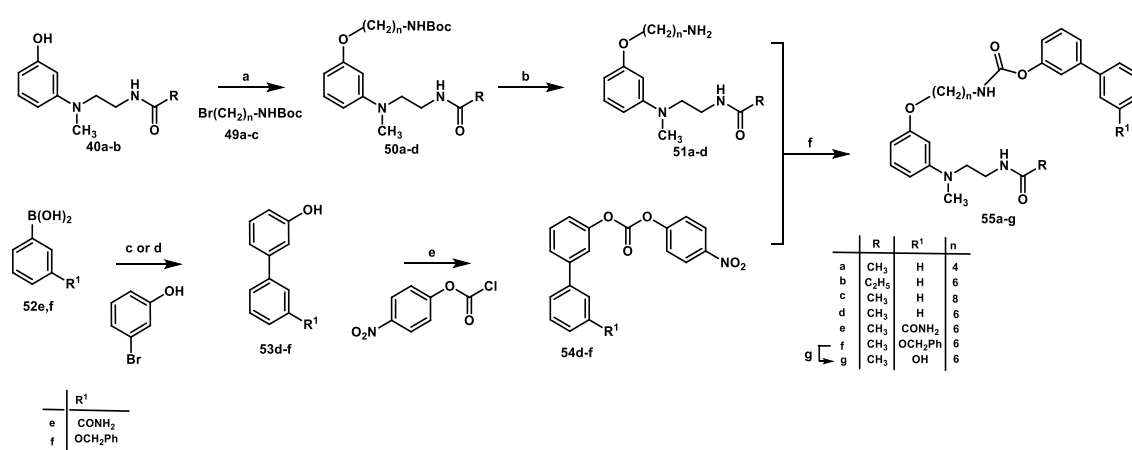
The first series of the designed dual-acting compounds (**45-48**) was prepared following the synthetic steps depicted in Scheme 5. The key intermediates **40a-b** were synthesized according to a well validated route to similar compounds,<sup>83</sup> involving a reductive *N*-alkylation of 3-methoxy-*N*-methylaniline with the suitable *N*-acylaminoacetaldehyde dimethylacetal **38a,b** (prepared in turn by acylation of the commercially available 2,2-dimethoxy-ethylamine) in the presence of TFA/Et<sub>3</sub>SiH, followed by methyl ether cleavage of **39a-b** using boron tribromide. Target carbamates **47-48** were prepared by *O*-alkylation of **40a-b** with the appropriate bromoalkylphenoxy derivative **41** or **42** (previously prepared by *O*-alkylation of 3-(benzyloxy)phenol with the suitable dibromoalkane) in the presence of NaH, followed by *O*-debenzylation by hydrogenolysis (**45-46**) and subsequent *O*-carbamoylation with *c*-hexylisocyanate in the presence of triethylamine.



Scheme 5 Synthesis of dual-acting compounds **45-48**. Reagents and conditions: (a) Et<sub>3</sub>SiH, TFA, CH<sub>2</sub>Cl<sub>2</sub>, rt, 20 h, yield 51–52%; (b) BBr<sub>3</sub>, CH<sub>2</sub>Cl<sub>2</sub>, 0°C to rt, 20 h, yield 68–76%; (c) K<sub>2</sub>CO<sub>3</sub>, acetone, 50 °C, 24 h, yield 68–82%; (d) NaH, DMF, –10 °C to rt, 16 h, yield 85–89%; (e) H<sub>2</sub> (1 atm), 10% Pd–C, EtOH/EtOAc, rt, 16 h, yield 78–92%; (f) Et<sub>3</sub>N, EtOH/CH<sub>3</sub>CN, rt, 18 h, yield 65–95%.

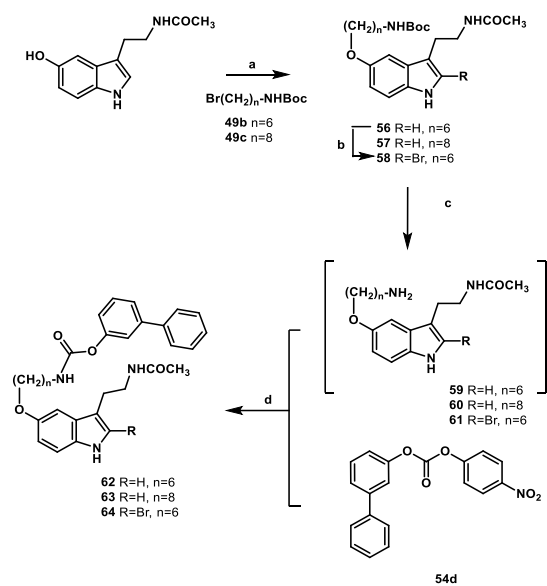


The second series of multifunctional compounds **55a–e** and **55g** were prepared in a convergent fashion following the steps outlined in Scheme 6. First, the aminoalkoxyphenyl intermediates **51a–d** were synthesized by *O*-alkylation of the previously cited phenol derivatives **40a, b** with the appropriate *tert*-butyl ( $\omega$ -bromoalkyl)carbamate **49a–c** in the presence of  $K_2CO_3/NaI$  and subsequent *N*-Boc-deprotection (TFA). The activated carbonates **54d–f** were then prepared by reaction of 1,1-biphenyl-3-ol derivatives (**53d–f**) [commercially available (**53d**) or prepared by a Suzuki coupling reaction of 3-bromophenol with the suitable phenylboronic acid **52e–f**] with *p*-nitrophenyl chloroformate in the presence of *N,N*-diisopropylethylamine (DIPEA). Finally, carbamates **55a–f** were obtained by coupling of the aminoalkoxyphenyl intermediates **51a–d** with the appropriate 4-nitrophenyl carbonate (**54d–f**). The final compound **55g** was achieved by hydrogenolysis of the benzyloxy precursor **55f**.



Scheme 6 Synthesis of dual-acting compounds **55a–g**. Reagents and conditions: (a)  $K_2CO_3$ ,  $NaI$ , acetone, 60 °C, 24 h, yield 20–44%; (b) TFA,  $CH_2Cl_2$ , rt, 16 h, yield 60–64%; (c) for **18e**  $Pd(PPh_3)_4$ ,  $Na_2CO_3$ ,  $CH_3CN$ , 90 °C, 1.5 h, yield 97%; (d) for **18f**  $Pd(OAc)_2$ ,  $Na_2CO_3$ ,  $H_2O$ , acetone, 35 °C, 40 min, yield 81%; (e) DIPEA,  $CH_3CN$ , rt, 1 h, yield 47–74%; (f)  $Et_3N$ ,  $CH_2Cl_2$ , rt, 4 h, yield 38–90%; (g)  $H_2$  (1 atm), 10% Pd–C,  $EtOH/EtOAc$ , rt, 20 h, yield 76%.

The dual acting-compounds (**62–64**), derived by bioisosteric replacement of the aniline moiety with the indole ring, were prepared according to the synthetic sequence outlined in Scheme 7 and including the condensation of 5-(aminoalkoxy)-*N*-acetyltryptamines **59–61** with the (4-nitrophenyl)carbonate derivative **54d**. The intermediate amines **59–61** were prepared by *O*-alkylation of *N*-acetylserotonin with *tert*-butyl (6-bromohexyl)carbamate (**49b**) or *tert*-butyl (8-bromooctyl)carbamate (**49c**) in the presence of  $K_2CO_3$  and subsequent *N*-Boc deprotection with trimethylsilyl bromide. The 2-bromoindole derivative **58** was obtained by bromination of **56** with trimethylphenylammonium tribromide in THF, before submitting it to *N*-Boc deprotection to give **61**.



Scheme 7 Synthesis of dual-acting compounds **62-64**. Reagents and conditions: (a)  $\text{K}_2\text{CO}_3$ ,  $\text{NaI}$ ,  $\text{CH}_3\text{CN}$ , reflux, 20 h, yield 47–59%; (b)  $(\text{CH}_3)_3\text{N}(\text{Br}_3)\text{C}_6\text{H}_5$ ,  $\text{THF}$ , rt, 30 min, yield 59%; (c)  $(\text{CH}_3)_3\text{SiBr}$ ,  $\text{CH}_3\text{CN}$ , rt, 1 h; (d)  $\text{Et}_3\text{N}$ ,  $\text{CH}_2\text{Cl}_2/\text{DMF}$ , rt, 3 h, two steps (c, d) yield 83–95%.

### 1.3.2.2. *In vitro* Pharmacological Studies and SARs

Newly synthesized compounds were evaluated for their binding affinity and intrinsic activity at *hMT*<sub>1</sub> and *hMT*<sub>2</sub> receptors (stably Expressed in NIH<sub>3</sub>T<sub>3</sub> Cells) and for their ability to inhibit the hydrolysis of [<sup>3</sup>H]-anandamide operated by the enzyme FAAH (prepared from rat brain homogenates) and the results are reported in Table 9.

The *O*-biphenylcarbamates hybrid compounds **55a-e, g** showed moderate binding affinity for MLT receptors (about one hundred times lower than that of MLT), but not very different (10-nanomolar range) from that of the MLT receptor ligand UCM871. Little differences in binding affinities were observed by modifying the length of the linker (*i.e.* **55a, 55c, 55d**) or introducing hydrophilic residues (e.g., carbamoyl, and hydroxyl groups) at the 3'-position of the biphenyl nucleus (**55e** and **55g**). Nevertheless, chain lengthening and/or introduction of polar substituents at C3'-position were correlated with an increase in intrinsic activity, with compounds **55c** and **55g** behaving as full agonists. Consistently with previously SAR profile of MLT ligands, a slight increase in binding affinity and intrinsic activity was observed by replacing the acetylamino group of **55c** with a propionylamino one (**55b**). We also synthesized and tested the aminoalkoxyphenyl derivatives **51a** and **51d** formally deriving from carbamate hydrolysis; these compounds do not display significant affinity for MLT receptors, and therefore the activity of *O*-biphenyl carbamates has to be ascribed to the whole hybrids, and not to metabolites deriving from FAAH hydrolysis.

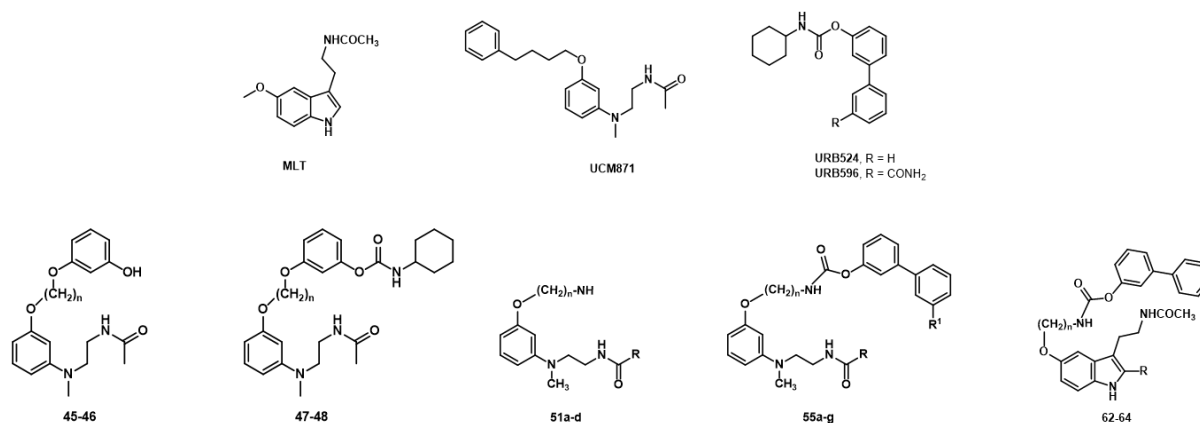
On the other hand, all these new bivalent ligands **55a-e, g** are more potent than the reference URB524 or URB597 at inhibiting FAAH activity *in vitro*, with a subnanomolar IC<sub>50</sub> value observed for compound **55c**. In general, increases in FAAH inhibitor potency were observed by lengthening the spacer from 4 to 8 carbon atoms (**55a**→**55d**→**55c**), and with the introduction of hydrophilic residues such as carbamoyl (**55e**) and hydroxyl (**55g**) groups at the 3'-position of the biphenyl nucleus. Inverting the arylcarbamate moiety (*N*-cyclohexylcarbamic acid *O*-phenyl esters **47** and **48**) resulted in significant decreases in FAAH inhibitory potency, without altering the affinity for MLT receptors.

The pharmacological results of the *O*-biphenylcarbamate derivatives **55a-e, g**, demonstrated that it is possible to merge the structural features required for FAAH inhibition and for MLT receptor binding activation in the same molecule. Unfortunately, activity at the two targets resulted rather unbalanced, as FAAH inhibitory potency is about 10–100 times higher than binding affinity at melatonin receptors.

In the attempt to improve MLT receptors binding affinity, the *N*-anilinoethyl fragment was replaced by the *N*-indolethyl portion of MLT. This bioisosteric replacement allowed to increase MLT receptor binding affinity of about 1 order of magnitude (**62-63**), with maintenance of FAAH inhibitory potency in the nanomolar range. Moreover, by the introduction of a bromine atom in position 2 of the

indole ring further increase in MLT receptor binding affinity were showed, consistent with previous SAR, leading to very potent dual-acting compound (**64**) with potencies in the low nanomolar concentration range for both molecular targets.

Table 9 Binding affinity and intrinsic activity of new dual-acting compounds at human MT<sub>1</sub> and MT<sub>2</sub> and FAAH receptors



Cpd	n	R <sup>1</sup>	R	MLT receptors				rFAAH IC <sub>50</sub> (nM) ± SEM <sup>c</sup>
				hMT <sub>1</sub>		hMT <sub>2</sub>		
				pK <sub>i</sub> ± SD <sup>a</sup>	IA <sub>r</sub> ± SD <sup>b</sup>	pK <sub>i</sub> ± SD <sup>a</sup>	IA <sub>r</sub> ± SD <sup>b</sup>	
MLT				9.69 ± 0.09	1.00 ± 0.01	9.54 ± 0.06	1.00 ± 0.03	nd <sup>d</sup>
UCM871				8.93 ± 0.17	0.68 ± 0.09	7.19 ± 0.04	0.64 ± 0.05	nd <sup>d</sup>
URB524				nd	nd	nd	nd	25.6 ± 2.0 <sup>e</sup>
URB597				nd	nd	nd	nd	4.6 ± 1.6 <sup>e</sup>
45	4			6.73 ± 0.08	0.27 ± 0.07	6.22 ± 0.07	0.18 ± 0.09	nd
46	6			7.23 ± 0.11	0.62 ± 0.14	6.48 ± 0.04	0.57 ± 0.08	nd
47	4			7.46 ± 0.10	0.07 ± 0.07	7.27 ± 0.01	0.05 ± 0.05	184 ± 3
48	6			7.56 ± 0.09	0.71 ± 0.04	6.53 ± 0.06	0.71 ± 0.05	197 ± 6
51a	4			5.51 ± 0.08	0.32 ± 0.09	4.89 ± 0.50	0.35 ± 0.04	nd
51d	6			6.35 ± 0.03	0.34 ± 0.05	6.40 ± 0.04	0.08 ± 0.04	nd
55a	4	H	CH <sub>3</sub>	7.89 ± 0.03	0.64 ± 0.07	7.35 ± 0.03	0.39 ± 0.07	1.45 ± 0.01
55b	6	H	CH <sub>2</sub> CH <sub>3</sub>	7.79 ± 0.04	0.77 ± 0.08	7.72 ± 0.02	0.88 ± 0.02	3.07 ± 0.08
55c	8	H	CH <sub>3</sub>	7.67 ± 0.01	0.70 ± 0.01	7.48 ± 0.02	0.75 ± 0.03	1.34 ± 0.03
55d	6	H	CH <sub>3</sub>	7.50 ± 0.01	0.85 ± 0.08	7.49 ± 0.02	0.96 ± 0.03	0.63 ± 0.04
55e	6	CONH <sub>2</sub>	CH <sub>3</sub>	7.41 ± 0.03	0.79 ± 0.06	7.81 ± 0.05	1.01 ± 0.02	0.43 ± 0.01
55g	6	OH	CH <sub>3</sub>	7.53 ± 0.02	0.89 ± 0.08	7.57 ± 0.01	0.94 ± 0.02	0.36 ± 0.01
62	6		H	8.22 ± 0.01	0.73 ± 0.08	8.34 ± 0.09	1.02 ± 0.02	2.38 ± 0.16
63	8		H	8.31 ± 0.70	0.73 ± 0.08	8.20 ± 0.02	0.53 ± 0.02	4.00 ± 0.10
64	6		Br	9.11 ± 0.10	0.73 ± 0.08	8.77 ± 0.03	0.97 ± 0.02	0.85 ± 0.01

<sup>a</sup>pK<sub>i</sub> values were calculated from IC<sub>50</sub> values, obtained from competition curves by the method of Cheng and Prusoff,<sup>84</sup> and are the mean of at least three determinations performed in duplicate. <sup>b</sup>The relative intrinsic activity values were obtained by dividing the maximum analogue-induced G protein activation by that of MLT. Measurements were performed in triplicate. <sup>c</sup>IC<sub>50</sub> values are the mean of at least two determinations. <sup>d</sup>nd: not determined. <sup>e</sup>Ref 57.

A representation of the docking solution obtained for the dual-acting compound **64** is provided in Figure 24.

Into the MT<sub>1</sub> receptor binding site the carbamoyl portion of **64** protrudes out of the TM region giving hydrogen bond interactions with amino acids belonging to extracellular loop 2. Into the active site of FAAH, the carbamate portion occupies the catalytic site, the biphenyl portion is accommodated in the cytoplasmic access channel and the bulky 2-bromoindole terminal portion has enough room to be properly accommodated in the ACB channel.

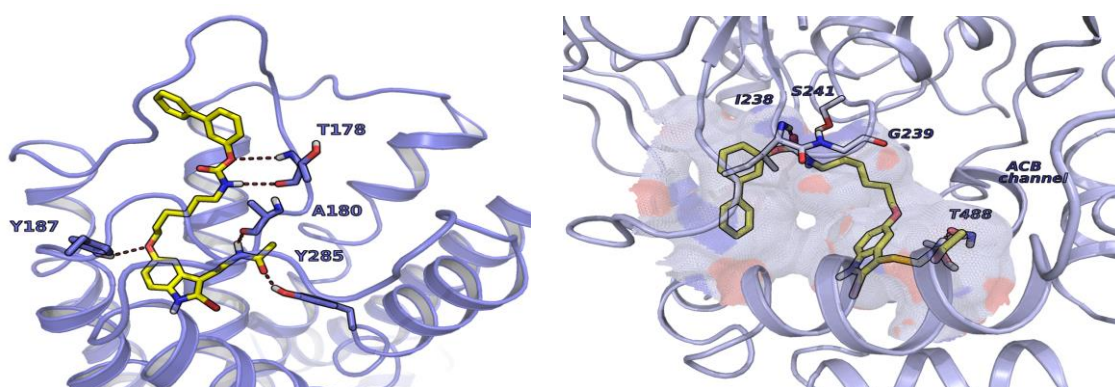


Figure 24 Induced-fit docking solution obtained for compound **64** into the homology model of the MT<sub>1</sub> receptor (left) and FAAH substrate binding site (right)

### 1.3.2.3. *In vivo* Intraocular Pressure (IOP) Lowering Effects

As both the endocannabinoid system and the melatonergic receptors are involved in the regulation of ocular homeostasis, some of the most interesting dual acting compounds (the aniline derivative **55e** and the indole derivative **64**) were evaluated in a normotensive glaucoma rabbit model for their intraocular pressure (IOP) lowering effects. Their behaviour was compared with that of the parent mono-ligands MLT and URB597 and of dorzolamide (**65**), a drug usually prescribed for the treatment of glaucoma. In these *in vivo* experiments, a transient ocular hypertension was induced by the injection of 0.1 mL of sterile hypertonic saline solution (5% distilled water) in the vitreous of New Zealand white rabbits, and then the tested compounds were topically administered (50  $\mu$ L of 1 mM solution).

As seen from the data of Figure 25, MLT and the reference URB597, when given topically to the eye of the animals, induce a prompt IOP lowering effect, visible at 60 min, which was maintained also at 120 min, even if with lower efficacy. Co-administration of compounds MLT and URB597 produced the same effect as the administration of each single agent at 60 min. However, the IOP reduction was maintained at 120 min, while single agents MLT and URB597 lost part of their efficacy at this time. The carbonic anhydrase inhibitor dorzolamide had a prompt effect, similar to that of MLT and URB597 at 60 min, which is maintained at 120 min as well. The *N*-anilinoethylamide derivative **55e** behaved similarly, showing limited effect after 60 min, which significantly increased at 120 min, exceeding those measured for the reference mono-ligands MLT and URB597. The most potent *in vitro* compound, the *N*-indolyethylamide derivative **64**, provided the highest IOP reduction at 120 min. Interestingly, the new hybrid compound **64** had a prolonged efficacy compared to the other tested compounds, showing efficacy even after 4 h post-administration, with an IOP drop of 3.5 mmHg.

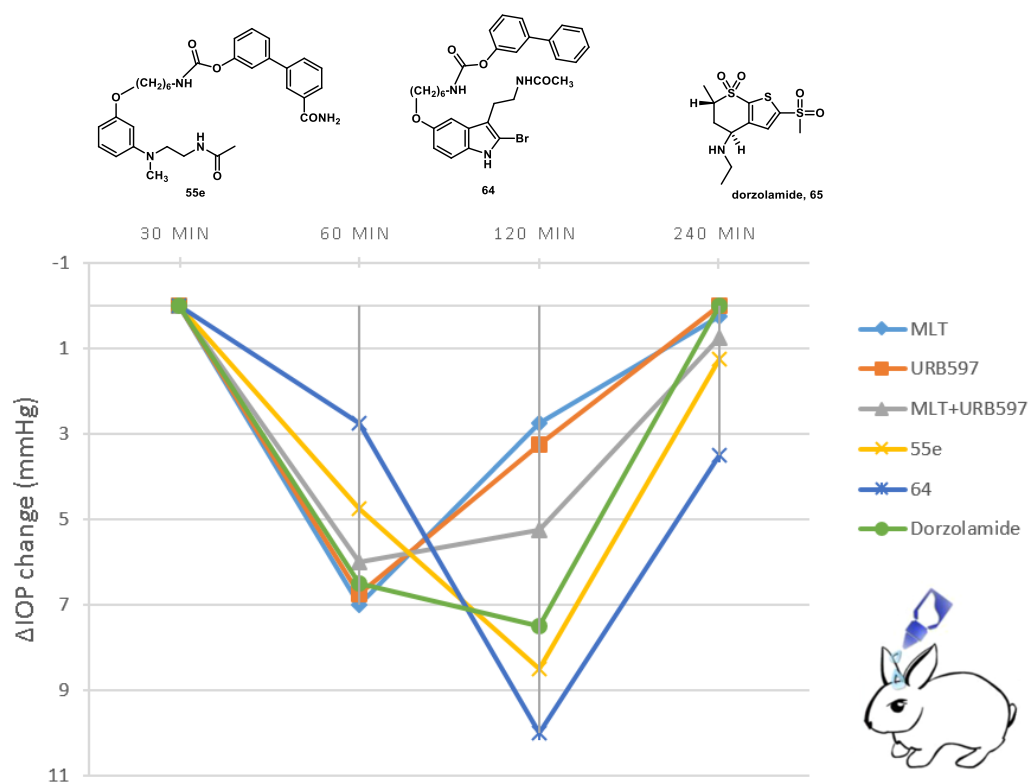


Figure 25 Drop of intraocular pressure ( $\Delta IOP$ , mm Hg) versus time (min) in hypertonic saline-induced ocular hypertension in New Zealand male albino rabbits measured after treatment with MLT, URB597, the combination of compounds MLT and URB597, the reference inhibitor dorzolamide, and dual-acting inhibitors 55e and 64, tested at 1 mM concentration (dorzolamide tested at 1% (w/v) concentration).

### 1.3.3 Conclusions

Novel multifunctional compounds behaving as melatonin receptor agonists and as inhibitors of the enzyme fatty acid amide hydrolase were discovered. Suitable combination of the structural features required for FAAH inhibition and for MLT receptor binding activation in the same molecule, led to compounds with remarkable and balanced activity at both targets. Since both targets are involved in the control of intraocular pressure, two of the most interesting dual acting compounds (**55e** and **64**) were tested for their potential IOP-lowering effects. In an *in vivo* rabbit model of high IOP **55e** and **64** showed promising anti-glaucoma activity. In particular, the IOP-lowering effects of compound **64** were significantly greater and long-lasting than those exerted by either melatonin or the FAAH-inhibitor URB597, and by dorzolamide, a currently used anti-glaucoma agent.



## 1.3.4 Experimental Section

### 1.3.4.1 Materials and Methods

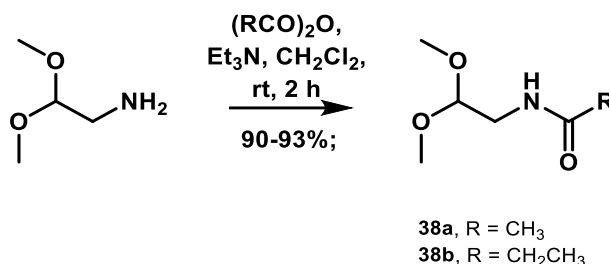
Melting points were determined on a Buchi B-540 capillary melting point apparatus and are uncorrected.  $^1\text{H}$  NMR and  $^{13}\text{C}$  NMR spectra were recorded on a Bruker AVANCE 200 or 400 instrument. Chemical shifts ( $\delta$  scale) are reported in parts per million (ppm) relative to the central peak of the solvent. Coupling constants ( $J$ ) are given in hertz (Hz).  $^1\text{H}$  and  $^{13}\text{C}$  signals were unambiguously assigned by COSY, NOESY, DEPT135, HMQC, and HMBC experiments. EI MS spectra (70 eV) were taken on a Fisons Trio 1000 instrument; only molecular ions ( $\text{M}^+$ ) and base peaks are given. ESI MS spectra were taken on a Waters Micromass ZQ instrument; only molecular ions ( $\text{M}+1$ )<sup>+</sup> or ( $\text{M}-1$ )<sup>-</sup> are given. High-resolution mass spectroscopy was performed on a Micro mass Q-ToF Micromass spectrometer (Micromass, Manchester, UK) using an ESI source. The purity of tested compounds, determined by high performance liquid chromatography (HPLC), was greater than 95%. These analyses were performed on a Waters HPLC/UV/MS system (separation module Alliance HT2795, Photo Diode Array Detector 2996, mass detector Micromass ZQ; software: MassLynx 4.1). Column chromatography purifications were performed under “flash” conditions using Merck 230–400 mesh silica gel. Analytical thin-layer chromatography (TLC) was carried out on Merck silica gel 60 F<sub>254</sub> plates. Chiral HPLC runs were conducted on a Jasco (Cremella, LC, Italy) HPLC system equipped with a Jasco AS-2055 plus autosampler, a PU2089 plus quaternary gradient pump, and an MD-2010 plus multiwavelength detector. Experimental data were acquired and processed by Jasco Borwin PDA and Borwin Chromatograph Software. Solvents used for chiral chromatography were HPLC grade and supplied by Carlo Erba (Milan, Italy). Optical rotation values were measured on a Jasco (Cremella, LC, Italy) photoelectric polarimeter DIP 1000 with a 0.2 dm cell at the sodium D line ( $\lambda = 589 \text{ nm}$ ); sample concentration values ( $c$ ) are given in  $10^{-2} \text{ g mL}^{-1}$ .

### 1.3.4.2 Reagents

*Tert*-butyl (4-bromobutyl)carbamate, *tert*-butyl (6-bromohexyl)carbamate, [1,1'-biphenyl]-3-ol, (3-carbamoylphenyl)boronic acid, [3-(benzyloxy)phenyl]boronic acid, 3-(benzyloxy)phenol, 2,2-dimethoxyethanamine and *N*-acetylserotonin were purchased from commercial suppliers and used without further purification.

### 1.3.4.3 Synthesis and Physicochemical Characterization of Dual-acting Compounds

#### General Procedure for the Synthesis of *N*-(2,2-Dimethoxyethyl)acylamines 38a, b



Acetic or propionic anhydride (12 mmol) and Et<sub>3</sub>N (1.65 mL, 12 mmol) were added to a solution of 2,2-dimethoxyethanamine (1.08 mL, 10 mmol) in dry CH<sub>2</sub>Cl<sub>2</sub> (16 mL), and the resulting mixture was stirred at room temperature for 2 h. The mixture was neutralized with a saturated solution of NaHCO<sub>3</sub> and extracted with CH<sub>2</sub>Cl<sub>2</sub>. The combined organic phases were washed with brine, dried (Na<sub>2</sub>SO<sub>4</sub>), filtered, and concentrated *in vacuo* affording a crude residue that was purified by silica gel column chromatography.

#### *N*-(2,2-Dimethoxyethyl)acetamide (38a)

Flash chromatography (CH<sub>2</sub>Cl<sub>2</sub>-MeOH 98:2 as eluent). Oil; 90% yield.

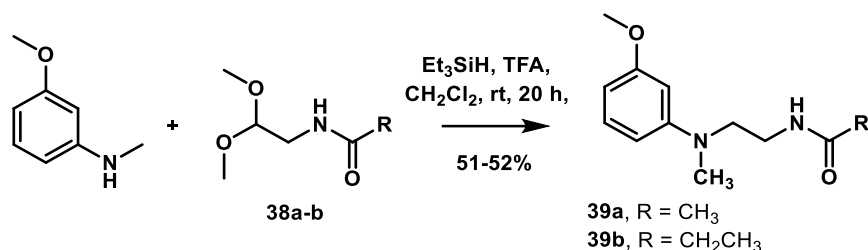
Chemical physical data were identical to those previously reported.<sup>85</sup>

#### *N*-(2,2-Dimethoxyethyl)propionamide (38b)

Flash chromatography (CH<sub>2</sub>Cl<sub>2</sub>-EtOAc 95:5 as eluent). Oil; 93% yield.

<sup>1</sup>H NMR (400 MHz, CDCl<sub>3</sub>): δ 5.70 (br s, 1H), 4.38 (t, 1H, *J* = 5.0), 3.39–3.44 (m, 2H), 3.40 (s, 6H), 2.23 (q, 2H, *J* = 7.5), 1.16 (t, 3H, *J* = 7.5). ESI MS (*m/z*): 184 [M + Na]<sup>+</sup>.

## General Procedure for the Synthesis of (Anilinoethyl)amido Derivatives 39a, b



Trifluoroacetic acid (2.2 mL, 29 mmol) and triethylsilane (0.9 mL, 5.6 mmol) were added to a solution of 3-methoxy-*N*-methylaniline (0.3 mL, 2.3 mmol) and the suitable acetal **38a,b** (3.1 mmol) in  $\text{CH}_2\text{Cl}_2$  (5 mL), and the resulting mixture was stirred at room temperature for 20 h under a nitrogen atmosphere. After cooling to 0 °C, the mixture was carefully neutralized with a saturated aqueous solution of  $\text{NaHCO}_3$ , and the aqueous layer was extracted with  $\text{CH}_2\text{Cl}_2$ . The combined organic phases were washed with brine, dried over  $\text{Na}_2\text{SO}_4$ , and concentrated under reduced pressure to give a crude residue that was purified by column chromatography.

### *N*-{2-[(3-Methoxyphenyl)methylamino]ethyl}acetamide (39a)

Purification by silica gel flash chromatography (EtOAc as eluent) and crystallization. White solid (diethyl ether/ petroleum ether), 51% yield.

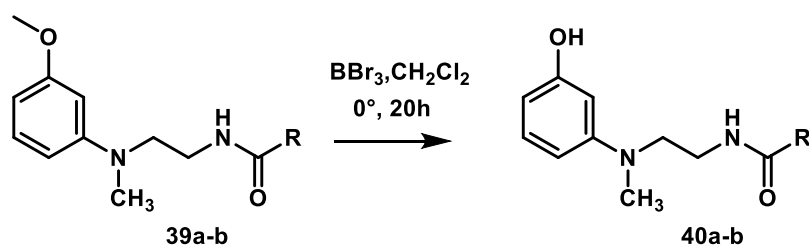
Chemical physical data were identical to those previously reported.<sup>23</sup>

### *N*-{2-[(3-Methoxyphenyl)methylamino]ethyl}propionamide (39b)

Purification by silica gel chromatography (EtOAc–cyclohexane 7:3 as eluent). Oil, 52% yield.

$^1\text{H NMR}$  (400 MHz,  $\text{CDCl}_3$ ):  $\delta$  7.16 (dd, 1H,  $J^1 = J^2 = 8.5$ ), 6.42 (dd, 1H,  $J^1 = 2.0$ ,  $J^2 = 8.0$  Hz), 6.31–6.33 (m, 2H), 5.70 (br s, 1H), 3.80 (s, 3H), 3.46–3.47 (m, 4H), 2.95 (s, 3H), 2.16 (q, 2H,  $J = 7.5$  Hz), 1.12 (t, 3H,  $J = 7.5$  Hz).  $^{13}\text{C NMR}$  (100 MHz,  $\text{CDCl}_3$ ):  $\delta$  174.0, 160.9, 150.6, 130.0, 105.8, 102.1, 99.3, 55.2, 52.0, 38.6, 37.2, 29.6, 9.7. ESI MS ( $m/z$ ): 237  $[\text{M} + \text{H}]^+$ .

## General Procedure for the Synthesis of (3-Hydroxyanilino)ethylamido Derivatives 40a,b



A 1 M solution of  $\text{BBr}_3$  in  $\text{CH}_2\text{Cl}_2$  (2.5 mL, 2.5 mmol) diluted with dry  $\text{CH}_2\text{Cl}_2$  (9 mL) was added dropwise to an ice-cooled solution of the suitable amide **39a, b** (1.23 mmol) in dry  $\text{CH}_2\text{Cl}_2$  (9 mL), and

the resulting mixture was stirred at room temperature for 20 h. After neutralization with a 2 N aqueous solution of  $\text{Na}_2\text{CO}_3$ , the mixture was extracted with  $\text{CH}_2\text{Cl}_2$ , and the combined organic phases were dried ( $\text{Na}_2\text{SO}_4$ ) and concentrated under reduced pressure to give a crude residue that was purified by column chromatography.

#### ***N*-{2-[(3-Hydroxyphenyl)methylamino]ethyl}acetamide (40a)**

Purification by silica gel flash chromatography ( $\text{CH}_2\text{Cl}_2$ -MeOH 98:2 as eluent). Oil, 76% yield.

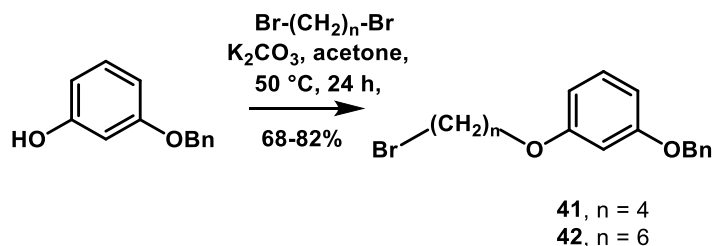
Chemical physical data were identical to those previously reported.<sup>86</sup>

#### ***N*-{2-[(3-Hydroxyphenyl)methylamino]ethyl}propionamide (40b)**

Purification by silica gel chromatography (EtOAc-cyclohexane 7:3 as eluent). Oil, 68% yield.

$^1\text{H}$  NMR (400 MHz,  $\text{CDCl}_3$ ):  $\delta$  7.09 (dd, 1H,  $J^1 = J^2 = 8.0$  Hz), 6.32–6.36 (m, 2H), 6.25 (d, 1H,  $J = 7.5$  Hz), 6.01 (br s, 1H), 5.71 (br s, 1H), 3.45–3.47 (m, 4H), 2.94 (s, 3H), 2.18 (q, 2H,  $J = 7.5$  Hz), 1.13 (t, 3H,  $J = 7.5$  Hz). ESI MS ( $m/z$ ): 223  $[\text{M} + \text{H}]^+$ .

#### **General Procedure for the Synthesis of Bromoalkylphenoxy Derivatives 41 and 42**



$\text{K}_2\text{CO}_3$  (0.31 g, 2.25 mmol) and the suitable dibromoalkane (2.25 mmol) were added to a solution of 3-(benzyloxy)phenol (0.3 g, 1.5 mmol) in dry acetone (4 mL), and the resulting mixture was stirred at  $50\text{ }^\circ\text{C}$  for 24 h. After addition of water, the mixture was extracted with EtOAc, and the combined organic phases were dried ( $\text{Na}_2\text{SO}_4$ ). After removing the solvent by distillation under reduced pressure, the crude residue was purified by silica gel column chromatography (cyclohexane-EtOAc 95:5 as eluent).

#### **1-(Benzyloxy)-3-(4-bromobutyloxy)benzene (41)**

Oil, 68% yield.

Analytical data were in agreement with those previously reported.<sup>87</sup>

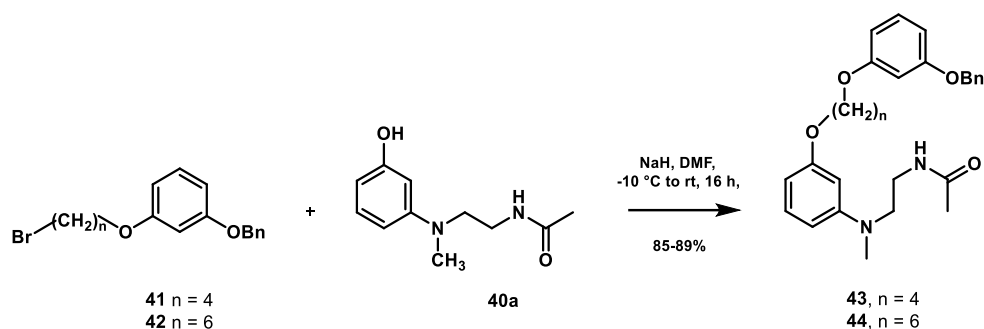
#### **1-(Benzyloxy)-3-(6-bromohexyloxy)benzene (42)**

Oil, 82% yield.

$^1\text{H}$  NMR (400 MHz,  $\text{CDCl}_3$ ):  $\delta$  7.28–7.45 (m, 5H), 7.19 (dd, 1H,  $J^1 = J^2 = 8.0$  Hz), 6.58–6.62 (m, 3H), 5.07 (s, 2H), 3.96 (t, 2H,  $J = 6.5$  Hz), 3.45 (t, 2H,  $J = 6.5$  Hz), 1.81–1.92 (m, 4H), 1.49–1.56 (m, 4H).

$^{13}\text{C}$  NMR (100 MHz,  $\text{CDCl}_3$ ):  $\delta$  160.3, 160.0, 137.0, 129.9, 128.6, 128.0, 127.5, 107.1, 106.9, 101.8, 70.0, 67.7, 33.9, 32.7, 29.1, 27.9, 25.3. ESI MS ( $m/z$ ): 363–365 [ $\text{M} + \text{H}$ ] $^+$ .

### General Procedure for the Synthesis of Derivatives **43** and **44**



NaH (60% in mineral oil, 0.026g, 0.65 mmol) was added to a solution of **40a** (0.13 g, 0.63 mmol) in dry DMF (1 mL), and the resulting mixture was stirred at  $-10^\circ\text{C}$  for 10 min under a nitrogen atmosphere. Then a solution of the suitable bromoalkylphenoxy derivative **41** or **42** (0.65 mmol) in dry DMF (1.5 mL) was added, and the resulting mixture was stirred at room temperature for 16 h. After addition of water, the mixture was extracted with EtOAc, the combined organic phases were dried ( $\text{Na}_2\text{SO}_4$ ), filtered, and concentrated under reduced pressure to afford a crude product that was purified by silica gel column chromatography (EtOAc as eluent).

#### *N*-[2-({3-[4-(3-Benzyloxy)phenoxy]butoxy}phenyl)methylaminoethyl]acetamide (**43**)

Oil, 89% yield.

$^1\text{H}$  NMR (400 MHz,  $\text{CDCl}_3$ ):  $\delta$  7.32–7.46 (m, 5H), 7.10–7.23 (m, 2H), 6.51–6.60 (m, 3H), 6.27–6.43 (m, 3H), 5.61 (br s, 1H), 5.05 (s, 2H), 3.98–4.09 (m, 4H), 3.45–3.47 (m, 4H), 2.94 (s, 3H), 1.94–1.98 (m, 4H), 1.94 (s, 3H). ESI MS ( $m/z$ ): 463 [ $\text{M} + \text{H}$ ] $^+$ .

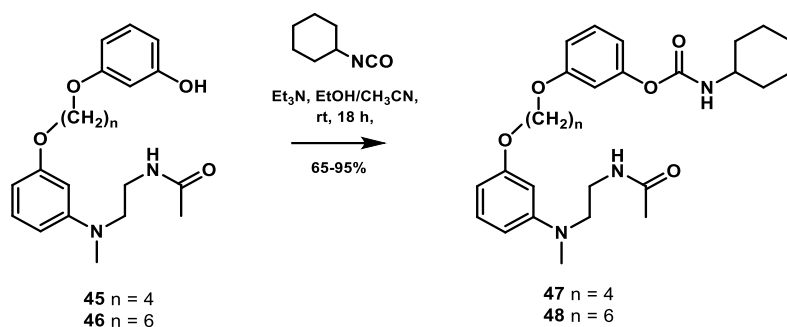
#### *N*-{2-([3-[6-(3-Benzyloxy)phenoxy]hexyloxy]phenyl(methylamino)ethyl]acetamide (**44**)

Oil, 85% yield.

$^1\text{H}$  NMR (400 MHz,  $\text{CDCl}_3$ ):  $\delta$  7.32–7.46 (m, 5H), 7.10–7.22 (m, 2H), 6.50–6.59 (m, 3H), 6.26–6.40 (m, 3H), 5.59 (br s, 1H), 5.05 (s, 2H), 3.92–4.00 (m, 4H), 3.44–3.49 (m, 4H), 2.93 (s, 3H), 1.94 (s, 3H), 1.75–1.90 (m, 4H), 1.50–1.57 (m, 4H). ESI MS ( $m/z$ ): 491 [ $\text{M} + \text{H}$ ] $^+$ .



## General Procedure for the Synthesis of Cyclohexyl Carbamates **47** and **48**



Cyclohexyl isocyanate (62  $\mu\text{L}$ , 0.48 mmol) and  $\text{Et}_3\text{N}$  (5  $\mu\text{L}$ ) were added to a solution of the appropriate phenol **45** or **46** (0.21 mmol) in absolute  $\text{EtOH}$  (0.6 mL) and dry  $\text{CH}_3\text{CN}$  (0.6 mL), and the resulting mixture was stirred at room temperature for 18 h under a nitrogen atmosphere. After removing the solvent by distillation under reduced pressure, the residue was purified by silica gel column chromatography ( $\text{EtOAc}$ –cyclohexane 7:3 as eluent) and crystallization.

### 3-(4-{3-[(2-Acetamidoethyl)methylamino]phenoxy}butyloxy)phenylcyclohexylcarbamate (**47**)

White solid, mp 115–6  $^\circ\text{C}$  ( $\text{EtOAc}$ –petroleum ether), 65% yield.

$^1\text{H}$  NMR (400 MHz,  $\text{CDCl}_3$ ):  $\delta$  7.10–7.23 (m, 2H), 6.70–6.74 (m, 3H), 6.30–6.40 (m, 3H), 5.72 (br s, 1H), 4.98 (br d, 1H), 4.00–4.06 (m, 4H), 3.54–3.58 (m, 1H), 3.44–3.47 (m, 4H), 2.94 (s, 3H), 1.92–2.05 (m, 4H), 1.93 (s, 3H), 1.58–1.80 (m, 4H), 1.14–1.50 (m, 6H).  $^{13}\text{C}$  NMR (100 MHz,  $\text{CDCl}_3$ ):  $\delta$  170.4, 160.2, 159.8, 153.5, 152.0, 150.9, 130.0, 129.6, 113.7, 111.6, 108.1, 105.5, 102.3, 99.7, 67.6, 67.3, 51.7, 50.1, 38.4, 37.3, 33.2, 26.0, 25.4, 24.7, 23.2. ESI MS ( $m/z$ ): 498  $[\text{M}+\text{H}]^+$ . HR MS (ESI):  $m/z$  calculated for  $\text{C}_{28}\text{H}_{40}\text{N}_3\text{O}_5$ ,  $[\text{M} + \text{H}]^+$ : 498.2968, found: 498.2961.

### 3-(6-{3-[(2-Acetamidoethyl)methylamino]phenoxy}hexyloxy)phenylcyclohexylcarbamate (**48**)

White solid, mp 99–101  $^\circ\text{C}$  ( $\text{EtOAc}$ –petroleum ether), 95% yield.

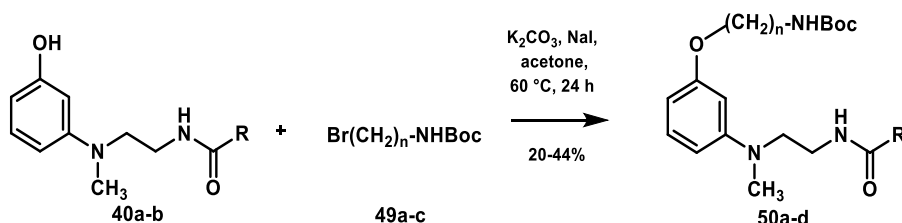
$^1\text{H}$  NMR (400 MHz,  $\text{CDCl}_3$ ):  $\delta$  7.10–7.24 (m, 2H), 6.69–6.75 (m, 3H), 6.31–6.40 (m, 3H), 5.66 (br s, 1H), 4.95 (br d, 1H), 3.92–4.01 (m, 4H), 3.54–3.59 (m, 1H), 3.45–3.47 (m, 4H), 2.94 (s, 3H), 1.94 (s, 3H), 1.72–2.04 (m, 8H), 1.48–1.65 (m, 4H), 1.17–1.46 (m, 6H).  $^{13}\text{C}$  NMR (100 MHz,  $\text{CDCl}_3$ )  $\delta$ : 170.4, 160.4, 159.9, 153.5, 152.0, 150.9, 130.0, 129.5, 113.6, 111.6, 108.1, 105.4, 102.3, 99.8, 67.9, 67.7, 51.8, 50.1, 38.4, 37.3, 33.2, 29.3, 29.1, 25.9, 25.8, 25.4, 24.7, 23.2. ESI MS ( $m/z$ ): 526  $[\text{M} + \text{H}]^+$ . HR MS (ESI):  $m/z$  calculated for  $\text{C}_{30}\text{H}_{44}\text{N}_3\text{O}_5$ ,  $[\text{M} + \text{H}]^+$ : 526.3281, found: 526.3251.

### Procedure for the Synthesis of *tert*-Butyl ( $\omega$ -Bromoalkyl)carbamates (**49a–c**)

*Tert*-Butyl (8-bromooctyl)carbamate (**49c**) was prepared according to literature procedure, and chemical physical data were identical with those previously reported.<sup>88</sup>

*Tert*-Butyl (4-bromobutyl)carbamate (**49a**) and *tert*-butyl (6-bromohexyl)carbamate (**49b**) are commercially available.

### General Procedure for the Synthesis of *N*-Boc-aminoalkoxyphenyl Derivatives **50a–d**



The suitable *tert*-butyl ( $\omega$ -bromoalkyl)carbamate **49a–c** (1.50 mmol),  $K_2CO_3$  (0.315 g, 2.25 mmol), and a catalytic amount of NaI were added to a solution of the appropriate (3-hydroxyanilino)ethylamido derivative **40a** or **40b** (1.50 mmol) in dry acetone (8 mL), and the resulting mixture was stirred at 60 °C for 24 h under a nitrogen atmosphere. After water addition the mixture was extracted with EtOAc, the combined organic phases were dried ( $Na_2SO_4$ ), and the solvent was removed by distillation under reduced pressure to afford a crude residue that was purified by column chromatography.

#### *tert*-Butyl {4-[3-((2-Acetamidoethyl)methylamino)phenoxy]butyl}carbamate (**50a**)

This product was obtained following the above general procedure by reacting **40a** with **49a**. Purification by silica gel chromatography (EtOAc as eluent). Oil, 37% yield.

$^1H$  NMR (400 MHz,  $CDCl_3$ ):  $\delta$  7.13 (dd, 1H,  $J^1 = J^2 = 8.0$  Hz), 6.28–6.38 (m, 3H), 5.71 (br s, 1H), 4.66 (br s, 1H), 3.98 (t, 2H,  $J = 6.5$  Hz), 3.44–3.48 (m, 4H), 3.17–3.21 (m, 2H), 2.94 (s, 3H), 1.94 (s, 3H), 1.77–1.83 (m, 2H), 1.65–1.71 (m, 2H), 1.45 (s, 9H). ESI MS ( $m/z$ ): 380 [ $M + H$ ] $^+$ .

#### *tert*-Butyl {4-[3-((2-Propionamidoethyl)methylamino)phenoxy]butyl}carbamate (**50b**)

This product was obtained following the above general procedure by reacting **40b** with **49b**. Purification by silica gel chromatography (EtOAc–cyclohexane 7:3 as eluent). Oil, 20% yield.

$^1H$  NMR (400 MHz,  $CDCl_3$ ):  $\delta$  7.13 (dd, 1H,  $J^1 = J^2 = 8.0$  Hz), 6.29–6.38 (m, 3H), 5.65 (br s, 1H), 4.55 (br s, 1H), 3.94 (t, 2H,  $J = 6.5$  Hz), 3.45–3.49 (m, 4H), 3.10–3.15 (m, 2H), 2.94 (s, 3H), 2.16 (q, 2H,  $J = 7.5$  Hz), 1.74–1.81 (m, 2H), 1.38–1.52 (m, 6H), 1.45 (s, 9H), 1.12 (t, 3H,  $J = 7.5$  Hz).  $^{13}C$  NMR (100 MHz,  $CDCl_3$ ):  $\delta$  174.0, 160.3, 156.0, 130.0, 105.5, 102.2, 99.7, 67.6, 51.8, 40.5, 38.4, 37.2, 30.0, 29.6, 29.2, 28.4, 26.5, 25.8, 9.7. ESI MS ( $m/z$ ): 422 [ $M + H$ ] $^+$ .

#### *tert*-Butyl {8-[3-((2-Acetamidoethyl)methylamino)phenoxy]octyl}carbamate (**50c**)

This product was obtained following the above general procedure by reacting **40a** with **49c**. Purification by silica gel chromatography (EtOAc as eluent). Oil, 37% yield.



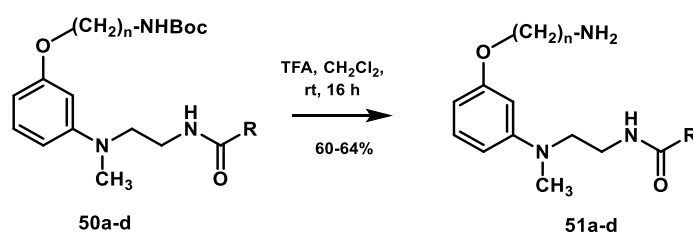
$^1\text{H}$  NMR (400 MHz,  $\text{CDCl}_3$ ):  $\delta$  7.12 (dd, 1H,  $J^1 = J^2 = 8.0$ ), 6.27–6.37 (m, 3H), 5.69 (br s, 1H), 4.52 (br s, 1H), 3.93 (t, 2H,  $J = 6.5$  Hz), 3.42–3.46 (m, 4H), 3.05–3.13 (m, 2H), 2.92 (s, 3H), 1.93 (s, 3H), 1.70–1.77 (m, 2H), 1.39–1.48 (m, 4H), 1.43 (s, 9H), 1.22–1.37 (m, 6H). ESI MS ( $m/z$ ): 436 [ $\text{M} + \text{H}$ ] $^+$ .

#### ***tert*-Butyl {6-[3-((2-Acetamidoethyl)methylamino)phenoxy]hexyl}carbamate (50d)**

This product was obtained following the above general procedure by reacting **40a** with **49b**. Purification by silica gel chromatography (EtOAc as eluent). Oil, 44% yield.

$^1\text{H}$  NMR (400 MHz,  $\text{CDCl}_3$ ):  $\delta$  7.14 (dd, 1H,  $J^1 = J^2 = 8.0$  Hz), 6.27–6.40 (m, 3H), 5.67 (br s, 1H), 4.55 (br s, 1H), 3.95 (t, 2H,  $J = 6.5$  Hz), 3.44–3.46 (m, 4H), 3.08–3.16 (m, 2H), 2.94 (s, 3H), 1.95 (s, 3H), 1.73–1.82 (m, 2H), 1.45 (s, 9H), 1.36–1.55 (m, 6H). ESI MS ( $m/z$ ): 408 [ $\text{M} + \text{H}$ ] $^+$ .

#### **General Procedure for *N*-Boc Deprotection: Synthesis of Aminoalkoxyphenyl Derivatives 51a–d**



Trifluoroacetic acid (0.8 mL, 10 mmol) was added to an ice-cooled solution of the suitable *N*-Boc derivative **50a–d** (0.3 mmol) in dry  $\text{CH}_2\text{Cl}_2$  (3.5 mL), and the resulting mixture was stirred at room temperature for 16 h under a nitrogen atmosphere. The reaction mixture was basified by dropwise addition of a 2 N aqueous solution of  $\text{Na}_2\text{CO}_3$  and extracted with  $\text{CH}_2\text{Cl}_2$ . The combined organic phases were washed with brine, dried ( $\text{Na}_2\text{SO}_4$ ), and the solvent removed by distillation under reduced pressure to give the desired crude amines that were used without further purification or purified by filtration through a pad of silica gel.

#### ***N*-{2-[(3-(4-Aminobutoxy)phenyl)methylamino]ethyl}acetamide (51a)**

Purification by filtration on silica gel (EtOAc–MeOH–conc.  $\text{NH}_3$  9:1:1 as eluent). Oil, 60% yield.

$^1\text{H}$  NMR (400 MHz,  $\text{CDCl}_3$ ):  $\delta$  7.12 (dd, 1H,  $J^1 = J^2 = 8.0$  Hz), 6.35–6.37 (m, 1H), 6.26–6.31 (m, 2H), 5.95 (br s, 1H), 3.97 (t, 2H,  $J = 6.0$  Hz), 3.42–3.44 (m, 4H), 2.93 (s, 3H), 2.81 (t, 2H,  $J = 7.0$  Hz), 1.93 (s, 3H), 1.77–1.85 (m, 2H), 1.64–1.71 (m, 2H).  $^{13}\text{C}$  NMR (100 MHz,  $\text{CDCl}_3$ ):  $\delta$  170.7, 160.5, 150.4, 130.1, 105.8, 102.5, 99.5, 67.9, 51.7, 42.0, 38.5, 37.1, 29.6, 26.7, 23.3. ESI MS ( $m/z$ ): 280 [ $\text{M} + \text{H}$ ] $^+$ . HR MS (ESI):  $m/z$  calculated for  $\text{C}_{15}\text{H}_{26}\text{N}_3\text{O}_2$ , [ $\text{M} + \text{H}$ ] $^+$ : 280.2020, found: 280.2031.

### ***N*-{2-[(3-(6-Aminohexyloxy)phenyl)methylamino]ethyl}propionamide (51b)**

This intermediate was used for the next step without any further purification.

ESI MS (*m/z*): 322 [M + H]<sup>+</sup>.

### ***N*-{2-[(3-(8-Aminoocetyloxy)phenyl)methylamino]ethyl}acetamide (51c)**

This intermediate was used for the next step without any further purification.

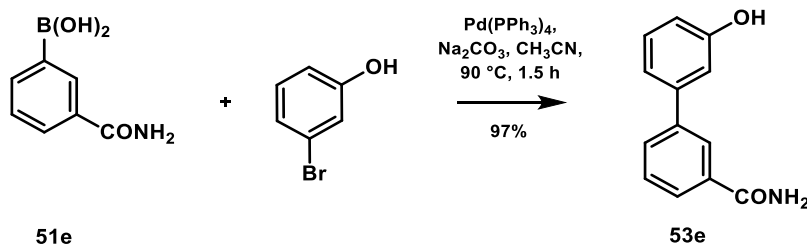
ESI MS (*m/z*): 336 [M + H]<sup>+</sup>.

### ***N*-{2-[(3-(6-Aminohexyloxy)phenyl)methylamino]ethyl}acetamide (51d)**

Purification by filtration on silica gel (EtOAc– MeOH–conc. NH<sub>3</sub> 9:1:1 as eluent). Oil, 64% yield.

<sup>1</sup>H NMR (400 MHz, CDCl<sub>3</sub>): δ 7.11 (dd, 1H, *J*<sup>1</sup> = *J*<sup>2</sup> = 8.0 Hz), 6.33–6.36 (m, 1H), 6.23–6.28 (m, 2H), 5.90 (br s, 1H), 3.92 (t, 2H, *J* = 6.5 Hz), 3.41–3.44 (m, 4H), 2.91 (s, 3H), 2.69 (t, 2H, *J* = 7.0 Hz), 1.91 (s, 3H), 1.72–1.79 (m, 2H), 1.35–1.51 (m, 6H). <sup>13</sup>C NMR (100 MHz, CDCl<sub>3</sub>) δ: 170.6, 160.3, 150.8, 129.9, 105.4, 102.2, 99.5, 67.6, 51.7, 41.7, 38.4, 37.2, 29.7, 29.2, 26.5, 25.9, 23.1. ESI MS (*m/z*): 308 [M+H]<sup>+</sup>. HR MS (ESI): *m/z* calculated for C<sub>17</sub>H<sub>30</sub>N<sub>3</sub>O<sub>2</sub>, [M+ H]<sup>+</sup>: 308.2338, found: 308.2321.

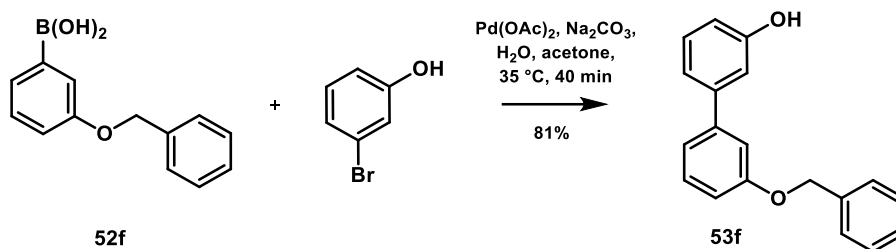
### **3'-Hydroxy-(1,1'-biphenyl)-3-carboxamide (53e)**



3-Bromophenol (0.25 g, 1.44 mmol) and a 0.4 M aqueous solution of Na<sub>2</sub>CO<sub>3</sub> (7.5 mL) were added to a solution of 3-carbamoylphenylboronic acid (51e) (0.25 g, 1.5 mmol) in CH<sub>3</sub>CN (7.5 mL); the reaction mixture was degassed by bubbling N<sub>2</sub> for 10 min and then added Pd(PPh<sub>3</sub>)<sub>4</sub> (10 mg). After stirring at 90 °C for 1.5 h, the reaction mixture was filtered on Celite, and the filtrate was poured in H<sub>2</sub>O and extracted with EtOAc. The combined organic phases were dried over Na<sub>2</sub>SO<sub>4</sub>, filtered, and concentrated *in vacuo* to yield a crude residue that was purified by silica gel column chromatography (EtOAc–cyclohexane 8:2 as eluent). White solid, 97% yield.

Chemical physical data were identical to those previously reported.<sup>89</sup>

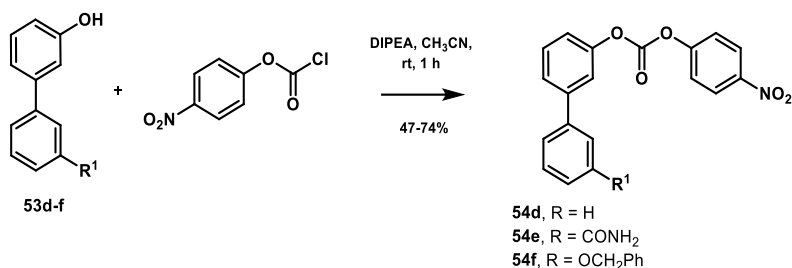
### 3'-(Benzyloxy)-[1,1'-biphenyl]-3-ol (**53f**)



Na<sub>2</sub>CO<sub>3</sub> (0.11 g, 2 mmol), Pd(OAc)<sub>2</sub> (0.001 g), and a solution of 3-bromophenol (0.17, 1 mmol) in H<sub>2</sub>O (0.7 mL) were added to a solution of 3-(benzyloxy)phenylboronic acid **52f** (0.336 g, 2 mmol) in acetone (3 mL), and the resulting mixture was stirred at 35 °C for 40 min. The mixture was extracted with EtOAc, the combined organic phases were dried (Na<sub>2</sub>SO<sub>4</sub>), and the solvent removed by distillation under reduced pressure to yield a crude residue that was purified by silica gel column chromatography (cyclohexane–EtOAc 9:1 as eluent). Oil, 81% yield.

<sup>1</sup>H NMR (400 MHz, CDCl<sub>3</sub>): δ 7.30–7.50 (m, 7H), 7.16–7.23 (m, 3H), 7.06–7.07 (m, 1H), 7.00 (ddd, 1H, *J*<sup>1</sup> = 1.0, *J*<sup>2</sup> = 2.5, *J*<sup>3</sup> = 8.0 Hz), 6.84 (ddd, 1H, *J*<sup>1</sup> = 1.0, *J*<sup>2</sup> = 2.5, *J*<sup>3</sup> = 8.0 Hz), 5.43 (br s, 1H), 5.14 (s, 2H). ESI MS (*m/z*): 275 [M – H]<sup>–</sup>.

### General Procedure for the Synthesis of Carbonates **54d–f**



DIPEA (0.15 mL, 0.8 mmol) and a solution of 4-nitrophenyl chloroformate (0.16 g, 0.8 mmol) in dry CH<sub>3</sub>CN (4 mL) were added dropwise to a solution of the suitable phenol **53d–f** (0.8 mmol) in dry CH<sub>3</sub>CN (2.5 mL), and the resulting mixture was stirred at room temperature for 1 h under a nitrogen atmosphere. Upon completion, the mixture was poured into water and filtered to separate the desired solid precipitate (for **54e**) or extracted with EtOAc (for cpds **54d** and **54f**). The combined organic phases were washed with brine, dried (Na<sub>2</sub>SO<sub>4</sub>), and the solvent removed by distillation under reduced pressure to give a crude residue that was purified by silica gel column chromatography (cyclohexane–EtOAc 9:1 as eluent) and crystallization.

### [1,1'-Biphenyl]-3-yl-(4-nitrophenyl)carbonate (**54d**)

White solid, mp 84–5 °C (EtOAc–petroleum ether); 47% yield.

$^1\text{H}$  NMR (400 MHz,  $\text{CDCl}_3$ ):  $\delta$  8.34 (d, 2H,  $J = 9.0$  Hz), 7.51 (d, 2H,  $J = 9.0$  Hz), 7.37–7.67 (m, 8H), 7.28–7.29 (m, 1H).

### 3'-Carbamoyl-[1,1'-biphenyl]-3-yl-(4-nitrophenyl)carbonate (**54e**)

Amorphous solid, 74% yield.

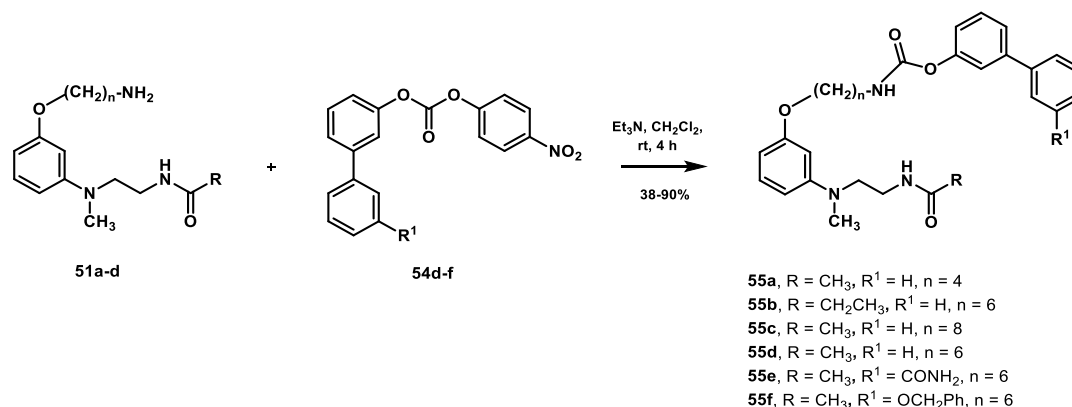
$^1\text{H}$  NMR ( $\text{DMSO}-d_6$ ):  $\delta$  8.38 (d, 2H,  $J = 9.0$  Hz), 8.21 (br s, 1H), 8.12 (br s, 1H), 7.83–7.92 (m, 3H), 7.74 (d, 2H,  $J = 9.0$  Hz), 7.73–7.76 (m, 1H), 7.57–7.64 (m, 2H), 7.45–7.47 (m, 2H). ESI MS ( $m/z$ ): 379  $[\text{M} + \text{H}]^+$ .

### 3'-(Benzyloxy)-[1,1'-biphenyl]-3-yl (4-nitrophenyl)carbonate (**54f**)

Amorphous solid, 50% yield.

$^1\text{H}$  NMR (400 MHz,  $\text{CDCl}_3$ ):  $\delta$  8.34 (d, 2H,  $J = 9.0$  Hz), 7.48 (d, 2H,  $J = 9.0$  Hz), 7.36–7.53 (m, 9H), 7.20–7.29 (m, 3H), 7.01 (dd, 1H,  $J^1 = 2.5$ ,  $J^2 = 8.0$  Hz), 5.14 (s, 2H).

### General Procedure for the Synthesis of *O*-Biphenyl Carbamate Derivatives **55a–f**



A solution of the appropriate amine **51a–d** (0.23 mmol) in dry  $\text{CH}_2\text{Cl}_2$  (2 mL, dry DMF for **55e**) and  $\text{Et}_3\text{N}$  (0.14 mL, 1.05 mmol) was added to an ice-cooled solution (room temperature for **55e**) of the suitable (4-nitrophenyl)carbonate **54d–f** (0.11 g, 0.33 mmol) in dry  $\text{CH}_2\text{Cl}_2$  (2 mL) under a nitrogen atmosphere, and the resulting mixture was stirred for 4 h at room temperature. Upon completion of the reaction, a saturated solution of  $\text{NaHCO}_3$  was added, and the aqueous phase was extracted with  $\text{CH}_2\text{Cl}_2$  (EtOAc for **55e**). The combined organic phases were washed with brine, dried ( $\text{Na}_2\text{SO}_4$ ), and the solvent removed by distillation under reduced pressure to afford a crude residue that was purified by silica gel column chromatography (EtOAc–cyclohexane 8:2 as eluent or EtOAc–MeOH 95:5 for **55e**).

### [1,1'-Biphenyl]-3-yl{4-[3-((2-acetamidoethyl)methylamino)phenoxy]butyl}carbamate (**55a**)

This product was obtained starting from amine **51a** and carbonate **54d**. Amorphous solid, 75% yield.

$^1\text{H}$  NMR(400 MHz,  $\text{CDCl}_3$ ):  $\delta$  7.55– 7.57 (m, 2H), 7.34–7.44 (m, 6H), 7.11–7.16 (m, 2H), 6.29–6.38 (m, 3H), 5.71 (br s, 1H), 5.38 (br s, 1H), 4.04 (t, 2H,  $J = 6.0$  Hz), 3.36– 3.43 (m, 6H), 2.93 (s, 3H), 1.87 (s, 3H), 1.64–1.94 (m, 4H).  $^{13}\text{C}$  NMR (100 MHz,  $\text{CDCl}_3$ ):  $\delta$  170.5, 160.1, 154.7, 151.4, 142.6, 140.3, 130.1, 129.5, 128.7, 128.0, 127.6, 127.1, 127.0, 124.0, 120.4, 105.6, 102.2, 99.6, 67.4, 51.7, 40.9, 38.4, 37.0, 26.7, 26.4, 23.1. ESI MS (m/z): 476 [M + H] $^+$ . HR MS (ESI): m/z calculated for  $\text{C}_{28}\text{H}_{34}\text{N}_3\text{O}_4$ , [M + H] $^+$ : 476.2549, found: 476. 2557.

**[1,1'-Biphenyl]-3-yl{6-[3-(methyl(2-propionamidoethyl)amino)phenoxy]hexyl}carbamate (55b)**

This product was obtained starting from amine **51b** and carbonate **54d**. Oil, 79% yield.

$^1\text{H}$  NMR (400 MHz,  $\text{CDCl}_3$ ):  $\delta$  7.54– 7.59 (m, 2H), 7.35–7.45 (m, 6H), 7.11–7.13 (m, 2H), 6.28–6.38 (m, 3H), 5.64 (br s, 1H), 5.14 (br s, 1H), 3.97 (t, 2H,  $J = 6.5$  Hz), 3.44–3.47 (m, 4H), 3.28–3.34 (m, 2H), 2.94 (s, 3H), 2.11–2.18 (m, 2H) 1.79– 1.83 (m, 2H), 1.61–1.66 (m, 2H), 1.47–1.54 (m, 4H), 1.11 (t, 3H,  $J = 7.5$  Hz).  $^{13}\text{C}$  NMR (100 MHz,  $\text{CDCl}_3$ ):  $\delta$  174.1, 160.3, 154.6, 151.4, 150.8, 142.6, 140.3, 130.0, 129.5, 128.7, 127.5, 127.2, 124.0, 120.4, 105.4, 102.1, 99.6, 67.6, 51.7, 41.2, 38.4, 37.2, 29.7, 29.6, 29.2, 26.4, 25.8, 9.7. ESI MS (m/z): 518 [M + H] $^+$ . HR MS (ESI): m/z calculated for  $\text{C}_{31}\text{H}_{40}\text{N}_3\text{O}_4$ , [M + H] $^+$ : 518.3019, found: 518.3015.

**[1,1'-Biphenyl]-3-yl{8-[3-((2-acetamidoethyl)methylamino)phenoxy]octyl}carbamate (55c)**

This product was obtained starting from amine **51c** and carbonate **54d**. Amorphous solid, 90% yield.

$^1\text{H}$  NMR (400 MHz,  $\text{CDCl}_3$ ):  $\delta$  7.55–7.61 (m, 2H), 7.32–7.47 (m, 6H), 7.09–7.17 (m, 2H), 6.27–6.41 (m, 3H), 5.63 (br s, 1H), 5.10 (br s, 1H), 3.95 (t, 2H,  $J = 6.5$  Hz), 3.44–3.46 (m, 4H), 3.25–3.31 (m, 2H), 1.48–1.52 (m, 2H), 1.34–1.47 (m, 6H).  $^{13}\text{C}$  NMR (100 MHz,  $\text{CDCl}_3$ ):  $\delta$  170.4, 160.4, 154.6, 151.4, 150.9, 142.6, 140.3, 130.0, 129.5, 128.7, 127.5, 127.2, 124.0, 120.4, 105.5, 102.3, 99.7, 67.7, 51.8, 41.3, 38.4, 37.4, 29.8, 29.3, 29.2, 29.1, 26.6, 26.0, 23.2. ESI MS (m/z): 532 [M + H] $^+$ . HR MS (ESI): m/z calculated for  $\text{C}_{32}\text{H}_{42}\text{N}_3\text{O}_4$ , [M + H] $^+$ : 532.3175, found: 532.3183.

**[1,1'-Biphenyl]-3-yl{6-[3-((2-acetamidoethyl)methylamino)phenoxy]hexyl}carbamate (55d)**

This product was obtained starting from amine **51d** and carbonate **54d**. Oil, 85% yield.

$^1\text{H}$  NMR (400 MHz,  $\text{CDCl}_3$ ):  $\delta$  7.56–7.61 (m, 2H), 7.28– 7.47 (m, 6H), 7.11–7.18 (m, 2H), 6.26–6.49 (m, 3H), 5.70 (br s, 1H), 5.18(br s, 1H), 3.98 (t, 2H,  $J = 6.0$  Hz), 3.44–3.46 (m, 4H), 3.26–3.37 (m, 2H), 2.95 (s, 3H), 1.93 (s, 3H), 1.71–1.89 (m, 2H), 1.58–1.65 (m, 6H).  $^{13}\text{C}$  NMR (100 MHz,  $\text{CDCl}_3$ ):  $\delta$  170.5, 160.1, 154.7, 151.4, 142.6, 140.3, 130.1, 129.5, 128.7, 128.0, 127.6, 127.1, 127.0, 124.0, 120.4, 105.6, 102.2, 99.6, 67.5, 51.7, 41.2, 38.5, 37.1, 29.7, 29.3, 26.4, 25.7, 23.1. ESI MS (m/z): 504 [M+H] $^+$ . HR MS (ESI): m/z calculated for  $\text{C}_{30}\text{H}_{38}\text{N}_3\text{O}_4$ , [M + H] $^+$ : 504.2862, found: 504.2856

**3'-Carbamoyl-[1,1'-biphenyl]-3-yl{6-[3-((2-acetamidoethyl) methylamino) phenoxy] hexyl} carbamate (55e)**

This product was obtained starting from amine **51a** and carbonate **54e**. Purification by silica gel chromatography (EtOAc–MeOH 95:5 as eluent). Amorphous solid, 38% yield.

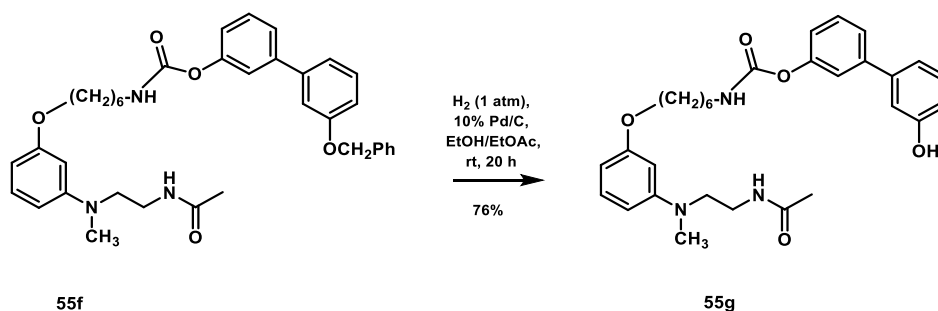
<sup>1</sup>H NMR (400 MHz, CDCl<sub>3</sub>): δ 7.99–8.01 (m, 1H), 7.81 (d, 1H, *J* = 8.0 Hz), 7.37 (d, 1H, *J* = 8.0 Hz), 7.36–7.54 (m, 4H), 7.11–7.15 (m, 2H), 6.46 (br s, 1H), 6.28–6.35 (m, 3H), 5.84 (br s, 1H), 5.73 (br s, 1H), 5.27 (br s, 1H), 3.97 (t, 2H, *J* = 6.5 Hz), 3.39–3.41 (m, 4H), 3.29–3.38 (m, 2H), 2.91 (s, 3H), 1.88 (s, 3H), 1.77–1.84 (m, 2H), 1.60–1.67 (m, 2H), 1.47–1.54 (m, 4H). <sup>13</sup>C NMR (100 MHz, CDCl<sub>3</sub>): δ 170.6, 169.3, 160.3, 154.7, 153.9, 151.5, 141.6, 140.8, 134.0, 130.6, 130.0, 129.7, 129.1, 126.5, 126.2, 124.1, 121.0, 120.6, 105.5, 102.2, 99.6, 67.6, 51.7, 41.1, 38.4, 37.2, 29.6, 29.1, 26.3, 25.7, 23.2. ESI MS (*m/z*): 547 [M + H]<sup>+</sup>. HR MS (ESI): *m/z* calculated for C<sub>31</sub>H<sub>39</sub>N<sub>4</sub>O<sub>5</sub>, [M + H]<sup>+</sup>: 547.2920, found: 547.2940.

**3'-(Benzyloxy)-[1,1'-biphenyl]-3-yl {6-[3-((2-acetamidoethyl) methylamino) phenoxy]hexyl} carbamate (55f)**

This product was obtained starting from amine **51a** and carbonate **54f**. Oil, 57% yield.

<sup>1</sup>H NMR (400 MHz, CDCl<sub>3</sub>): δ 7.32–7.48 (m, 9H), 7.10–7.22 (m, 4H), 6.97 (dd, 1H, *J*' = 2.0, *J*' = 8.0 Hz), 6.29–6.41 (m, 3H), 5.66 (br s, 1H), 5.13 (br s, 1H), 5.12 (s, 2H), 3.97 (t, 2H, *J* = 6.5 Hz), 3.43–3.45 (m, 4H), 3.29–3.34 (m, 2H), 2.93 (s, 3H), 1.92 (s, 3H), 1.77–1.83 (m, 2H), 1.47–1.66 (m, 6H). ESI MS (*m/z*): 610 [M + H]<sup>+</sup>.

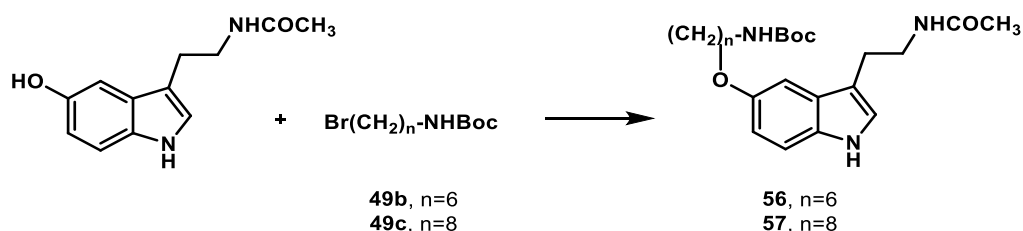
**3'-Hydroxy-[1,1'-biphenyl]-3-yl {6-[3-((2-acetamidoethyl) methylamino) phenoxy] hexyl} carbamate (55g)**



A solution of the benzyloxy derivative **55f** (0.13 g, 0.21 mmol) in EtOH (0.5 mL) and EtOAc (2.5 mL) was hydrogenated (1 atm) at room temperature in the presence of 10% Pd–C (0.03 g) for 20 h. The catalyst was removed by filtration on Celite and the filtrate concentrated under reduced pressure to afford a crude product, which was purified by silica gel chromatography (EtOAc as eluent). Amorphous solid, 76% yield.

$^1\text{H}$  NMR (400 MHz,  $\text{CDCl}_3$ ):  $\delta$  7.38–7.40 (m, 2H), 7.30–7.32 (m, 1H), 7.25–7.29 (m, 2H), 7.07–7.18 (m, 3H), 7.02–7.04 (m, 1H), 6.84 (dd, 1H,  $J^1 = 2.0$ ,  $J^2 = 8.0$  Hz), 6.32–6.37 (m, 3H), 5.81 (br s, 1H), 5.18 (br s, 1H), 3.98 (t, 2H,  $J = 6.5$  Hz), 3.42–3.44 (m, 4H), 3.28–3.33 (m, 2H), 2.91 (s, 3H), 1.93 (s, 3H), 1.76–1.83 (m, 2H), 1.58–1.66 (m, 2H), 1.44–1.57 (m, 4H).  $^{13}\text{C}$  NMR (100 MHz,  $\text{CDCl}_3$ ):  $\delta$  170.1, 160.3, 156.7, 154.9, 151.3, 142.5, 141.7, 130.1, 129.9, 129.5, 124.0, 120.4, 120.3, 119.0, 114.8, 114.2, 105.6, 102.7, 99.9, 67.8, 51.9, 41.1, 38.5, 37.2, 29.6, 29.0, 26.3, 25.7, 23.1. ESI MS ( $m/z$ ): 520 [ $M + H$ ] $^+$ . HR MS (ESI):  $m/z$  calculated for  $\text{C}_{30}\text{H}_{38}\text{N}_3\text{O}_5$ , [ $M + H$ ] $^+$ : 520.2811, found: 520.2798.

### General Procedure for the Synthesis of 5-(*N*-Boc-aminoalkoxy)-*N*-acetyltryptamines **56**–**57**



$\text{K}_2\text{CO}_3$  (0.19 g, 1.4 mmol) was added to a solution of *N*-acetylserotonin (0.10 g, 0.46 mmol) in dry  $\text{CH}_3\text{CN}$  (3 mL), and the resulting mixture was stirred under reflux for 1 h under a nitrogen atmosphere. Then a solution of the suitable *N*-Boc derivative **49b** or **49c** (0.46 mmol) in dry  $\text{CH}_3\text{CN}$  (2 mL) and a catalytic amount of NaI were added, and the resulting mixture was refluxed for 20 h. Water was added to quench the reaction, and the aqueous phase was extracted with EtOAc. The combined organic phases were dried ( $\text{Na}_2\text{SO}_4$ ) and concentrated under reduced pressure to give a crude residue that was purified by silica gel column chromatography (EtOAc as eluent).

#### *tert*-Butyl (6-[[3-(2-Acetamidoethyl)-1*H*-indol-5-yl]oxy]hexyl)carbamate (**56**)

Amorphous solid; 59% yield.

$^1\text{H}$  NMR (400 MHz,  $\text{CDCl}_3$ ):  $\delta$  7.97 (br s, 1H), 7.26 (d, 1H,  $J = 8.5$  Hz), 7.03–7.05 (m, 2H), 6.87 (dd, 1H,  $J^1 = 2.0$ ,  $J^2 = 8.5$  Hz), 5.75 (br s, 1H), 4.55 (br s, 1H), 4.00 (t, 2H,  $J = 6.5$  Hz), 3.59–3.61 (m, 2H), 3.13–3.15 (m, 2H), 2.95 (t, 2H,  $J = 6.5$  Hz), 1.96 (s, 3H), 1.78–1.85 (m, 4H), 1.48 (s, 9H), 1.38–1.56 (m, 4H).

ESI MS ( $m/z$ ): 418 [ $M + H$ ] $^+$ . ESI MS ( $m/z$ ): 416 [ $M - H$ ] $^-$ .

#### *tert*-Butyl (8-[[3-(2-Acetamidoethyl)-1*H*-indol-5-yl]oxy]octyl)carbamate (**57**)

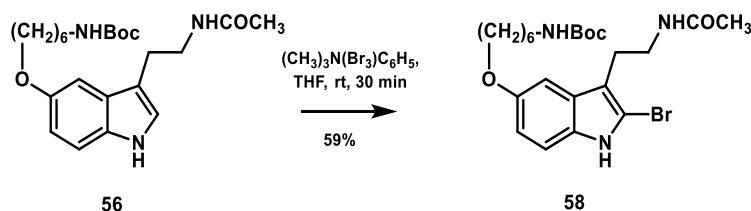
White solid, mp 75–6 °C; (EtOAc petroleum ether), 47% yield.

$^1\text{H}$  NMR (400 MHz,  $\text{CDCl}_3$ ):  $\delta$  8.01 (br s, 1H), 7.27 (d, 1H,  $J = 8.5$  Hz), 7.02–7.04 (m, 2H), 6.88 (dd, 1H,  $J^1 = 2.0$ ,  $J^2 = 8.5$  Hz), 5.75 (br s, 1H), 4.52 (br s, 1H), 4.00 (t, 2H,  $J = 6.5$  Hz), 3.58–3.61 (m, 2H),

3.08–3.11 (m, 2H), 2.95 (t, 2H,  $J = 6.5$  Hz), 1.95 (s, 3H), 1.78–1.82 (m, 2H), 1.45 (s, 9H), 1.42–1.54 (m, 4H), 1.29–1.41 (m, 6H).

ESI MS ( $m/z$ ): 446  $[M + H]^+$ . ESI MS ( $m/z$ ): 444  $[M - H]^-$ .

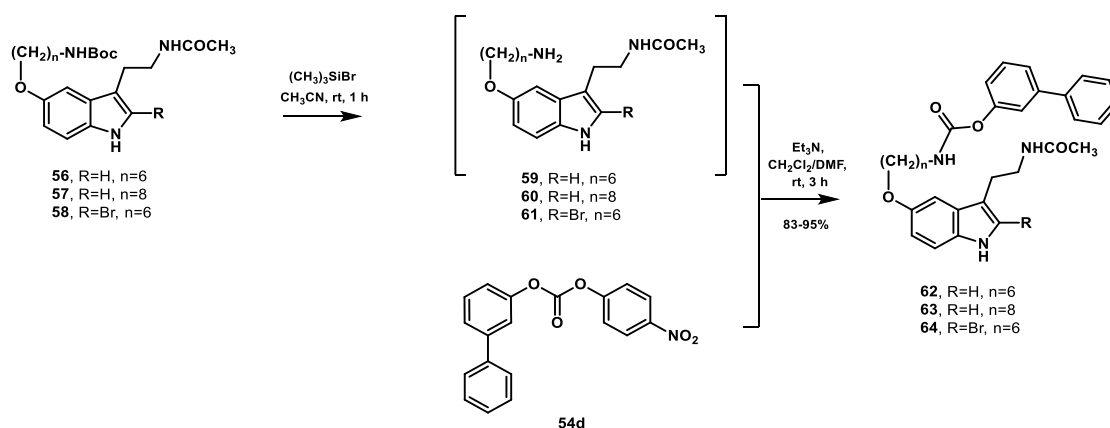
### *tert*-Butyl (6-{{3-(2-Acetamidoethyl)-2-bromo-1*H*-indol-5-yl}oxy}hexyl)carbamate (**58**)



Trimethylphenyl ammonium tribromide (0.050 g, 0.132 mmol) was added to a solution of **56** (0.055 g, 0.132 mmol) in dry THF (2.5 mL), and the resulting mixture was stirred at room temperature for 30 min under a nitrogen atmosphere. After removing the solvent by distillation under reduced pressure, the residue was partitioned between water and EtOAc. The combined organic phases were dried ( $Na_2SO_4$ ) and concentrated under reduced pressure to afford a crude residue that was purified by silica gel column chromatography (EtOAc–cyclohexane 6:4 as eluent). Oil, 59% yield.

$^1H$  NMR (400 MHz,  $CDCl_3$ ):  $\delta$  8.71 (br s, 1H), 7.19 (d, 1H,  $J = 8.5$  Hz), 6.94–6.96 (m, 1H), 6.81 (dd, 1H,  $J^1 = 2.0$ ,  $J^2 = 8.5$  Hz), 5.72 (br s, 1H), 4.63 (br s, 1H), 3.96 (t, 2H,  $J = 6.5$  Hz), 3.51–3.54 (m, 2H), 3.11–3.15 (m, 2H), 2.90 (t, 2H,  $J = 6.5$  Hz), 1.94 (s, 3H), 1.76–1.80 (m, 2H), 1.45 (s, 9H), 1.34–1.52 (m, 6H). ESI MS ( $m/z$ ): 496  $[M + H]^+$ .

### General Procedure for the Synthesis of Indole Target Compounds **62–64**



$(CH_3)_3SiBr$  (48  $\mu$ L, 0.36 mmol) was added to a solution of the suitable *N*-Boc-derivative **56–58** (0.12 mmol) in dry  $CH_3CN$  (1.2 mL), and the resulting mixture was stirred at room temperature for 1 h under a nitrogen atmosphere. Upon completion of the reaction, MeOH was added, and the resulting mixture was concentrated *in vacuo* to give the corresponding crude amine that was used for the next step without any further purification.  $Et_3N$  (0.075 mL, 0.53 mmol) and a solution of the suitable above crude amine



(**59–61**) in dry CH<sub>2</sub>Cl<sub>2</sub> (2 mL) and DMF (0.2 mL) were added to an ice-cooled solution of carbonate **54d** (0.06 g, 0.17 mmol) in dry CH<sub>2</sub>Cl<sub>2</sub> (1 mL) under a nitrogen atmosphere, and the resulting mixture was stirred at room temperature for 3 h. The reaction mixture was neutralized by addition of an aqueous saturated solution of NaHCO<sub>3</sub> and extracted with CH<sub>2</sub>Cl<sub>2</sub>. The combined organic phases were dried (Na<sub>2</sub>SO<sub>4</sub>) and concentrated under reduced pressure to afford a crude residue that was purified by column chromatography.

**[1,1'-Biphenyl]-3-yl(6-((3-(2-aminoethyl)-1H-indol-5-yl)oxy)hexyl)carbamate (62)**

Purification by silica gel chromatography (EtOAc as eluent) and crystallization. White solid, mp 100–1 °C (EtOAc–petroleum ether); 83% yield.

<sup>1</sup>H NMR (400 MHz, CDCl<sub>3</sub>): δ 8.02 (br s, 1H), 7.55–7.59 (m, 2H), 7.41–7.45 (m, 4H), 7.33–7.37 (m, 2H), 7.24–7.26 (m, 1H), 7.10–7.13 (m, 1H), 7.05 (d, 1H, *J* = 2.0 Hz), 6.99–7.02 (m, 1H), 6.89 (dd, 1H, *J*<sup>1</sup> = 2.0, *J*<sup>2</sup> = 8.5 Hz), 5.70 (br s, 1H), 5.20 (br s, 1H), 4.03 (t, 2H, *J* = 6.5 Hz), 3.57–3.60 (m, 2H), 3.31–3.34 (m, 2H), 2.93 (t, 2H, *J* = 6.5 Hz), 1.93 (s, 3H), 1.81–1.88 (m, 2H), 1.43–1.70 (m, 6H). <sup>13</sup>C NMR (100 MHz, CDCl<sub>3</sub>): δ 170.8, 154.6, 153.5, 151.4, 142.6, 140.3, 131.5, 129.5, 128.7, 127.8, 127.5, 127.2, 127.1, 124.0, 122.7, 120.4, 113.0, 112.7, 111.9, 101.8, 68.7, 41.2, 39.8, 29.8, 29.3, 26.5, 25.8, 25.3, 23.3. ESI MS (*m/z*): 514 [M + H]<sup>+</sup>. HR MS (ESI): *m/z* calculated for C<sub>31</sub>H<sub>36</sub>N<sub>3</sub>O<sub>4</sub>, [M + H]<sup>+</sup>: 514.2706, found: 514.2700.

**[1,1'-Biphenyl]-3-yl(8-((3-(2-aminoethyl)-1H-indol-5-yl)oxy)octyl)carbamate (63)**

Purification by silica gel chromatography (EtOAc as eluent) and crystallization. White solid, mp 108–9 °C (EtOAc–petroleum ether); 95% yield.

<sup>1</sup>H NMR (400 MHz, CDCl<sub>3</sub>): δ 7.96 (br s, 1H), 7.57–7.60 (m, 2H), 7.41–7.46 (m, 4H), 7.35–7.38 (m, 2H), 7.25–7.29 (m, 1H), 7.10–7.14 (m, 1H), 7.04–7.05 (d, 1H, *J* = 2.0 Hz), 7.01–7.03 (m, 1H), 6.88 (dd, 1H, *J*<sup>1</sup> = 2.0, *J*<sup>2</sup> = 8.5), 5.68 (br s, 1H), 5.10 (br s, 1H), 4.01 (t, 2H, *J* = 6.5 Hz), 3.57–3.62 (m, 2H), 3.27–3.32 (m, 2H), 2.94 (t, 2H, *J* = 6.5 Hz), 1.93 (s, 3H), 1.80–1.85 (m, 2H), 1.26–1.67 (m, 10H). <sup>13</sup>C NMR (100 MHz, CDCl<sub>3</sub>): δ 170.8, 154.6, 153.5, 151.4, 142.6, 140.3, 131.5, 129.5, 128.7, 127.8, 127.5, 127.2, 124.0, 122.7, 120.4, 113.0, 112.7, 111.9, 101.7, 68.8, 41.3, 39.8, 29.8, 29.4, 29.2, 29.1, 26.6, 26.0, 25.2, 23.3. ESI MS (*m/z*): 542 [M + H]<sup>+</sup>. HR MS (ESI): *m/z* calculated for C<sub>33</sub>H<sub>40</sub>N<sub>3</sub>O<sub>4</sub>, [M + H]<sup>+</sup>: 542.3019, found: 542.3044.

**[1,1'-Biphenyl]-3-yl(6-((3-(2-aminoethyl)-2-bromo-1H-indol-5-yl)oxy)hexyl)-carbamate (64):**

Purification by silica gel chromatography (cyclohexane–EtOAc 7:3 as eluent). Amorphous solid; 83% yield. <sup>1</sup>H NMR (400 MHz, CDCl<sub>3</sub>): δ 8.18 (br s, 1H), 7.54–7.57 (m, 2H), 7.40–7.43 (m, 4H), 7.37–7.39 (m, 2H), 7.13 (d, 1H, *J* = 8.5 Hz), 7.11–7.15 (m, 1H), 6.97–6.99 (m, 1H), 6.83 (dd, 1H, *J*<sup>1</sup> = 2.0, *J*<sup>2</sup> =

8.5 Hz), 6.18 (br s, 1H), 5.27 (br s, 1H), 4.01 (t, 2H,  $J = 6.5$  Hz), 3.48–3.52 (m, 2H), 3.30–3.31 (m, 2H), 2.89 (t, 2H,  $J = 6.5$  Hz), 1.94 (s, 3H), 1.80–1.84 (m, 2H), 1.62–1.67 (m, 2H), 1.44–1.57 (m, 4H).  $^{13}\text{C}$  NMR (100 MHz,  $\text{CDCl}_3$ ):  $\delta$  171.0, 154.8, 153.8, 151.4, 142.6, 140.3, 131.3, 129.6, 128.7, 128.1, 127.6, 127.2, 124.0, 120.4, 120.4, 112.8, 111.9, 111.5, 108.9, 101.2, 68.7, 41.2, 39.6, 29.7, 29.2, 26.5, 25.8, 24.7, 22.9. ESI MS ( $m/z$ ): 592  $[\text{M}+\text{H}]^+$ . HR MS (ESI):  $m/z$  calculated for  $\text{C}_{31}\text{H}_{35}\text{N}_3\text{O}_4\text{Br}$ ,  $[\text{M} + \text{H}]^+$ : 592.1811, found: 592.1844.

## **Section II: C8-Substituted Temozolomide Derivatives: SAR Studies and Effects on Stability**

The following work has been conducted during my period of visiting spent abroad at the University of Illinois at Urbana-Champaign under the guidance of Professor Paul Hergenrother

## 2.1 Introduction and Aim of the Work

### 2.1.1 General Introduction

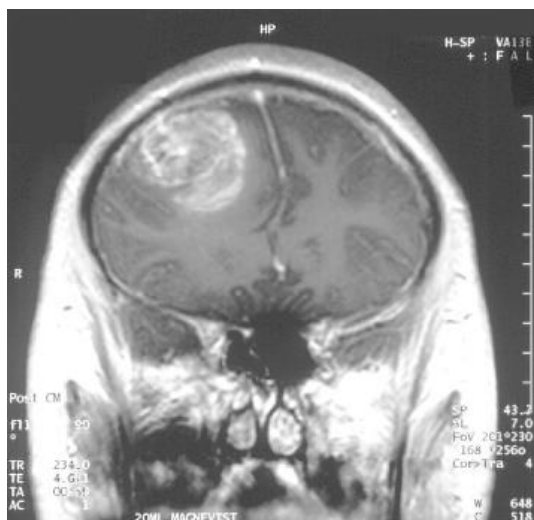
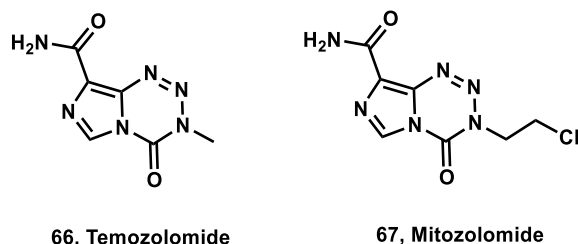


Figure 26 Glioblastoma (astrocytoma) WHO grade IV - MRI coronal view, post contrast. 15 year old boy.

Gliomas are the most common adult primary tumors affecting the central nervous system (CNS) with an annual incidence in the USA of 5–8/ 100,000 population.<sup>90</sup> Gliomas are neuroepithelial tumors currently subclassified by the World Health Organization (WHO) according to the morphological appearance into astrocytic, oligodendroglial, ependymal, and choroid plexus tumors, ranging from low (grade I) to high (grade IV) based on histological tumor aberrations hallmarks such as nuclear atypia, mitotic activity, endothelial hyperplasia, and necrosis.<sup>91</sup> About half of all newly diagnosed gliomas

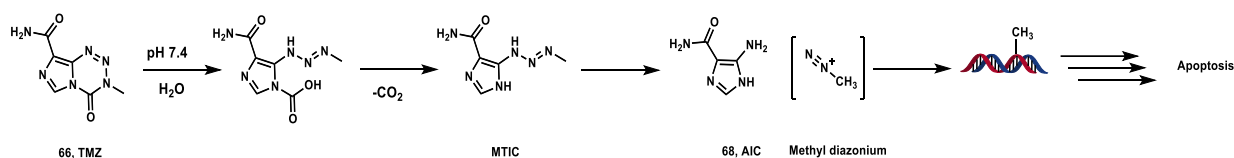
are neoplastic astrocytes and are classified as Glioblastoma (GBM, Astrocytomas grade IV, Figure 26). GBM are the most infiltrative and lethal types of brain cancers and manifest three or four morphological abnormalities. Standard treatment of GBM consists of maximal surgical resection, radiotherapy, and concomitant and adjuvant chemotherapy with temozolomide (TMZ, **66**, Figure 27). Despite surgical resection and genotoxic treatment, median reported survival does not exceed 1 year, highlighting the need for better treatment strategies.<sup>92,93</sup>

TMZ is a small molecule DNA alkylating agent developed for the first time at Aston University, in Great Britain, in 1984 as one of the second-generation imidazotetrazine series.<sup>94</sup> The most active compound of this series was the *N*3- $\beta$ -chloroethyl derivative mitozolomide (**67**, Figure 27). However, mitozolomide development was discontinued during Phase I-II clinical trials after it was found to cause severe and irreversible thrombocytopenia, due to its high DNA-cross-linking ability.<sup>95</sup> Replacement of *N*3- $\beta$ -chloroethyl group by methyl led to the less toxic analogue, with comparable antitumor activity, temozolomide that was approved in 1999, by the US Food and Drug Administration (FDA), for the treatment of anaplastic astrocytoma patients who were refractory to both nitrosourea drug (BCNU or CCNU) and procarbazine. In 2005, FDA and the European Agency approved temozolomide (Temodar® and Temodal® respectively) also for newly diagnosed GBM patients.



*Figure 27 Imidazotetrazine drugs*

Among the beneficial properties contributing to TMZ commercial and clinical success is the benefit of the drug to be administered orally in an outpatients setting. It is well established that TMZ acts as a prodrug, stable at acidic pH values, a property which permits oral administration, but labile above pH 7, with a plasma half-life of 1.8 hours at pH 7.4. Thus, TMZ is rapidly absorbed intact by the digestive system, and once in the bloodstream, easily crosses the BBB due to its lipophilic characteristics. Once TMZ reaches alkaline pH (in tissue such as cerebrospinal fluid and brain), it is spontaneously hydrolyzed in a ring-opening reaction to the open chain triazene active metabolite 5-(3-methyltriazen-1-yl)imidazole-4-carboxamide (MTIC) through a pH dependent hydrolytic attack at C4. MTIC, which is also unstable, breaks down into two parts: 5-aminoimidazole-4-carboxamide (AIC) excreted by kidneys, and the highly reactive methyl diazonium cation, the real active species (Scheme 8).<sup>96</sup>



*Scheme 8 Mechanism of TMZ activation*

The methyl diazonium ion reacts with nucleophilic groups on DNA, resulting in DNA methylation, preferentially at *N7* positions of guanine (*N7*-MG; 70%), but also at the *N3* position of adenine (*N3*-MA; 9%) and at the *O6* position of guanine (*O6*-MG; 6%) (Figure 28).

Products of *N*-methylation are readily repaired by the base-excision repair pathway (BER) and are not major contributors to cytotoxicity. In contrast, the least frequent, methylation of guanine at *O6* (*O6*-MG) is critical for temozolomide cytotoxicity.

There is a narrow pH window close to physiological pH at which the whole process of TMZ prodrug activation to methyl diazonium can occur. Brain tumours possess a more alkaline pH compared with surrounding healthy tissue, a situation that favours prodrug activation preferentially within tumour tissue.<sup>97,98,99,100</sup> Thus TMZ is used to treat (but not exclusively) brain tumours, imparting significant therapeutic benefit to GBM patients.<sup>101</sup>

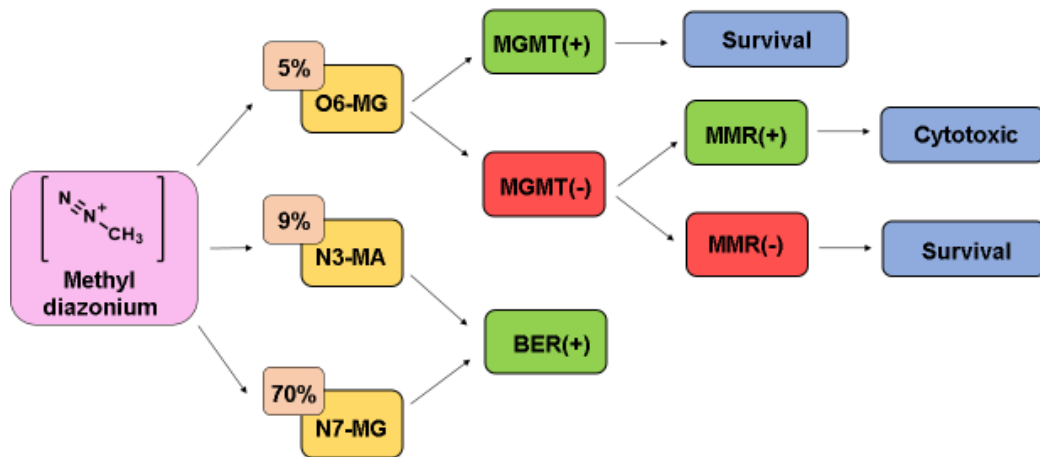


Figure 28 Methyl diazonium-alkylating sites

In normal cells, *O*6-methylguanine (*O*6-MG) lesions are reversed by the suicide enzyme methylguanine DNA methyltransferase (MGMT), which removes the methyl adduct and restores the guanine (Figure 29). Specifically, a cysteine residue in MGMT active site removes the alkyl group through a  $S_N2$  mechanism, protecting cells from carcinogens.

Unrepaired *O*6-MG alerts DNA mismatch repair (MMR) that recognizes this mispairing in the DNA daughter strands and excises it. Therefore, after many cycles of thymine re-insertion and removal, the replication fork collapse, inducing cell cycle arrest and apoptosis.<sup>102,103,104,105</sup>

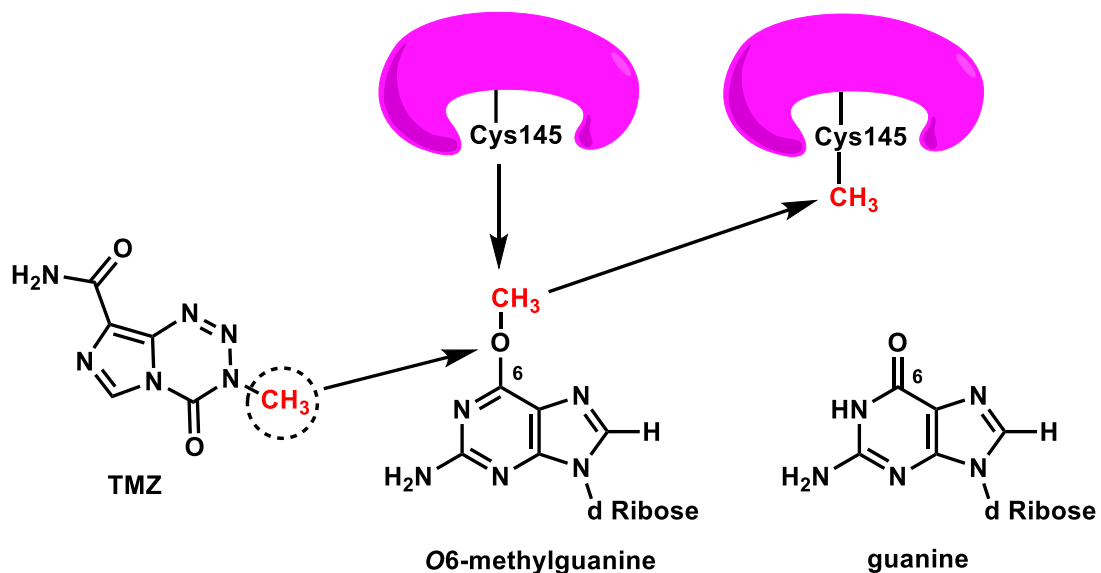


Figure 29 Repair of *O*6-methylguanine adducts by MGMT

However, this suicide enzyme is also able to protect cancer cells from chemotherapeutic drugs such as TMZ and a strong positive correlation exists between MGMT activity and alkylating agent resistance. In gliomas, high MGMT expression has been detected in 45% - 70% of cases.<sup>106,107</sup>

## 2.1.2 Summary of Known SAR on Imidazotetrazines Derivatives

SAR expansion of this class of compounds was limited both by the high sensibility to protic solvents and basic reagents, and by the fact that the usually exploited synthetic procedures require the use of isocyanate, a poisonous gas, or reagents such as *N*-succinimidyl, *N*-methylcarbamate or *N*-methylcarbamic chloride<sup>108</sup> that drastically reduce the cyclization yield. Furthermore, a broad exploration of the link between imidazotetrazine structure and biological activity was precluded by the fact that most of these SAR studies refer to non CNS cancer models,<sup>109</sup> making their translation to GBM tumor models difficult.

The *N*3 substituent seems to be very important for imidazotetrazines antitumor activity. Compounds such as mitozolomide, bearing a *N*3  $\beta$ -chloroethyl substituent, result the most potent ones. Replacement of chloroethyl group by methyl group leads to analogues with retained activity, although slightly lower, whereas substitution by ethyl, bromoethyl, methoxyethyl, chloropropyl, allyl, and other alkyl groups gives compounds without good antitumor activity.<sup>110</sup> The *N*3 substituent also plays a pivotal role in MGMT mediated resistance. In fact, while TMZ shows low potency across MGMT positive tumors, *N*3-methyl replacement by groups such as an alkyne or a 2-(trimethylsilyl)ethoxymethyl (SEM), leads to interesting analogues with *in vitro* growth-inhibitory potency higher than that of TMZ in both MGMT deficient and positive cell lines. Nitrogen shifts from position 7 to 6 is tolerated and leads to pyrazolotriazines series, but these compounds showed lower cytotoxicity than the corresponding imidazotetrazines and are more difficult to synthesize.<sup>111,112</sup> C6 position tolerates hydrogen or small straight-chain alkyl groups, but not branched alkyl substituents.<sup>113</sup>

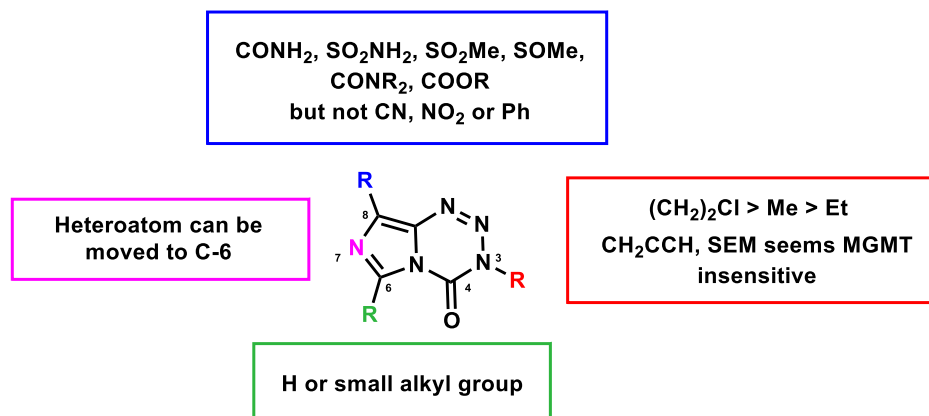
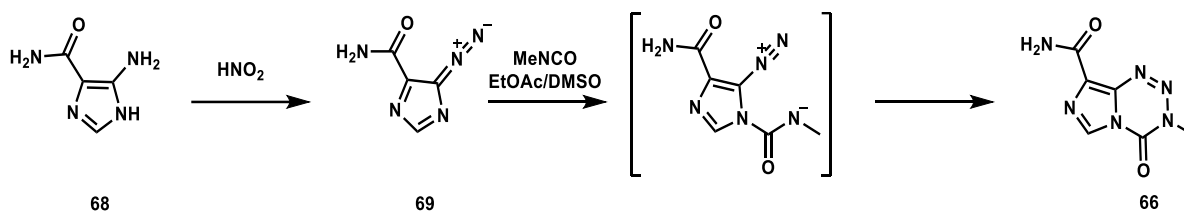


Figure 30 Current SARs of Imidazotetrazines

The TMZ C8 position has never been fully explored. It has been previously suggested that the C8-amide is essential for anticancer activity. Such claims were supported by NMR studies outlining the importance of a C8 hydrogen bond donator to enable TMZ ring-opening in solution.<sup>114,115</sup> However, more recent studies have shown that other functionalities, such as amides and esters, can be tolerated at this position.<sup>116,117,118</sup>

The C8-amide requirement is probably an artifact related to the synthetic approach originally used to prepare imidazotetrazines, involving the reaction of 5-diazoimidazole-4-carboxamide (**69**), prepared by nitrosation of AIC, and an isocyanate (Scheme 9).<sup>119,120</sup> The remarkable stability of diazo **69** that rapidly precipitates out of solution as pure compound, in spite of other soluble diazonium, favored its use in imidazotetrazines synthesis.<sup>121,122</sup>



*Scheme 9 TMZ original synthesis*



### 2.1.3 Aim of the Work

Despite enormous sums of money and vast efforts to identify alternative treatments, even in the era of personalized medicine temozolomide remains the front line drug for treatment of glioblastoma, in patients whose tumors do not express *O6*-methylguanine DNA methyltransferase.<sup>123</sup> However, due to inherent and acquired resistance conferred by multiple mechanisms,<sup>124</sup> TMZ does not increase median survival to over one year, highlighting the need for better treatment strategies.

The principal aspect governing the anticancer activity of imidazotetrazines is the hydrolytic activation of the prodrug. The half-life of TMZ is ~2 hours *in vivo* and in aqueous solution *in vitro*, enabling a discrete TMZ accumulation within the central nervous system before methyldiazonium release (cerebral spinal fluid: blood ratio of 17:83 in human cancer patients).<sup>125,126</sup>

Despite the fact that TMZ has been FDA approved for two decades, the relationship between TMZ half-life and anticancer activity has never been clarified. Indeed, there is lack of information about compound optimal half-life and it is still unclear if these two hours are suitable to maximize its antitumor effect or if longer or shorter half-lives improve the prodrug efficacy.

To understand the relationship between its structure, hydrolytic stability, and anticancer activity, we synthesized new imidazotetrazine derivatives bearing new previously unexplored functionality at the C8 position (such as aliphatic, ketone, halogen, and aryl groups). Specifically, we hypothesized that electronics at C8 may directly translate through imidazotetrazine ring to the C4, and strategic substitutions at this position could be used to tune the hydrolytic stability of imidazotetrazines. Additionally, C8-substitution could also affect the CNS penetrance, with consequences on brain accumulation and the systemic toxicity profile (since myelosuppression limits TMZ dosage).<sup>127,128,129</sup>

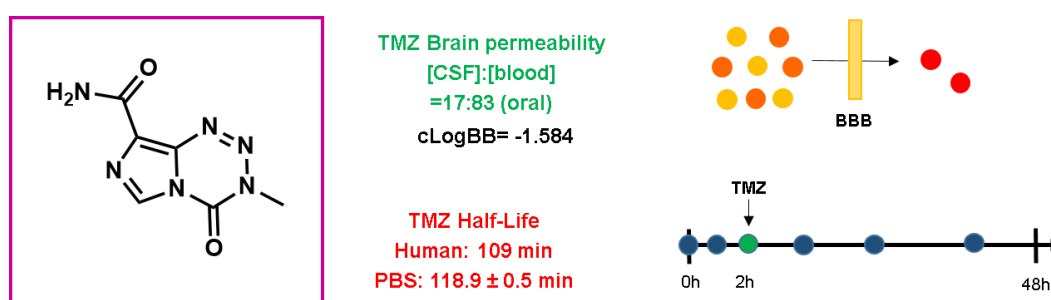


Figure 31 TMZ BBB penetrance and hydrolytic stability

Groups with different electronic characters were inserted at C8, after developing new synthetic approaches. To enhance BBB penetrance, the C8 substituents were also chosen by using calculated cLogBB values<sup>130</sup> (based on compound's cLogP and total polar surface area)<sup>i</sup> and CNS multiparameter optimization (MPO) tool<sup>131,132</sup> (which score is based on six physicochemical properties and spans from

<sup>i</sup> Brain-to-plasma ratio:  $c\text{LogBB} = \text{Log P} - (\text{N} + \text{O})$ ; (N + O) is the number of nitrogen and oxygen atoms).

0 to 6.0) (Figure 32). These types of *in silico* metrics are a well-established measure of compounds hydrophilicity and have been used reliably on several occasions to predict relative changes in biological phenomena, among which the blood-brain barrier penetrance.<sup>133,134,135</sup>

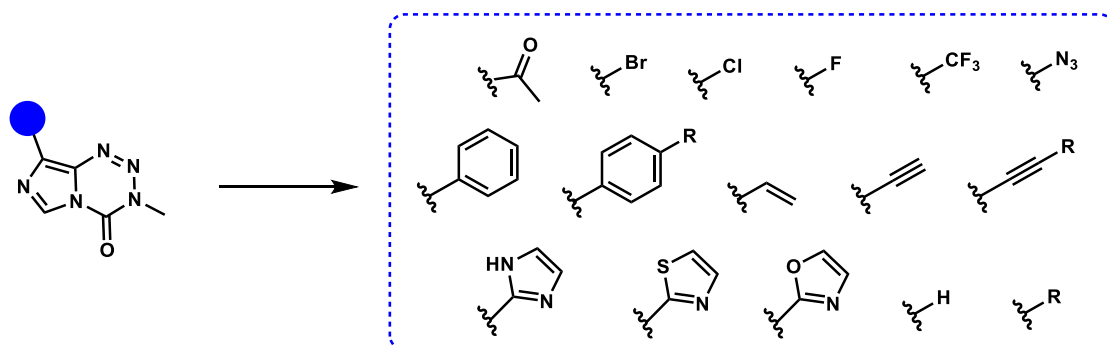


Figure 32 TMZ C8-derivatives with interesting *cLogBB* values, missing from the literature

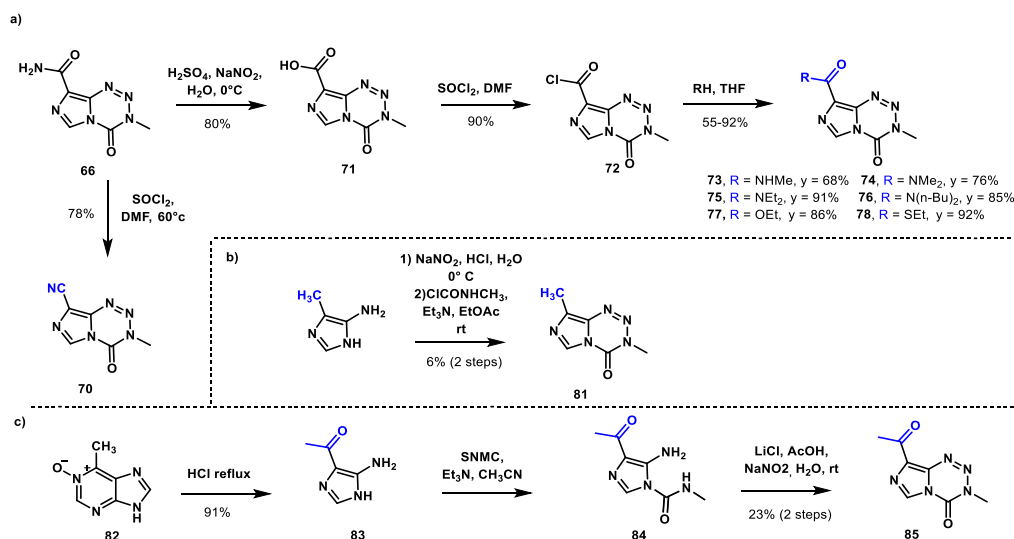
## 2.2 Result and Discussions

To widen the relationship between the structure, hydrolytic stability, and anticancer activity of imidazotetrazines we studied the effects deriving from strategic substitutions at the C8 position.

We began our C8 exploration by alkylation of TMZ amide in order to improve the lipophilicity of the resulting compounds. Derivatives (**73-78**), were synthesized employing established synthetic procedures depicted in Scheme 10a.<sup>136</sup> TMZ amide was converted to the corresponding carboxylic acid derivative **71** in good yield, by using specific acid conditions (a water solution of sodium nitrite and Sulfuric acid).<sup>137</sup> The carboxylic acid **71** was transformed to the corresponding acid chloride (**72**) and then converted to the desired amide (**73-76**), ester (**77**) or thioester (**78**) derivatives by treatment with the appropriate nucleophile. To provide access to cyano derivative **70**, a previously reported procedure of dehydration was employed (thionyl chloride in DMF at 60° C; Scheme 10a).<sup>138</sup>

While certain derivatives (e.g. amides and esters) can be obtained directly from TMZ using validated routes developed for mitozolomide, other derivatives of interest, such as the ketone derivative and those eliminating the carbonyl (aliphatic, halogen and aryl groups), cannot be synthesized using known methods. To have access to these previously unexplored functionality new synthetic methods have been developed.

The synthetic route adopted for the preparation of C8-methyl derivative **81** is outlined in Scheme 10b, and involves the diazotization of commercially available 5-amino-4-methylimidazole, followed by cyclization with the methyl isocyanate surrogate *N*-methylcarbonyl chloride. Considering the imidazotetrazine ring instability to Grignard and alkyl lithium reagents, the ketone derivative **85** was prepared starting from 5-amino-4-methylimidazole **83** that was converted to the intermediate **84** by treatment with *N*-succinimidyl *N*-methylcarbamate, followed by diazotization in the presence of LiCl and spontaneous compound cyclization. The ketone intermediate **83** was prepared according to a previous reported strategy, starting from 6-methylpurine *N*-oxide **82** by oxidation and subsequently hydrolytic degradation (Scheme 10c).<sup>139</sup>



Scheme 10 Synthesis of new C8- derivatives of temozolomide

To introduce an aryl group to the C8 position, two synthetic routes seemed to be feasible (Figure 33). Firstly, a modular intermediate, such as one containing a reactive cross-coupling partner (or a group primed for displacement) can be developed (Figure 33a). This first strategy could give access to a small library of unique derivatives appended directly to the C8 carbon, as the last step of the synthetic sequence.

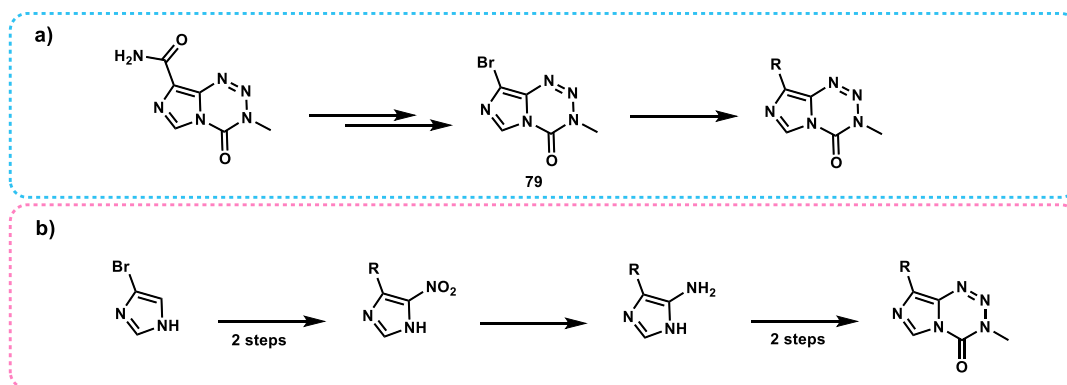
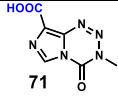
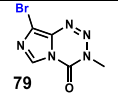


Figure 33 Modular synthetic routes

A classic method to generate carbon–carbon bonds is the palladium-catalysed Suzuki–Miyaura cross-coupling reaction of organoboronic acids with aryl halides.<sup>140</sup> To prepare the C8-bromo key intermediate (**79**), TMZ amide was hydrolyzed to the carboxylic acid derivative (**71**)<sup>141</sup> that was then submitted to several decarboxylative bromination strategies. Classical brominating agents, such as NBS or Ag(II)/Br<sub>2</sub>, were not useful. Conversely, hypervalent iodine reagents, such as Dess–Martin periodinane (DMP) and 2-iodoxybenzoic acid (IBX), in combination with tetraethylammonium bromide (TEAB) allowed getting the desired bromine derivative (**79**), even if in traces (Table 10, entry

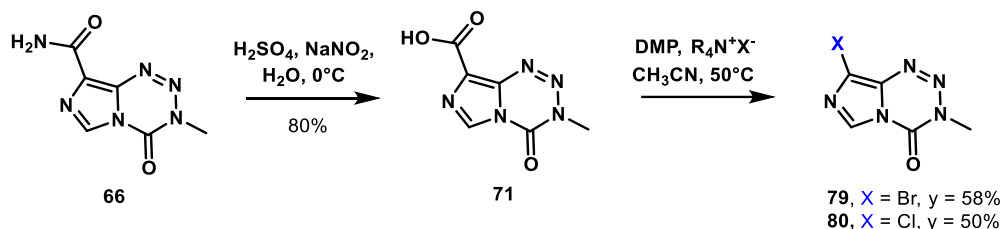
b and d). To improve the product yield, a HPLC screening of the reaction condition have been performed (Table 10), enhancing isolated yield to 58% (Table 10, entry r and Scheme 11). The value of this new strategy, which has never been applied to imidazole rings, is largely due to the employment of mild conditions to successfully convert carboxylic acid compounds in bromine derivatives.

Table 10 Decarboxylative halogenation; Condition screening (HPLC conversion)

Entry	Solvent	Conditions	Temperature (°C)	Time (h)			Isolated yield 79 (%)
a	CH <sub>2</sub> Cl <sub>2</sub>	IBX : TEAB 2 : 2	rt	1	trace	3.3	nd
b	CH <sub>2</sub> Cl <sub>2</sub>	IBX : TEAB 2 : 2	rt	4	trace	8.3	trace
c	CH <sub>2</sub> Cl <sub>2</sub>	DMP : TEAB 1 : 1	rt	1	72.9	13.3	nd
d	CH <sub>2</sub> Cl <sub>2</sub>	DMP : TEAB 1 : 1	rt	4	63.4	16.3	trace
e	CH <sub>2</sub> Cl <sub>2</sub>	DMP : TEAB 1 : 1	rt	20	53.8	8	nd
f	CH <sub>2</sub> Cl <sub>2</sub>	DMP : TEAB 2 : 2	rt	1	82	16.1	nd
g	CH <sub>2</sub> Cl <sub>2</sub>	DMP : TEAB 2 : 2	rt	2	46.6	36.5	nd
h	CH <sub>2</sub> Cl <sub>2</sub>	DMP : TEAB 2 : 2	rt	6	40.6	48	23
i	CH <sub>2</sub> Cl <sub>2</sub>	DMP : TEAB 2 : 2	rt	20	40	23.4	nd
l	CH <sub>2</sub> Cl <sub>2</sub>	DMP : TEAB 3 : 3	rt	2	40	31	nd
m	CH <sub>3</sub> CN	DMP : TEAB 1 : 1	50	2	52.5	31.1	nd
n	CH <sub>3</sub> CN	DMP : TEAB 1 : 1	50	4	52	30.3	nd
o	CH <sub>3</sub> CN	DMP : TEAB 1 : 1	80	1	52	39.4	nd
p	CH <sub>3</sub> CN	DMP : TEAB 1 : 1	80	2	51	28.7	nd
q	CH <sub>2</sub> Cl <sub>2</sub>	DMP : TEAB 2 : 2	50	2	trace	45.6	nd
r	CH <sub>3</sub> CN	DMP : TEAB 2 : 2	50	2	trace	62.9	58
s	CH <sub>2</sub> Cl <sub>2</sub>	DMP : TEAB 3 : 3	rt	2	40	31	nd

nd = not determined

We also explored the possibility to apply this new methodology to synthesize other halo-derivatives by using different tetraalkylammonium salts. While this method worked properly for the chlorine derivative (**80**) (using tetramethylammonium chloride), both iodo and fluorine derivatives cannot be obtained according to this method (Scheme 11).



Scheme 11 Synthesis of C8-halogenated derivatives of temozolomide

In order to obtain the C8-phenyl-imidazotetrazine **89a**, several cross coupling reaction were tested starting from the bromo derivative **79**. However, all coupling attempts were unsuccessful (Table 11), probably due to imidazotetrazine sensitivity to protic solvent and basic reagents.

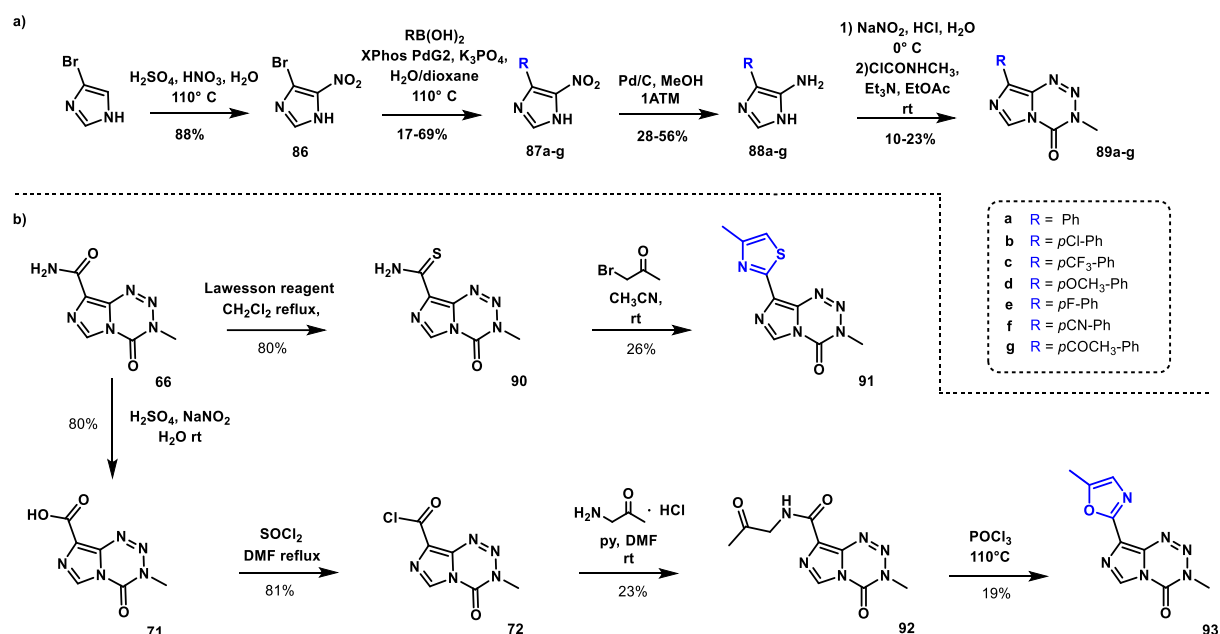
Table 11 Coupling attempts (\*Reaction performed using  $\text{PhSn}(\text{Bu})_3$ ; \*\*Reaction performed on carboxylic acid **71**)

	Catalyst	Additive or Base	Solvent	Temperature °C
<b>a</b>	$\text{Pd}(\text{PPh}_3)_4$	TEBAC / $\text{CsF}$	toluene/ $\text{H}_2\text{O}$	rt; 50; 70
<b>b*</b>	$\text{Pd}(\text{PPh}_3)_2$	$\text{CsF}$	toluene	rt; 50; 70
<b>c</b>	$\text{Pd}(\text{PPh}_3)_4$	$\text{Na}_2\text{CO}_3$	DME/ $\text{H}_2\text{O}$	rt; 110
<b>d</b>	$\text{PdCl}_2$	$\text{Bu}_2\text{NH}$	DMF	rt; 60; 100
<b>e</b>	XPhos PdG2	$\text{Na}_2\text{CO}_3$	DME/ $\text{H}_2\text{O}$	rt; 90
<b>f**</b>	BrettPhos PdG1	$\text{Cu}(\text{OAc})_2 / \text{LiCl}$	$\text{CH}_3\text{CN}$	rt; 50
<b>g</b>	XPhos PdG2	$\text{K}_3\text{PO}_4$	Dioxane/ $\text{H}_2\text{O}$	rt; 110
<b>h</b>	BrettPhos PdG1	$\text{K}_3\text{PO}_4$	Dioxane/ $\text{H}_2\text{O}$	rt; 110

A second alternative method involves imidazole scaffold functionalization, followed by imidazole-derivative cyclization (Figure 33b). This second route, even if longer, appears to be more feasible. Briefly, 5-nitro-4-bromimidazole (**86**) was submitted to Suzuki coupling reaction with the suitable phenylboronic acids in the presence of a different palladium catalyst. While classic catalyst (e.g.  $\text{PdCl}_2(\text{PPh}_3)_2$ ,  $\text{Pd}(\text{dba})_2$ ) did not prove useful, XPhos Palladacycle enabled the preparation of the desired compound **87a-h**, which were subsequently reduced to corresponding **88a-h** by Pd-catalyzed hydrogenation. The obtained amines **88** were then cyclized to the final aryl-substituted imidazotetrazine

(**89a-h**) by diazotization and subsequently treatment with *N*-methylcarbamic chloride in EtOAc (Scheme 12a).

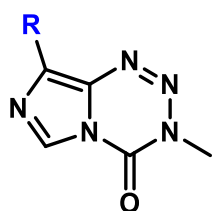
Finally, to further explore C8-SAR, heterocyclic compounds **91** and **93** were built on TMZ amide. Specifically, using Lawesson reagent, TMZ amide was converted to corresponding thioamide (**90**) which, upon cyclization with  $\alpha$ -bromoacetone, led to the target 4-methylthiazole **91**. The target compound **93** was prepared according to a well-validated route for similar compounds,<sup>118</sup> involving TMZ amide activation to the corresponding acid chloride **72**, followed by nucleophilic substitution with the suitable amide and final cyclization with POCl<sub>3</sub> (Scheme 12b).



Scheme 12 Synthesis of C8-aryl and -heteroaryl derivatives of temozolomide

Anticancer activity of new C8-substituted imidazotetrazines was evaluated against a series of human GBM cell lines (Table 12). Cell lines both expressing and lacking MGMT were included and cytotoxicity of each compound was compared to that of TMZ. Consistently with the literature, MGMT deficient cell lines were sensitive to TMZ ( $IC_{50} \leq 51 \mu M$ ), whereas those MGMT positive were resistant ( $IC_{50} \geq 322 \mu M$ ). Cyano derivative **70** and carboxylic acid derivative **71**, similarly to mitozolomide analogues, were inactive. Conversely, amide, ester and thioester derivatives proved to be as active as TMZ in the absence of MGMT and more potent in cell lines expressing the enzyme. The retention of activity for these compounds supports our hypothesis concerning the C8-hydrogen bond donating non-necessity. Likewise, imidazotetrazines lacking the carbonyl group (e.g. halogenated, aryl and heteroaryl derivatives) proved to be as or more effective against U87 and D54 cell lines, and significantly more potent in those expressing MGMT (U118MG, T98G and U3054MG). In particular, insertion of methyl or phenyl substituent at C8 position afforded to the most active compounds across all cell lines.

Table 12 C8 substituted imidazotetrazines-IC<sub>50</sub> value (μM) in multiple GBM cell lines



MGMT(-)    MGMT(-)    MGMT(+)    MGMT(+)    MGMT(+)

Compound	R	U87	D54	U118MG	T98G	U3054MG
<b>66</b> (TMZ)	CONH <sub>2</sub>	51 ± 8	12 ± 1	322 ± 7	660 ± 10	370 ± 40
<b>70</b>	CN	500 ± 60	91 ± 6	670 ± 20	>1000	870 ± 60
<b>71</b>	COOH	320 ± 7	130 ± 8	370 ± 20	321 ± 8	nd
<b>73</b>	CONHMe	49 ± 7	11 ± 1	280 ± 20	580 ± 20	229 ± 20
<b>74</b>	CONMe <sub>2</sub>	40 ± 20	12 ± 5	130 ± 30	250 ± 60	132 ± 6
<b>75</b>	CONEt <sub>2</sub>	80 ± 30	13 ± 2	80 ± 10	160 ± 40	nd
<b>76</b>	CON(n-Bu) <sub>2</sub>	27 ± 6	11 ± 2	62 ± 2	140 ± 20	nd
<b>77</b>	COOEt	66 ± 3	7 ± 1	180 ± 20	236 ± 10	nd
<b>78</b>	COSEt	64 ± 21	8 ± 1	165 ± 4	327 ± 4	nd
<b>79</b>	Br	26 ± 7	20 ± 1	84 ± 17	55 ± 14	nd
<b>80</b>	Cl	15 ± 4	21 ± 4	60 ± 20	60 ± 10	87 ± 4
<b>81</b>	Me	3 ± 1	6 ± 3	7 ± 1	6 ± 1	nd
<b>85</b>	COMe	44 ± 6	18 ± 1	115 ± 9	240 ± 20	125 ± 4
<b>89a</b>	Ph	9 ± 1	7 ± 1	3 ± 1	14 ± 1	18 ± 1
<b>89c</b>	pCF <sub>3</sub> -Ph	16 ± 1	nd	nd	>100	nd
<b>91</b>	4-Me-Thiaz	9 ± 1	8 ± 1	12 ± 2	31 ± 4	nd
<b>93</b>	5Me-Ox	27 ± 4	9 ± 1	70 ± 20	100 ± 20	123 ± 6

Panel of C8-substituted imidazotetrazines and associated IC<sub>50</sub> values (μM) in multiple GBM cell lines. Cell lines were incubated with compound for 7 days then viability was assessed using the Alamar Blue assay. Error is SEM, n≥3.

As already mentioned, despite being known since 1984, FDA approved since 1999, and reaching \$1 billion in sales in 2009, the relationship between TMZ hydrolytic stability and anticancer activity is unknown and specifically, there is a scarce information on the compound optimal half-life. Towards this end, effects of compounds with C8 substituents were evaluated in buffered saline, using PBS, which mimics *in vivo* conditions. A HPLC assay was developed to quantify the fraction of prodrug in solution remained intact after 2 hours at pH 7.4, 37°C. In this condition, TMZ showed a half-life of 119 minutes. The results of this experiment confirmed that the electronic effects of the substituent hanging at C8 dramatically influenced prodrug stability, leading to 2 h-stabilities ranging from 0% to 97% (Figure 34).

Since the electronic character of the group at C8 has a clear effect on the hydrolysis rate of the prodrug, substituents Hammett constants ( $\sigma_p$ )<sup>142</sup> were mapped against the percentage remaining after two hours. This value, derived by Hammett in 1937 from the ionization constants of benzoic acids para substituted, is based on substituent inductive and mesomeric effects. As shown in Figure 34, rendering C8 positions more electron-rich increases the prodrug stability (e.g. **81**;  $\sigma_p = -0.17$ , half-life 40 h), while replacing the amide with more electron withdrawing functionality decreases the stability (e.g. **70**;  $\sigma_p =$



0.66, half-life 0.5 h). Additionally, compound stability seems strictly related to *in vitro* anticancer activity. While compounds displaying lower anticancer activities against cell lines are mainly characterized by very short hydrolytic half-lives, those with remarkable stability and very long half-lives showed the greatest potency *in vitro*. Indeed, a very short half-life probably give rise to hydrolysis too quickly, which will release methyl diazonium before accumulating in the DNA microenvironment. Conversely, long half-life, enable compound distribution to the nucleus before its activation, thus leading to a high anticancer potency. Compounds possessing substituents with electronic sigma values ranging from  $0.23 \leq \sigma_p \leq 0.50$ , then close to TMZ ones ( $\sigma_p = 0.36$ , half-life  $\sim 2$  h) showed similar stability and potency in culture.

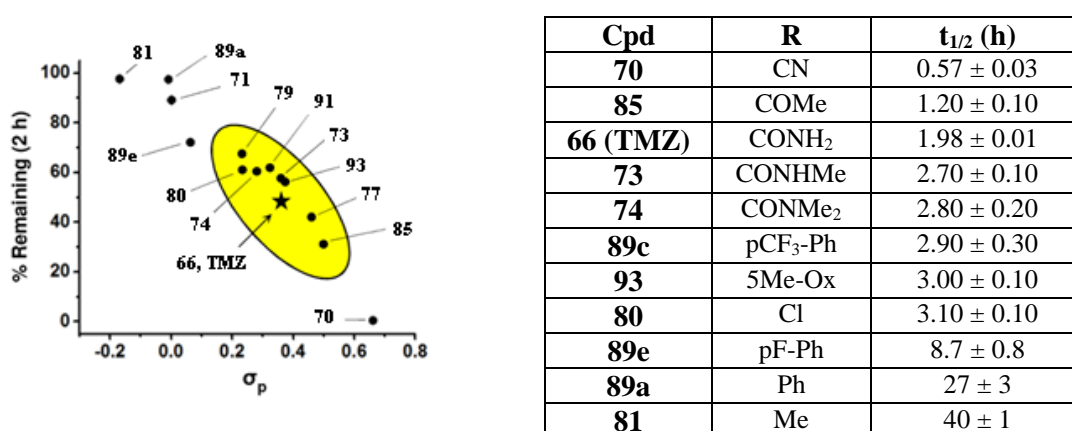


Figure 34 Hydrolytic stability of C8-substituted imidazotetrazines. (left) The percentage of compound remaining after 2 hours plotted against the Hammett constant of its C8 substituent. Compounds with hydrolytic stability similar to TMZ are enclosed in the oval. (right) Half-lives of select C8 derivatives in PBS (pH 7.4, 37°C).

Among beneficial pharmacokinetic properties of TMZ is its ability to avoid primary metabolism. To determine if the C8 modifications lead to significant metabolic liability, the stabilities of select compounds were tested in the presence of mouse liver microsomes and compared to control runs without microsomes. As shown in Table 13, TMZ is insensitive to metabolic perturbation. Amide-alkylation (**73-75**) enhances microsomes susceptibility and particularly, alkylation with larger substituents, as shown for compound **76**, proved to be detrimental for compounds metabolic stability. The ketone (**85**) and the chlorine (**80**) have revealed compounds with interesting microsomes stability, suggesting that for these compounds hydrolysis could drive the *in vivo* pharmacokinetics as for TMZ.

Table 13 C8-Metabolic stability and cLogBB and CNS MPO values for relevant C8 analogs

Compound	Stability 2h, Microsomes	Stability 2h, No Microsomes	cLogBB	CNS MPO
<b>Propranolol</b>	68 ± 2	102 ± 3	nd	nd
<b>66, TMZ</b>	87 ± 6	86 ± 4	-1.58	4.9
<b>73</b>	86 ± 1	93 ± 1	-1.34	5.7
<b>74</b>	81 ± 2	92 ± 3	-1.18	6.0
<b>75</b>	81 ± 1	95 ± 2	-1.07	6.0
<b>76</b>	1 ± 1	98 ± 3	-0.78	5.6
<b>80</b>	91 ± 3	91 ± 1	-0.72	6.0
<b>85</b>	70 ± 1	77 ± 3	-1.08	6.0
<b>89a</b>	44 ± 2	103 ± 5	-0.56	5.7
<b>93</b>	71 ± 1	95 ± 4	-1.19	5.9

The metabolic stability was assessed in mouse liver microsomes. Compounds were incubated in microsomes for 2 h, then the residual substrate was quantified relative to t0. Experiments assessing stability in the absence of microsomes were identical but replacing liver microsomes with PBS. Error is SEM, n≥2. Internal standard = N3-propyl TMZ. Blood

To verify if replacing the amide at C8 could be a viable strategy to increase BBB penetrance and to reach enhanced brain concentrations, selected compounds showing great antitumor activity, appropriate hydrolytic and metabolic stability, and optimal cLogBB and CNS MPO values, have been assessed *in vivo* for their brain penetrance.

First, the BBB penetrance of top compounds was evaluated head-to-head with TMZ. In an initial experiment, the mono- (**73**) and di- (**74**) methylated compounds were tested (Figure 35b). Unfortunately, due to their fast metabolisms, **73** and **74**, even if showed enhanced brain concentration after five minutes, displayed brain-blood *ratio* equivalent to TMZ ones.

To verify if compounds with higher predicted BBB penetrance could reach an increased brain permeability, in a second experiment the oxazole **93** and the ketone **85** were assessed with TMZ and the dimethyl derivative **74**. While TMZ had an absolute brain-blood *ratio* of 8:92, **93** and **85** boasted this *ratio* of 55:45 and 69:31, respectively, confirming our hypothesis (Figure 35e).

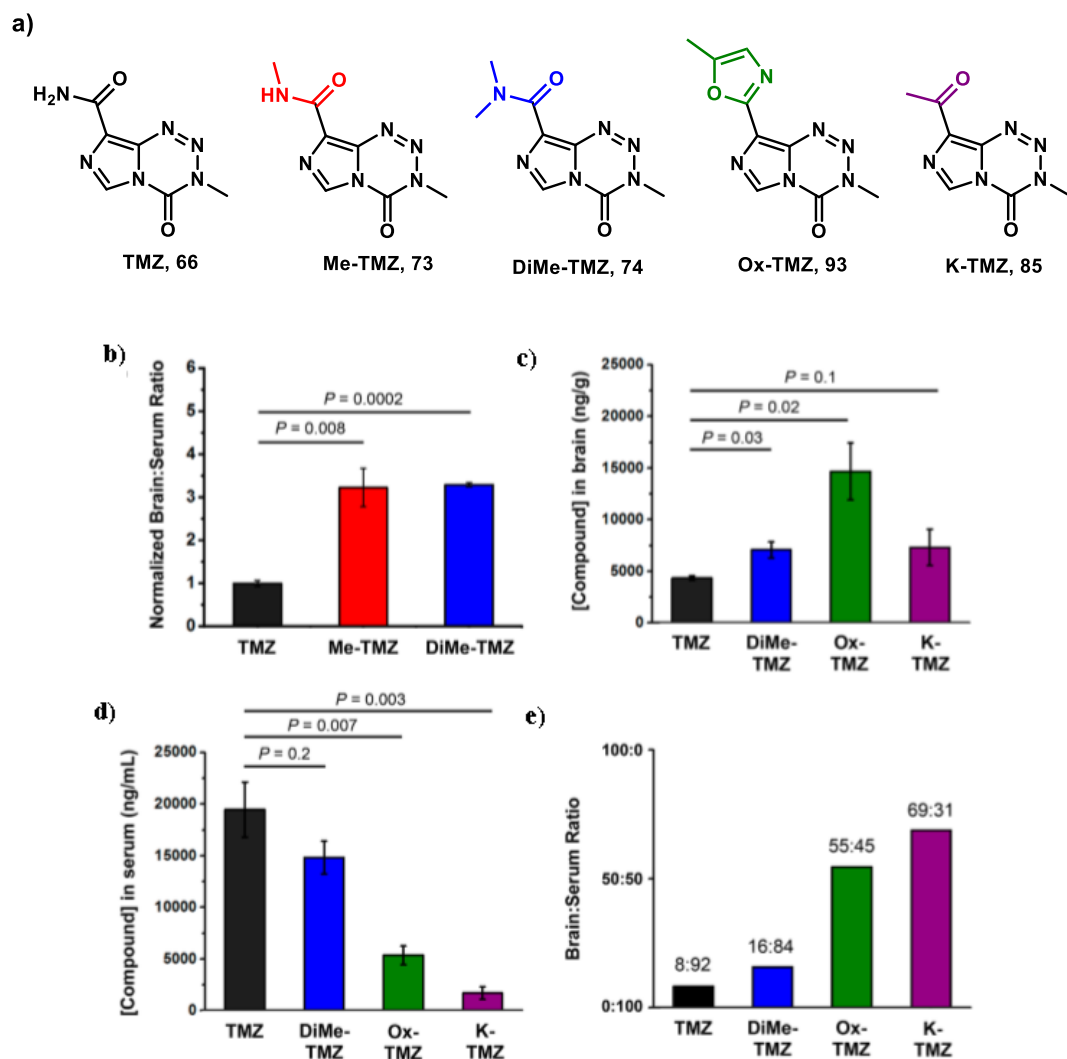


Figure 35 Blood-brain barrier permeability of imidazotetrazines. (a) Structures of lead C8-substituted compounds. (b) Relevant brain:serum ratios of TMZ, Me-TMZ, and DiMe-TMZ (25 mg/kg) were measured 5 minutes after IV injection into mice. Values are the fold change of brain:serum ratio relative to TMZ. In a second experiment, brain (c) and serum (d) concentrations of TMZ and C8 analogs (25 mg/kg) were quantitated 5 minutes after IV injection into mice. (e) Brain:serum ratios were calculated based on (c) and (d) assuming a mouse blood volume of 58.5 mL/kg. Error is SEM, number of mice per cohort = 3. Statistical significance was determined by using a two-sample Student's *t*-test (two-tailed test, assuming equal variance).

The elevated brain concentration of compounds **93** and **85** might decrease *in vivo* hematological toxicity of imidazotetraazines. Since myelosuppression, which occurs in ~20% of TMZ-treated patients, is the major dose-limiting TMZ toxicity,<sup>143</sup> in order to prove our hypothesis an *in vivo* study have been assessed. Specifically, mice were treated with a single dose of 125 mg/kg TMZ, **93** or **85** intravenously and, after 7 days, their blood was collected and analyzed. In this experiment, while TMZ produced severe myelosuppression by white blood cell (WBC) depletion and both lymphocyte and neutrophil concentration decrease, treatment with **93** or **85** did not give rise to hematological toxicity (Figure 36 and 37).

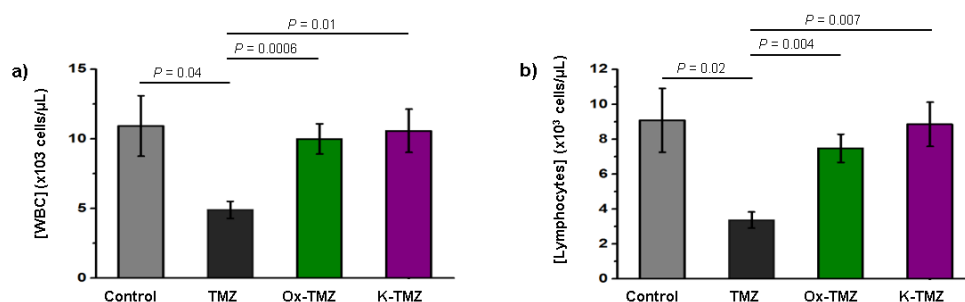


Figure 36 Assessment of the hematological toxicity of imidazotetraazines *in vivo*. Mice were administered a single IV dose of 125 mg/kg imidazotetraazine. After 7 days, whole blood was collected and a complete blood count was obtained for each individual mouse. (a) Total WBC count. Control vs. Ox-TMZ:  $P = 0.7$ , Control vs. K-TMZ:  $P = 0.9$ . (b) Lymphocyte concentrations. Control vs. Ox-TMZ:  $P = 0.5$ , Control vs. K-TMZ:  $P = 0.9$ . Error is SEM, number of mice per cohort = 4. Statistical significance was determined by using a two-sample Student's *t*-test (two-tailed test, assuming equal variance).

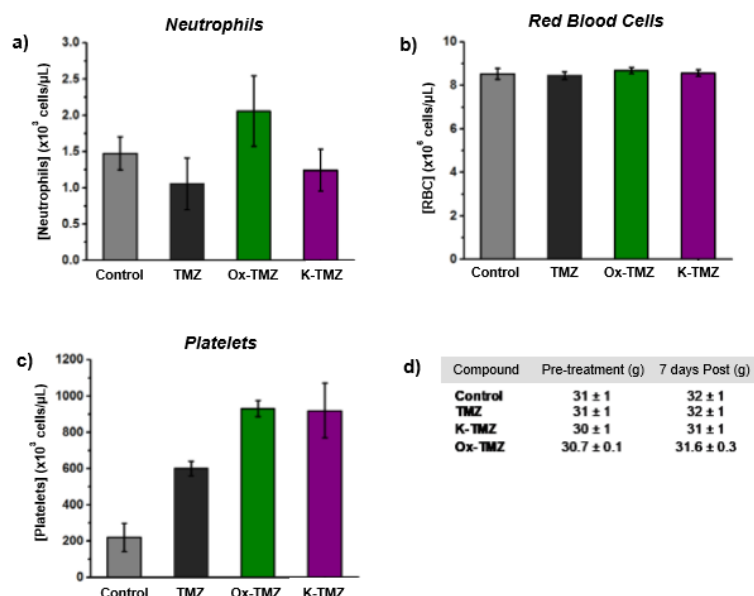


Figure 37 Assessment of the hematological toxicity of imidazotetraazines *in vivo*. Mice were treated with a single IV dose of 125 mg/kg imidazotetraazine and a complete blood count was obtained for each mouse after 7 days. (a) Neutrophil concentrations (b) RBC concentrations (c) Platelet concentrations (d) Cohort weights of mice prior to treatment and at the time of blood collection 7 days post-treatment. Error is SEM, number of mice per cohort = 4.

Finally, *in vivo* anticancer activity of most interesting imidazotetrazines was evaluated. Mice were implanted intracranial with GBM oncosphere Br23c cells, which accurately recapitulate the genetic and histopathological features of human GBM.<sup>144</sup> In the first experiment, five days post implantation, mice were orally treated with 15 mg/kg TMZ or equimolar equivalent of Me-TMZ (**73**) or DiMe-TMZ (**74**). Compounds **73** and **74** outperformed TMZ by increasing median survival by 24% and 46%, respectively, suggesting that increasing the BBB permeability of imidazotetrazine prodrugs is a viable strategy to improve anticancer efficacy (Figure 38a). For this reason, in a second experiment mice were orally treated with TMZ or DiMe-TMZ (**74**) or ketone **85**. This study (Figure 38b) supported our hypothesis, since mice treated with **85** achieved an extended median survival over 50 days past TMZ-treated mice.

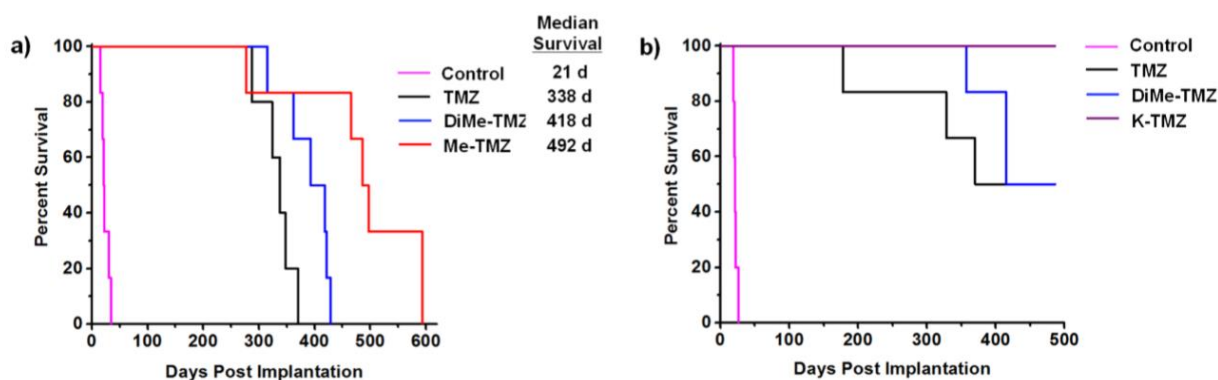


Figure 38 Evaluation of imidazotetrazines in intracranial mouse models of GBM. GBM Br23c oncospheres were intracranially implanted into female athymic nude mice. Treatment was started 5 days post implantation. (a) Mice were administered 15 mg/kg TMZ or an equimolar dose of Me-TMZ (16.1 mg/kg) or DiMe-TMZ (17.2 mg/kg) orally once per-day, 5x/week for 7 weeks. Control vs. TMZ:  $P = 0.0014$ , TMZ vs. DiMe-TMZ:  $P = 0.061$ , TMZ vs. Me-TMZ:  $P = 0.016$ . (b) Mice were administered 15 mg/kg TMZ or an equimolar dose of DiMe-TMZ (17.2 mg/kg) or K-TMZ (14.9 mg/kg) orally once-per-day for 5 total doses. Control vs. TMZ:  $P = 0.0007$ , DiMe-TMZ vs. TMZ:  $P = 0.7$ , K-TMZ vs. TMZ:  $P = 0.055$ . Compounds were formulated in 10% PEG in PBS immediately prior to each treatment. Number of mice per treatment cohort  $\geq 5$ . Survival curves were compared using log-rank test.

Importantly, the methyl derivative **81**, which displays the highest efficacy in cell culture and an extended half-life in aqueous solution (around 40 hours), had no effect in this *in vivo* model (Figure 39), suggesting that dramatically elongated half-lives are less likely *in vivo*, as compounds clearance occurs before activation following alternative pathways.

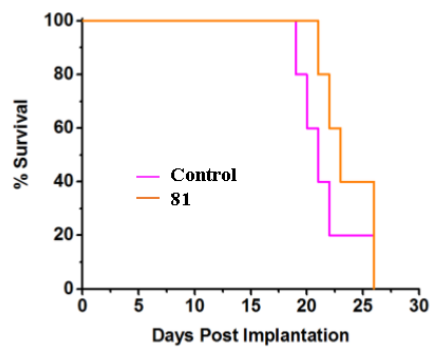


Figure 39 GBM oncosphere Br23c cells were intracranially implanted into female athymic nude mice. Treatment was started 5 days post implantation. Mice were administered compound 81 (12.8 mg/kg, equimolar to 15 mg/kg TMZ) orally once-per-day for 5 doses. Compound was formulated in 10% PEG in PBS.  $n \geq 5$ .

## 2.3 Conclusions

New synthetic methods enabling the construction of novel C8-substituted imidazotetrazines have been developed. These challenging approaches allowed us to construct a panel of compounds that were previously inaccessible. Evaluation of these novel imidazotetrazines against a set of human GBM cell lines and in *in vivo* assays led us to definitively conclude that the C8 amide is not required for anticancer activity.

The principal aspect governing the anticancer activity of imidazotetrazines is the hydrolytic activation of the prodrug. We demonstrated that the electronic properties of the C8-substituent (Hammett constant  $\sigma_p$  value) affect the *in vitro* hydrolytic stability of the novel imidazotetrazines, as well as the cytotoxic activity in multiple GBM cell lines. However, the *in vivo* anticancer activity of TMZ derivatives seems to be depend on additional factors. Our analysis suggested the *in vivo* existence of a critical threshold of aqueous stability ( $\sim 1$  hour), below which hydrolysis occurs too quickly to methylate target DNA. Based on these studies, it appears that compounds with C8-substituents having electronic properties close to those of TMZ, ranging from  $0.23 \leq \sigma_p \leq 0.50$ , are favorites *in vivo*.

The C8-substitution seems also to influence the BBB-penetrance of imidazotetrazines. Compounds such as the oxazole **93** and the ketone **85** displayed higher brain: serum rate compared to TMZ ones. These compounds demonstrated lower *in vivo* toxicity profile and enhanced efficacy *in vivo* intracranial models of glioblastoma. As such, the novel imidazotetrazines synthesized could hold considerable promise for treatment of GBM and other cancers. Indeed, the C8-ketone derivative **85** is the first imidazotetrazine – ever – to provide a notable survival benefit relative to TMZ in animal models.

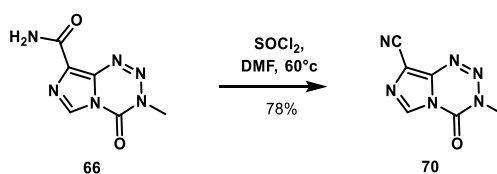
## 2.4 Experimental Section

### 2.4.1 Materials and Methods

$^1\text{H}$  and  $^{13}\text{C}$  NMR spectra were recorded on Bruker 500 (500 MHz,  $^1\text{H}$ ; 125 MHz,  $^{13}\text{C}$ ) or Varian Unity Inova 500 (500 MHz,  $^1\text{H}$ ) MHz spectrometers. Chemical shifts ( $\delta$  scale) are reported in parts per million (ppm) relative to the central peak of the solvent. Coupling constants (J) are given in hertz (Hz). Multiplicities are indicated by s (singlet), d (doublet), t (triplet), q (quartet), m (multiplet), and br (broad). High resolution mass spectrometry (HR MS) was performed on a Waters Q-ToF Ultima or Waters Synapt G2-Si instrument with electrospray ionization (ESI) or electron impact ionization (EI). The purity of tested compounds, determined by high performance liquid chromatography (HPLC), was greater than 95%. Chemical reagents were purchased from commercial sources and used without further purification. Column chromatography purifications were performed under “flash” conditions using 230–400 mesh silica gel. Anhydrous solvents were dried after being passed through columns packed with activated alumina under positive pressure of nitrogen. Unless otherwise noted, all reactions were carried out in oven-dried glassware with magnetic stirring under nitrogen atmosphere.

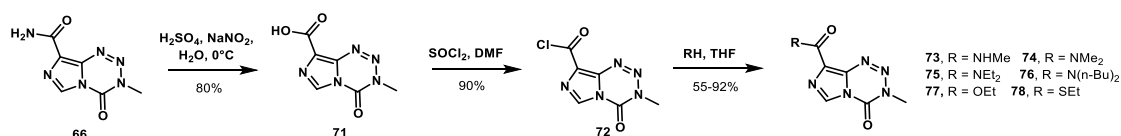
### 2.4.2 Synthesis and Physicochemical Characterization of C8-Temozolomide Derivatives

#### Procedure for Preparation of 3-methyl-4-oxo-3,4-dihydroimidazo[5,1-d][1,2,3,5]tetrazine-8-carbonitrile (70):



Synthetic procedures and experimental data for the compound have been published.<sup>145</sup>

#### General Scheme for Preparation of Amide, Ester, and Thioester Derivatives 73–78:



Synthetic procedures and experimental data for compounds 71,<sup>146</sup> 72,<sup>108</sup> and 77<sup>147</sup> have been previously reported.



In an oven-dried 25 mL round bottom flask, acyl chloride **72** (148.6 mg, 0.70 mmol) was dissolved in anhydrous THF (2.8 mL). The appropriate amine, alcohol or thiol (0.73 mmol) was then added and the reaction was stirred for 3 h at room temperature. When complete, the reaction was stopped and the solvent was evaporated. The crude solid was purified by flash silica gel chromatography (100% EtOAc) to yield desired compound as pure solid.

***N*,3-dimethyl-4-oxo-3,4-dihydroimidazo[5,1-d][1,2,3,5]tetrazine-8-carboxamide (73):**

68% yield as a white solid.

<sup>1</sup>H NMR (500 MHz, DMSO-*d*<sub>6</sub>): δ 8.84 (s, 1H), 8.45 (d, 1H, *J* = 4.9 Hz), 3.86 (s, 3H), 2.81 (d, 3H, *J* = 4.8 Hz). <sup>13</sup>C NMR (125 MHz, DMSO-*d*<sub>6</sub>): δ 160.1, 139.2, 134.3, 130.6, 128.4, 36.1, 25.8. HR MS (ESI) calc. for C<sub>7</sub>H<sub>8</sub>N<sub>6</sub>O<sub>2</sub>Na, [M+Na]<sup>+</sup>: 231.0606, found: 231.0608.

***N,N*,3-trimethyl-4-oxo-3,4-dihydroimidazo[5,1-d][1,2,3,5]tetrazine-8-carboxamide (74):**

76% yield as a white solid.

<sup>1</sup>H NMR (500 MHz, DMSO-*d*<sub>6</sub>): δ 8.81 (s, 1H), 3.85 (s, 3H), 3.06 (s, 6H). <sup>13</sup>C NMR (125 MHz, DMSO-*d*<sub>6</sub>): δ 161.8, 139.2, 133.6, 132.0, 128.6, 38.1, 36.0, 34.8. HR MS (ESI) calc. for C<sub>8</sub>H<sub>11</sub>N<sub>6</sub>O<sub>2</sub>, [M+H]<sup>+</sup>: 223.0938, found: 223.0943.

***N,N*-diethyl-3-methyl-4-oxo-3,4-dihydroimidazo[5,1-d][1,2,3,5]tetrazine-8-carboxamide (75):**

91% yield as a white solid.

<sup>1</sup>H NMR (500 MHz, DMSO-*d*<sub>6</sub>): δ 8.81 (s, 1H), 3.84 (s, 3H), 3.49 (q, 2H, *J* = 7.1 Hz), 3.38 (q, 2H, *J* = 7.0 Hz), 1.18 (t, 3H, *J* = 7.1 Hz), 1.11 (t, 3H, *J* = 7.0 Hz). <sup>13</sup>C NMR (125 MHz, DMSO-*d*<sub>6</sub>): δ 161.3, 139.2, 133.5, 132.7, 128.4, 42.5, 36.0, 14.4, 12.8. HR MS (ESI) calc. for C<sub>10</sub>H<sub>15</sub>N<sub>6</sub>O<sub>2</sub>, [M+H]<sup>+</sup>: 251.1256, found: 251.1250.

***N,N*-dibutyl-3-methyl-4-oxo-3,4-dihydroimidazo[5,1-d][1,2,3,5]tetrazine-8-carboxamide (76):**

85% yield as a white solid.

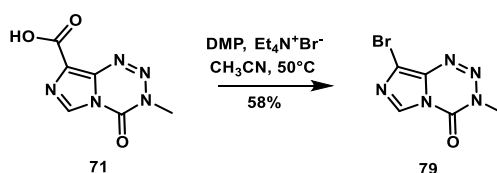
<sup>1</sup>H NMR (500 MHz, DMSO-*d*<sub>6</sub>): δ 8.80 (s, 1H), 3.84 (s, 3H), 3.45 (m, 2H), 3.34 (m, 2H), 1.59 (m, 2H), 1.49 (m, 2H), 1.35 (h, 2H, *J* = 7.4 Hz), 1.11 (h, 2H, *J* = 7.4 Hz), 0.94 (t, 3H, *J* = 7.4 Hz), 0.76 (t, 3H, *J* = 7.4 Hz). <sup>13</sup>C NMR (125 MHz, DMSO-*d*<sub>6</sub>): δ 161.7, 139.2, 133.3, 132.8, 128.4, 47.7, 44.4, 36.0, 30.5, 29.2, 19.6, 19.2, 13.8, 13.5. HR MS (ESI) calc. for C<sub>14</sub>H<sub>23</sub>N<sub>6</sub>O<sub>2</sub>, [M+H]<sup>+</sup>: 307.1882, found: 307.1881.

**S-ethyl 3-methyl-4-oxo-3,4-dihydroimidazo[5,1-d][1,2,3,5]tetrazine-8-carbothioate (78):**

92% yield as a white solid.

$^1\text{H}$  NMR (500 MHz,  $\text{DMSO-}d_6$ ):  $\delta$  8.86 (s, 1H), 3.89 (s, 3H), 3.02 (q, 2H,  $J = 7.4$  Hz), 1.28 (t, 3H,  $J = 7.4$  Hz).  $^{13}\text{C}$  NMR (125 MHz,  $\text{DMSO-}d_6$ ):  $\delta$  184.6, 139.0, 133.8, 131.5, 129.2, 36.5, 22.1, 14.7. HR MS (ESI) calc. for  $\text{C}_8\text{H}_{10}\text{N}_5\text{O}_2\text{S}$ ,  $[\text{M}+\text{H}]^+$ : 240.0555, found: 240.0551.

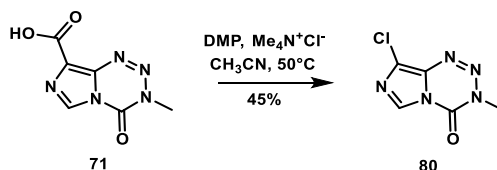
**Procedure for Preparation of 8-bromo-3-methylimidazo[5,1-d][1,2,3,5]tetrazin-4(3H)-one (79):**



To a stirred suspension of Dess-Martin periodinane (477 mg, 1.12 mmol) in anhydrous  $\text{CH}_3\text{CN}$  (2.6 mL), tetraethylammonium bromide (240 mg, 1.12 mmol) was added. Reaction was stirred 5 min at room temperature before **71** (100 mg, 0.51 mmol) was added. The resultant reaction mixture was heated at  $50^\circ\text{C}$  for 2 h. Upon completion, the solvent was concentrated under reduced pressure to give the crude product that was purified by flash silica gel chromatography (9:1 hexane:EtOAc) to afford 73 mg (58%) of **79** as a white solid.

$^1\text{H}$  NMR (500 MHz,  $\text{CDCl}_3$ ):  $\delta$  8.37 (s, 1H), 3.98 (s, 3H).  $^{13}\text{C}$  NMR (125 MHz,  $\text{CDCl}_3$ ):  $\delta$  138.7, 133.3, 128.6, 117.2, 36.4. HR MS (ESI) calc. for  $\text{C}_5\text{H}_5\text{N}_5\text{OBr}$ ,  $[\text{M}+\text{H}]^+$ : 229.9677, found: 229.9684.

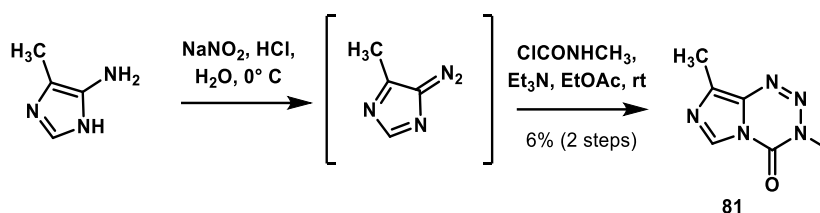
**Procedure for Preparation of 8-chloro-3-methylimidazo[5,1-d][1,2,3,5]tetrazin-4(3H)-one (80):**



To a stirred suspension of Dess-Martin periodinane (477 mg, 1.12 mmol) in anhydrous  $\text{CH}_3\text{CN}$  (2.6 mL), tetramethylammonium chloride (123 mg, 1.12 mmol) was added. The reaction was stirred 5 min at room temperature before **71** (100 mg, 0.51 mmol) was added. The resultant reaction mixture was heated at  $50^\circ\text{C}$  for 2 hours. Upon completion, the solvent was concentrated under reduced pressure to give the crude product that was purified by flash silica chromatography (9:1 hexane:EtOAc) to afford 43 mg (45%) of **80** as a white solid.

$^1\text{H}$  NMR (500 MHz,  $\text{CDCl}_3$ ):  $\delta$  8.33 (s, 1H), 3.98 (s, 3H).  $^{13}\text{C}$  NMR (125 MHz,  $\text{CDCl}_3$ ):  $\delta$  138.7, 130.8, 129.8, 127.2, 36.4. HR MS (ESI) calc. for  $\text{C}_5\text{H}_5\text{N}_5\text{OCl}$ ,  $[\text{M}+\text{H}]^+$ : 186.0183, found: 186.0186.

### Procedure for Preparation of 3,8-dimethylimidazo[5,1-d][1,2,3,5]tetrazin-4(3H)-one (**81**):

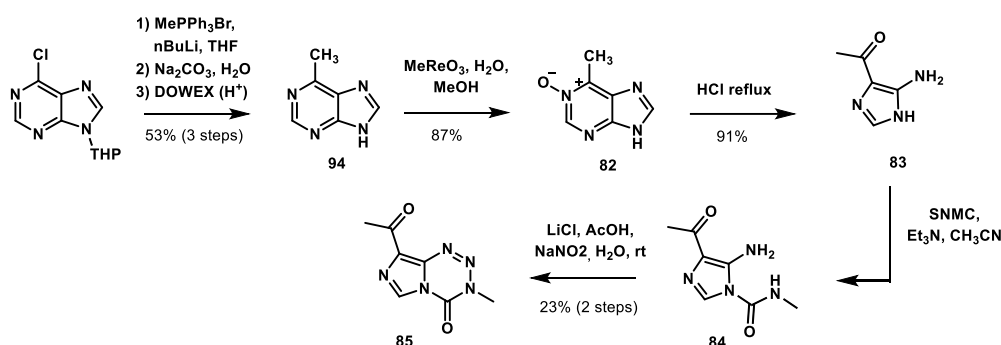


To a 15 mL round bottom flask, 4-methyl-1H-imidazol-5-amine dihydrochloride (44.2 mg, 0.3 mmol) was added and dissolved in 1M HCl (0.4 mL) before  $\text{NaNO}_2$  (26.2 mg, 0.4 mmol) in water (0.4 mL) was added at  $0^\circ\text{C}$  in the dark. The solution was stirred 30 minutes then concentrated and azeotroped twice with toluene to afford crude 4-diazo-5-methyl-4H-imidazole. To the crude diazo suspended in ethyl acetate (1.3 mL), anhydrous triethylamine (0.08 mL, 0.6 mmol) and methylcarbamic chloride (79 mg, 0.8 mmol) were added in the dark. The reaction was stirred overnight before being purified via flash silica gel chromatography (4:1 hexane:EtOAc) to afford 2.4 mg (6%) **81** as a pale yellow solid.

Note: To minimize decomposition of the crude diazo species, concentration was done (without heating) in the dark as quickly as possible.

$^1\text{H}$  NMR (500 MHz,  $\text{CDCl}_3$ ):  $\delta$  8.35 (s, 1H), 3.94 (s, 3H), 2.66 (s, 3H).  $^{13}\text{C}$  NMR (125 MHz,  $\text{CDCl}_3$ ):  $\delta$  139.7, 139.6, 132.5, 127.9, 35.8, 12.5. HR MS (EI) calc. for  $\text{C}_6\text{H}_7\text{N}_5\text{O}$ ,  $[\text{M}+\text{H}]^+$ : 165.0651, found: 165.0654.

### Procedure for Preparation of 8-acetyl-3-methylimidazo[5,1-d][1,2,3,5]tetrazin-4(3H)-one (**85**):



Synthetic procedures and experimental data for compounds **94**,<sup>148</sup> **82**,<sup>149</sup> and **83**<sup>150</sup> have been published.

### 4-acetyl-5-amino-N-methyl-1H-imidazole-1-carboxamide (**84**):

To an oven-dried 25 mL round bottom flask, **83** (186 mg, 0.89 mmol) and *N*-succinimidyl *N*-methylcarbamate (321 mg, 1.86 mmol) were added and suspended in anhydrous acetonitrile (1.5 mL). Next, under nitrogen, dry triethylamine (0.34 mL, 2.4 mmol) was slowly added and the solution was stirred overnight at room temperature. Upon completion, the mixture was concentrated and purified by

silica gel flash chromatography (100% CH<sub>2</sub>Cl<sub>2</sub> to 4:1 CH<sub>2</sub>Cl<sub>2</sub>:methanol) to afford 106 mg (66%) of intermediate **84** as a gold solid.

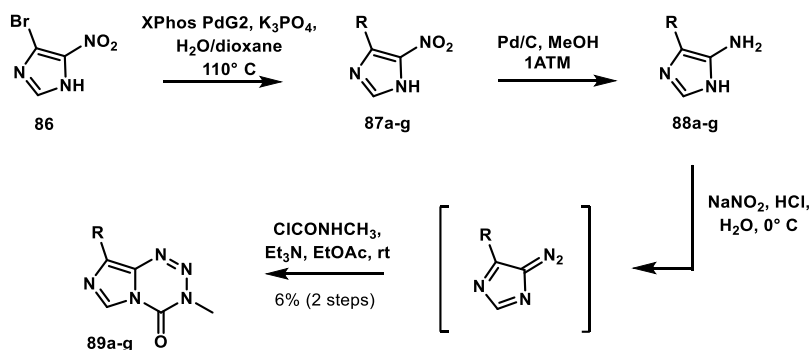
<sup>1</sup>H NMR (500 MHz, DMSO-*d*<sub>6</sub>): δ 8.17 (br s, 1H), 7.97 (s, 1H), 7.56 (s, 2H), 3.36 (d, 3H, *J* = 4.5 Hz), 2.73 (s, 3H).

#### 8-acetyl-3-methylimidazo[5,1-d][1,2,3,5]tetrazin-4(3H)-one (**85**):

In a 15 mL round bottom flask, LiCl (802 mg, 19 mmol) was dissolved in distilled water (1.3 mL) and AcOH (0.10 mL) and stirred for 30 minutes until the exotherm dissipated. Intermediate **84** (96.3 mg, 0.53 mmol) was added in one portion and stirred for 30 minutes. The suspension was then cooled to 0°C in an ice bath before a solution of NaNO<sub>2</sub> (57 mg, 0.8 mmol) in a minimal amount of distilled water was added dropwise. The resultant mixture was stirred at 0°C for 30 minutes, then warmed to room temperature and stirred an additional 5 hours. Upon completion, the reaction mixture was diluted with CH<sub>2</sub>Cl<sub>2</sub> and the organic layer was separated. The aqueous layer was extracted with CH<sub>2</sub>Cl<sub>2</sub> (x6) and the combined organic layers were dried over Na<sub>2</sub>SO<sub>4</sub> and concentrated to yield crude solid which was purified by flash silica chromatography (1:1 hexane:EtOAc) to afford 36 mg (35%) of **85** as a white solid.

<sup>1</sup>H NMR (500 MHz, DMSO-*d*<sub>6</sub>): δ 8.86 (s, 1H), 3.90 (s, 3H), 2.68 (s, 3H). <sup>13</sup>C NMR (125 MHz, DMSO-*d*<sub>6</sub>): δ 191.5, 139.0, 135.6, 133.3, 129.1, 36.4, 28.3. HR MS (ESI) calc. for C<sub>7</sub>H<sub>8</sub>N<sub>5</sub>O<sub>2</sub>, [M+H]<sup>+</sup>: 194.0678, found: 194.0683.

#### General Scheme for Preparation of Aryl Derivatives **89a-g**:



#### General Procedure for Suzuki Coupling Reaction (**87a-g**):

A mixture of 4-bromo-5-nitro-1H-imidazole **86** (400 mg, 2.08 mmol), phenylboronic acid (507 mg, 4.17 mmol), XPhos PdG2 (164 mg, 0.2 mmol) and K<sub>3</sub>PO<sub>4</sub> (1.32 g, 6.24 mmol) under nitrogen was suspended in degassed 1:1 H<sub>2</sub>O:dioxane (16 mL). The resulting mixture was stirred at 110°C for 16 h. The reaction was cooled to room temperature and H<sub>2</sub>O was added. The aqueous layer was extracted x3 with EtOAc and the combined organic layers were dried over Na<sub>2</sub>SO<sub>4</sub> and concentrated. The residue

obtained was purified by flash silica gel chromatography (100% EtOAc) to afford desired compounds, which were used for next step as crude without further purification.

**5-nitro-4-phenyl-1H-imidazole (87a):**

Compound was obtain using the procedure above as a dark solid, ~55% yield.

<sup>1</sup>H NMR (500 MHz, DMSO-*d*<sub>6</sub>): δ 13.50 (br s, 1H), 7.92 (s, 1H), 7.66-7.65 (m, 2H), 7.53-7.51 (m, 3H).

<sup>13</sup>C NMR (125 MHz, DMSO-*d*<sub>6</sub>): δ 143.1, 135.1, 131.7, 130.1, 130.0, 128.8, 128.2. HPLC-MS ESI = 190.06 [M+H]<sup>+</sup>.

**4-(4-chlorophenyl)-5-nitro-1H-imidazole (87b):**

Compound was obtain using the procedure above as a dark solid, ~19% yield.

<sup>1</sup>H NMR (500 MHz, DMSO-*d*<sub>6</sub>): δ 13.56 (br s, 1H), 7.94 (s, 1H), 7.69 (d, 2H, *J* = 8.5 Hz), 7.60 (d, 2H,

*J* = 8.5 Hz). HPLC-MS ESI = 224.02 [M+H]<sup>+</sup>.

**5-nitro-4-(4-(trifluoromethyl)phenyl)-1H-imidazole (87c):**

Compound was obtain using procedure above as a brown solid, ~49% yield.

<sup>1</sup>H NMR (500 MHz, DMSO-*d*<sub>6</sub>): 13.69 (s, 1H), 8.00 (s, 1H), 7.89 (br s, 4H). <sup>13</sup>C NMR (125 MHz,

DMSO-*d*<sub>6</sub>): δ 143.6, 135.6, 132.3, 130.9, 130.2, 129.9, 125.6 (q, *J* = 3.7 Hz, 1C), 123.39. HPLC-MS ESI = 208.05 [M+H]<sup>+</sup>.

**4-(4-methoxyphenyl)-5-nitro-1H-imidazole (87d):**

Product was obtain using procedure above as a dark solid, ~17% yield.

<sup>1</sup>H NMR (500 MHz, DMSO-*d*<sub>6</sub>): δ 13.37 (s, 1H), 7.87 (s, 1H), 7.61 (dt, 2H, *J*<sup>1</sup> = 8.8, *J*<sup>2</sup> = 2.9 Hz), 7.07

(dt, 2H, *J*<sup>1</sup> = 8.8, *J*<sup>2</sup> = 2.9 Hz), 3.83 (s, 3H). HPLC-MS ESI = 220.07 [M+H]<sup>+</sup>.

**4-(4-fluorophenyl)-5-nitro-1H-imidazole (87e)**

Compound was obtain using procedure above as a dark solid, ~35% yield.

HPLC-MS ESI = 208.05 [M+H]<sup>+</sup>.

**4-(5-nitro-1H-imidazol-4-yl)benzotrile (87f):**

Compound was obtain using procedure above as a dark solid, ~69% yield.

<sup>1</sup>H NMR (500 MHz, DMSO-*d*<sub>6</sub>): δ 13.72 (br s, 1H), 8.41 (s, 1H), 8.00-7.98 (m, 1H), 7.94-7.78 (m, 1H).

HPLC-MS ESI = 115.06 [M+H]<sup>+</sup>.

**1-(4-(5-nitro-1H-imidazol-4-yl)phenyl)ethan-1-one (87g):**

Product was obtained using procedure above as a dark solid, ~31% yield.

<sup>1</sup>H NMR (500 MHz, DMSO-*d*<sub>6</sub>): δ 13.69 (br s, 1H), 8.07 (dt, 2H, *J*<sup>1</sup> = 8.5, *J*<sup>2</sup> = 1.8 Hz), 8.00 (s, 1H), 7.81 (dt, 2H, *J*<sup>1</sup> = 8.5, *J*<sup>2</sup> = 1.8 Hz), 2.64 (s, 3H). <sup>13</sup>C NMR (125 MHz, DMSO-*d*<sub>6</sub>): δ 198.1, 137.6, 135.6, 134.7, 132.5, 130.5, 130.3, 128.5, 27.4. HPLC-MS ESI = 232.07 [M+H]<sup>+</sup>.

**General Procedure for Nitro Reduction (88a-g):**

Compounds **87a-g** were dissolved in dry MeOH (10 mL) containing 10% Pd/C before H<sub>2</sub> (1 atm) was introduced. The reaction was stirred for 16 h at room temperature before the catalyst was filtered over Celite. The filtrate was concentrated under reduced pressure and purified by flash silica gel chromatography (95:5 CH<sub>2</sub>Cl<sub>2</sub>:MeOH) providing the desired compounds **88a-g**, which were used for next step as crude without further purification.

**4-phenyl-1H-imidazol-5-amine (88a):**

Compound was obtained using procedure above as a purple solid, ~54% yield.

<sup>1</sup>H NMR (500 MHz, DMSO-*d*<sub>6</sub>): δ 11.77 (br s, 1H), 7.53 (br s, 2H), 7.32 (t, 2H, *J* = 7.5 Hz), 7.03 (t, 1H, *J* = 7.5 Hz), 4.51 (br s, 2H). <sup>13</sup>C NMR (125 MHz, DMSO-*d*<sub>6</sub>): δ 143.1, 135.1, 131.7, 130.1, 130.0, 128.8, 128.2. HPLC-MS ESI = 160.09 [M+H]<sup>+</sup>.

**4-(4-chlorophenyl)-1H-imidazol-5-amine (88b):**

Compound was obtained using procedure above as a purple solid, ~56% yield.

<sup>1</sup>H NMR (500 MHz, DMSO-*d*<sub>6</sub>): δ 11.78 (br s, 1H), 7.56 (br d, 2H, *J* = 7.0 Hz), 7.33 (d, 2H, *J* = 8.5 Hz), 7.28 (br s, 1H), 4.68 (br s, 2H). HPLC-MS ESI = 194.05 [M+H]<sup>+</sup>.

**4-(4-(trifluoromethyl)phenyl)-1H-imidazol-5-amine (88c):**

Compound was obtained using procedure above as a brown solid, ~55% yield.

<sup>1</sup>H NMR (500 MHz, DMSO-*d*<sub>6</sub>): δ 7.75 (d, 2H, *J* = 8.32 Hz), 7.63 (d, 2H, *J* = 8.3 Hz), 7.41 (br s, 1H), 5.04 (br s, 2H). HPLC-MS ESI = 178.08 [M+H]<sup>+</sup>.

**4-(4-methoxyphenyl)-1H-imidazol-5-amine (88d):**

Compound was obtained using procedure above as a dark green solid, ~35% yield.

<sup>1</sup>H NMR (500 MHz, DMSO-*d*<sub>6</sub>): δ 11.73 (s, 1H), 7.54-7.61 (d, 2H, *J* = 8.6 Hz), 7.28 (s, 1H), 6.98 (d, 2H, *J* = 8.6 Hz), 4.42 (br s, 2H), 3.81 (s, 3H). HPLC-MS ESI = 190.10 [M+H]<sup>+</sup>.

**4-(4-fluorophenyl)-1H-imidazol-5-amine (88e):**

Compound was obtained using procedure above as a brown solid, ~39% yield.

<sup>1</sup>H NMR (500 MHz, DMSO-*d*<sub>6</sub>): δ 11.76 (br s, 1H), 7.58 (br s, 2H), 7.26 (br s, 1H), 7.15 (t, 2H, *J* = 8.8 Hz), 4.54 (br s, 2H). HPLC-MS ESI = 178.08 [M+H]<sup>+</sup>.

**4-(5-amino-1H-imidazol-4-yl)benzotrile (88f):**

Compound was obtained using procedure above as a dark solid, ~28% yield.

HPLC-MS ESI<sup>+</sup> = 185.08 [M+H]<sup>+</sup>.

**1-(4-(5-amino-1H-imidazol-4-yl)phenyl)ethan-1-one (88g)**

Compound was obtained using procedure above as a dark solid, ~43% yield.

HPLC-MS ESI = 202.10 [M+H]<sup>+</sup>.

**General Procedure for Cyclization (89a-g):**

To a suspension of intermediate **88a-g** in 1 M HCl (2.9 mL) at 0°C was added a pre-formed solution of NaNO<sub>2</sub> (186 mg, 2.7 mmol) in H<sub>2</sub>O (2.9 mL) dropwise. The resultant mixture was stirred at 0°C in the dark for 30 min. Upon completion, the solvent was evaporated and the crude diazo compound was dissolved in EtOAc (9.6 mL, 0.2 M) before triethylamine (544 μL, 4.6 mmol) and methylcarbamic chloride (1010 mg, 10.8 mmol) were added. The reaction mixture was stirred at room temperature for 16 h protected from light. Upon reaction completion, the solvent was concentrated under reduced pressure and the residue was purified by flash silica gel chromatography (9:1 hexane:EtOAc) to afford **89a-g** as pure solids.

Note: To minimize decomposition of the crude diazo species, concentration was done (without heating) in the dark as quickly as possible.

**3-methyl-8-phenylimidazo[5,1-d][1,2,3,5]tetrazin-4(3H)-one (89a):**

White solid, 6% yield (3 steps).

<sup>1</sup>H NMR (500 MHz, DMSO-*d*<sub>6</sub>): δ 8.84 (s, 1H), 8.31-8.29 (m, 2H), 7.57-7.53 (m, 2H), 7.44 (tt, 1H, *J*<sup>1</sup> = 7.4, *J*<sup>2</sup> = 1.3 Hz), 3.85 (s, 3H). <sup>13</sup>C NMR (125 MHz, CDCl<sub>3</sub>): δ 140.0, 137.0, 132.3, 131.9, 129.9, 129.5, 129.4, 127.1, 36.3. HR MS (ESI) calc. for C<sub>11</sub>H<sub>10</sub>N<sub>5</sub>O, [M+H]<sup>+</sup>: 228.0885, found: 228.0878.

**8-(4-chlorophenyl)-3-methylimidazo[5,1-d][1,2,3,5]tetrazin-4(3H)-one (89b):**

Yellow solid, 1.2% yield (3 steps).

<sup>1</sup>H NMR (500 MHz, DMSO-*d*<sub>6</sub>): δ 8.86 (s, 1H), 8.30 (dt, 2H, *J*<sup>1</sup> = 9.25, *J*<sup>2</sup> = 2.5 Hz), 7.62 (dt, 2H, *J*<sup>1</sup> = 9.25, *J*<sup>2</sup> = 2.5 Hz), 3.86 (s, 3H). <sup>13</sup>C NMR (125 MHz, *d*-DMSO): δ 139.9, 135.7, 133.97, 132.4, 130.7, 130.0, 129.6, 128.6, 36.4. HR MS (ESI) calc. for C<sub>11</sub>H<sub>9</sub>N<sub>5</sub>OCl, [M+H]<sup>+</sup>: 262.0496, found: 262.0489.

**3-methyl-8-(4-(trifluoromethyl)phenyl)imidazo[5,1-d][1,2,3,5]tetrazin-4(3H)-one (89c):**

Yellow solid, 5% yield (3 steps).

<sup>1</sup>H NMR (500 MHz, CDCl<sub>3</sub>): δ 8.52 (d, 2H, *J* = 8.2 Hz), 8.48 (s, 1H), 7.75 (d, 2H, *J* = 8.2 Hz), 4.02 (s, 3H). <sup>13</sup>C NMR (125 MHz, CDCl<sub>3</sub>): δ 139.3, 137.9, 134.3, 131.9, 131.0 (q, 1C, *J* = 32.3 Hz), 128.8, 127.6, 125.8 (q, 1C, *J* = 3.8 Hz), 123.0, 36.1. HR MS (ESI) calc. for C<sub>12</sub>H<sub>9</sub>N<sub>5</sub>OF<sub>3</sub>, [M+H]<sup>+</sup>: 296.0759, found: 296.0754.

**8-(4-methoxyphenyl)-3-methylimidazo[5,1-d][1,2,3,5]tetrazin-4(3H)-one (89d):**

Yellow solid, 0.7% yield (3 steps).

<sup>1</sup>H NMR (500 MHz, CDCl<sub>3</sub>): δ 8.42 (s, 1H), 8.34 (dt, 2H, *J* = 9.7, 2.9 Hz), 7.03 (dt, 2H, *J*<sup>1</sup> = 9.7, *J*<sup>2</sup> = 2.9 Hz), 3.97 (s, 3H), 3.88 (s, 3H). <sup>13</sup>C NMR (125 MHz, CDCl<sub>3</sub>): δ 160.8, 139.9, 139.8, 130.5, 129.0, 128.5, 123.7, 114.4, 55.4, 35.9. HR MS (ESI) calc. for C<sub>12</sub>H<sub>12</sub>N<sub>5</sub>O<sub>2</sub>, [M+H]<sup>+</sup>: 258.0991, found: 258.0998.

**8-(4-fluorophenyl)-3-methylimidazo[5,1-d][1,2,3,5]tetrazin-4(3H)-one (89e):**

Yellow solid, 3% yield (3 steps).

<sup>1</sup>H NMR (500 MHz, CDCl<sub>3</sub>): δ 8.46 (s, 1H), 8.44-8.40 (m, 2H), 7.24-7.19 (m, 2H), 4.01 (s, 3H). <sup>13</sup>C NMR (125 MHz, CDCl<sub>3</sub>): δ 164.6, 162.6, 139.2 (d, 1C, *J* = 86.4 Hz), 131.0, 129.4 (d, 1C, *J* = 8.3 Hz), 128.6, 127.3 (d, 1C, *J* = 3.3 Hz), 116.0 (d, 1C, *J* = 21.6 Hz), 36.0. HR MS (ESI) calc. for C<sub>11</sub>H<sub>9</sub>FN<sub>5</sub>O, [M+H]<sup>+</sup>: 246.0791, found: 246.0788.

**8-(4-acetylphenyl)-3-methylimidazo[5,1-d][1,2,3,5]tetrazin-4(3H)-one (89f):**

White solid, 1.3% yield (3 steps).

<sup>1</sup>H NMR (500 MHz, CDCl<sub>3</sub>): δ 8.92 (s, 1H), 8.44 (dt, 2H, *J*<sup>1</sup> = 8.5, *J*<sup>2</sup> = 1.8 Hz), 8.14 (dt, 2H, *J*<sup>1</sup> = 8.5, *J*<sup>2</sup> = 1.8 Hz), 3.87 (s, 3H), 2.63 (s, 3H). <sup>13</sup>C NMR (125 MHz, CDCl<sub>3</sub>): δ 197.9, 139.9, 136.9, 136.1, 135.4, 133.2, 130.2, 129.5, 127.0, 36.5, 27.3. HR MS (ESI) calc. for C<sub>13</sub>H<sub>12</sub>N<sub>5</sub>O<sub>2</sub>, [M+H]<sup>+</sup>: 270.0991, found: 270.0993.



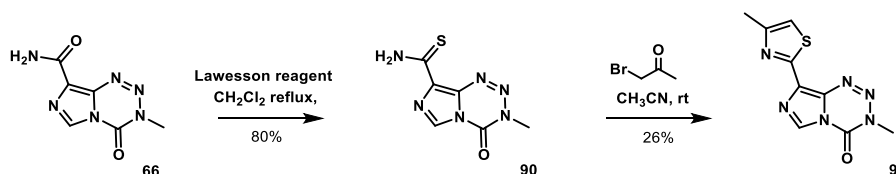
#### 4-(3-methyl-4-oxo-3,4-dihydroimidazo[5,1-d][1,2,3,5]tetrazin-8-yl)benzotrile (89g):

White solid, 4.4% yield (3 steps).

$^1\text{H}$  NMR (500 MHz,  $\text{CDCl}_3$ ):  $\delta$  8.53 (d, 2H,  $J^1 = 8.4$ ,  $J^2 = 1.8$  Hz), 8.49 (s, 1H), 7.79 (d, 2H,  $J^1 = 8.4$ ,  $J^2 = 1.8$  Hz), 4.03 (s, 3H). HR MS (ESI) calc. for  $\text{C}_{12}\text{H}_9\text{N}_6\text{O}$ ,  $[\text{M}+\text{H}]^+$ : 296.0838, found: 253.0835.

Note: Compound **89g** results extremely unstable, it decomposes during  $^{13}\text{C}$ -NMR times.

#### Procedure for Preparation of 3-methyl-8-(4-methylthiazol-2-yl)imidazo[5,1-d][1,2,3,5]tetrazin-4(3H)-one (91):



The route to 4-substituted thiazol-2-yls at the C8 position of imidazotetrazines is known,<sup>118</sup> however, the synthesis of compound **91** had never been reported.

#### 3-methyl-4-oxo-3,4-dihydroimidazo[5,1-d][1,2,3,5]tetrazine-8-carbothioamide (90):

Compound was synthesized following a different route from that used in the literature.

A mixture of temozolomide (500 mg, 2.6 mmol) and Lawesson reagent (1146 mg, 2.83 mmol) was refluxed in  $\text{CH}_2\text{Cl}_2$  (13.5 mL) for 18h. Reaction was quenched with water and the precipitate was filtered and washed with water and diethyl ether. Solid was purified by flash chromatography over silica gel (EtOAc) to afford 433 mg (80%) of pure **24** as yellow solid.

The experimental data are conform to literature.<sup>118</sup>

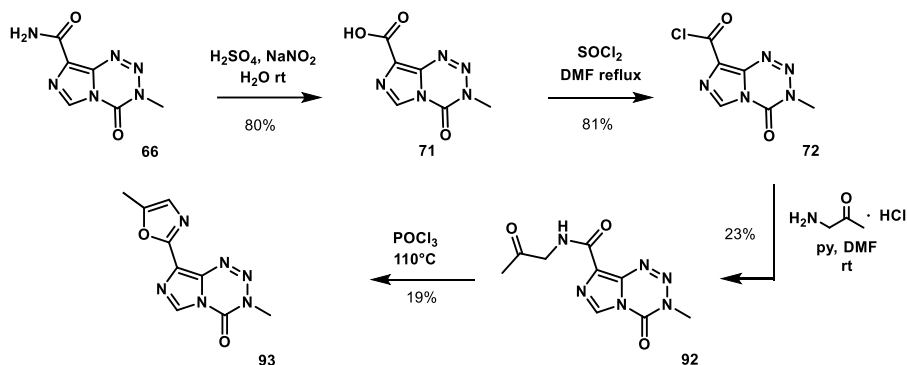
$^1\text{H}$  NMR (500 MHz,  $\text{DMSO}-d_6$ ):  $\delta$  9.92 (br s, 1H), 9.44 (br s, 1H), 8.81 (s, 1H), 3.87 (s, 3H).  $^{13}\text{C}$  NMR (125 MHz,  $\text{DMSO}-d_6$ ):  $\delta$  188.3, 139.6, 135.0, 134.4, 128.2, 36.6. HPLC-MS ESI = 211.04  $[\text{M}+\text{H}]^+$ .

#### 3-methyl-8-(4-methylthiazol-2-yl)imidazo[5,1-d][1,2,3,5]tetrazin-4(3H)-one (91):

To a solution of **90** (550 mg, 2.6 mmol) in acetonitrile (40 mL) was added  $\alpha$ -bromo acetone (220  $\mu\text{L}$ , 2.6 mmol) and the solution was stirred at room temperature for 18 h. Upon completion, the reaction was stopped, and the precipitate was filtered and purified by flash silica gel chromatography (4:6 hexane:EtOAc) to afford 167 mg (26%) of the desired product **91** as a yellow solid.

$^1\text{H}$  NMR (500 MHz,  $\text{DMSO}-d_6$ ):  $\delta$  8.87 (s, 1H), 7.46 (d, 1H,  $J = 0.9$  Hz), 3.86 (s, 3H), 2.48 (d, 3H,  $J = 0.9$  Hz).  $^{13}\text{C}$  NMR (125 MHz,  $\text{DMSO}-d_6$ ):  $\delta$  158.6, 154.6, 139.7, 131.9, 131.8, 130.2, 116.6, 36.5, 17.4. HR MS (ESI) calc. for  $\text{C}_9\text{H}_9\text{N}_6\text{OS}$ ,  $[\text{M}+\text{H}]^+$ : 249.0559, found: 249.0559.

**Procedure for Preparation of 3-methyl-8-(5-methyloxazol-2-yl)imidazo[5,1-d][1,2,3,5]tetrazin-4(3H)-one (93):**



The route to 4-substituted oxazol-2-yls at the C8 position of imidazotetrazines is known,<sup>118</sup> however, the synthesis of compound **93** via intermediate **92** had never been reported.

**3-methyl-4-oxo-N-(2-oxopropyl)-3,4-dihydroimidazo[5,1-d][1,2,3,5]tetrazin-8-carboxamide (92):**

To **72** (447 mg, 2.09 mmol) and 2-aminoacetophenone hydrochloride (229 mg, 2.09 mmol) were added DMF (4.4 mL) and pyridine (0.9 mL). The reaction mixture was stirred for 16 h at room temperature. Water was added and the aqueous layer was extracted x5 with EtOAc. The combined organic layers were dried over  $\text{Na}_2\text{SO}_4$  and concentrated. The residue obtained was purified by flash silica gel chromatography (100% EtOAc) to afford 266 mg (51%) of **92** as an orange solid.

$^1\text{H}$  NMR (500 MHz,  $\text{DMSO}-d_6$ ):  $\delta$  8.87 (s, 1H), 8.59 (t, 1H,  $J = 5.7$  Hz), 4.17 (d, 2H,  $J = 5.7$  Hz), 3.88 (s, 3H), 2.15 (s, 3H).  $^{13}\text{C}$  NMR (125 MHz,  $\text{DMSO}-d_6$ ):  $\delta$  204.5, 160.1, 139.6, 135.1, 130.2, 129.1, 49.6, 36.7, 27.5. LC-MS (ESI) calc. for  $\text{C}_9\text{H}_{11}\text{N}_6\text{O}_3$   $[\text{M}+\text{H}]^+$ : 251.0893, found: 251.09.

**3-methyl-8-(5-methyloxazol-2-yl)imidazo[5,1-d][1,2,3,5]tetrazin-4(3H)-one (93):**

Intermediate **92** (266 mg, 1.06 mmol) was added to phosphoryl chloride (6.5 mL) and the stirred mixture was heated at  $110^\circ\text{C}$  for 3 h. Upon completion, ice water was added and the aqueous layer was extracted x4 with EtOAc. The combined organic layers were dried over  $\text{Na}_2\text{SO}_4$  and concentrated. The residue obtained was purified by flash silica gel chromatography (100% EtOAc) to afford 80 mg (32%) of the product **93** as a yellow solid.

$^1\text{H}$  NMR (500 MHz,  $\text{DMSO}-d_6$ ):  $\delta$  8.89 (s, 1H), 7.13 (br d, 1H,  $J = 1.2$  Hz), 3.87 (s, 3H), 2.44 (d, 3H,  $J = 1.2$  Hz).  $^{13}\text{C}$  NMR (125 MHz,  $\text{DMSO}-d_6$ ):  $\delta$  154.1, 150.5, 139.6, 133.6, 130.4, 126.1, 125.4, 36.6, 11.2. HR MS (ESI) calc. for  $\text{C}_9\text{H}_9\text{N}_6\text{O}_2$ ,  $[\text{M}+\text{H}]^+$ : 233.0782, found: 233.0787.

## List of Abbreviations

**4-P-PDOT** = 4-Phenyl-2-propionamidotetralin

**Ac** = Acetyl

**ACB** = Acyl chain binding

**AIC** = 5-aminoimidazole-4-carboxamide

**BBB** = Blood brain barrier

**BCNU** = Carmustine or bis-chloroethylnitrosourea

**BER** = DNA base excision repair

**BINAP** = (1,1'-Binaphthalene-2,2'-diyl)bis(diphenylphosphine), (R)-(+)-2,2'-Bis(diphenylphosphino)-1,1'-binaphthalene

**Bn** = Benzyl

**BrettPhos PdG1** = Chloro[2-(dicyclohexylphosphino)-3,6-dimethoxy-2',4', 6'-triisopropyl-1,1'-biphenyl][2-(2-aminoethyl)phenyl]palladium(II)

**Bu** = Butyl

**CA** = Cytoplasmic access

**CB** = Cannabinoid receptor

**CCNU** = Lomustine

**CNS** = Central nervous system

**COSY** = Correlation spectroscopy

**CP** = Cytosolic port

**Cpd** = Compound

**CSF** = Cerebrospinal fluid

**DIPEA** = *N,N*-diisopropylethylamine

**DMF** = *N,N*-dimethylformamide

**DMP** = Dess-Martin periodinane

**DMSO** = Dimethyl sulfoxide

**EDG** = Electron donating groups

**Et** = Ethyl

**EWG** = Electron withdrawing groups

**FAAH** = Fatty acid amide hydrolase

**FDA** = US Food and Drug Administration

**GBM** = Glioblastoma Multiforme

**GPCR** = G protein-coupled receptors

**HPLC** = High Performance Liquid Chromatography

**IBX** = 2-iodoxybenzoic acid  
**IOP** = Intraocular pressure  
**MAC** = Membrane access channel  
**Me** = Methyl  
**MGMT** = O6-methylguanine DNA methyl transferase  
**MLT** = Melatonin  
**MMR** = DNA mismatch repair  
**MPO** = CNS multiparameter optimization  
**MT** = Melatonin receptor  
**MTIC** = 5-(3methyl)1-triazenyl)imidazole-4-carboxamide  
**N3MA** = N3-methyladenine  
**N7MG** = N3-methylguanine  
**NBS** = *N*-Bromosuccinimide  
**nc** = Not computable  
**nd** = Not determined  
**NOE** = Nuclear overhauser effect  
**NOESY** = Nuclear overhauser effect spectroscopy  
**NMDA** = *N*-methyl-D-aspartate receptor  
**NMR** = Nuclear magnetic resonance  
**Nrf2** = Nuclear factor (erythroid-derived 2)-like 2  
**O6MG** = O6-methylguanine  
**Ox** = Oxazole  
**PBS** = Phosphate-buffered saline  
**Pd(dba)<sub>2</sub>** = Palladium(0) bis(dibenzylideneacetone)  
**Ph** = Phenyl  
**PK** = Pharmacokinetics  
**Py** = Pyridine  
**QSAR** = Quantitative structure-activity relationship  
**RGC** = Retinal ganglion cells  
**SAR** = Structure-activity relationship  
**SCN** = Suprachiasmatic nucleus  
**SEM** = 2-(trimethylsilyl)ethoxymethyl  
**SNMC** = *N*-succinimidyl *N*-methylcarbamate  
**TEA** = Triethylamine  
**TEAB** = Tetraethylammonium bromide

**TEBAC** = Benzyltriethylammonium chloride

**TFA** = Trifluoroacetic acid

**THF** = Tetrahydrofuran

**Thiaz** = Thiazole

**THQ** = Tetrahydroquinoline

**TM** = Transmembrane

**TMZ** = Temozolomide

**WBC** = White blood cell

**WHO** = World Health Organization

**XPhos PdG2** = Chloro(2-dicyclohexylphosphino-2',4',6'-triisopropyl-1,1'-biphenyl)[2-(2'-amino-1,1'-biphenyl)]palladium(II)

$\sigma_p$  = Hammett constants

## Acknowledgements

*This research was carried out at the Department of Biomolecular Sciences, University of Urbino (Section I) and Roger Adams Laboratory, University of Illinois at Urbana-Champaign (Section II). In particular, I would like to express my sincere gratitude to my mentor at University of Urbino, Prof. Gilberto Spadoni, who has assisted me through all the phases of this work, providing me with valuable advice and encouragement even when results were still far from being obtained. I would like also to thank my supervisor at UIUC, Professor Paul Hergenrother, for the help, the encouragement and the support during my fruitful months abroad. I would like to thanks Prof.ssa Annalida Bedini, for the support and help during these years, and all the Researchers of the Department of Biomolecular Sciences of University of Urbino. I would also like to thank the University of Parma for the computational analysis and Riley Svec for the biological data. A sincere thanks go to the Hergenrother Group, to make me feeling at home. Now, it is time to express my gratitude to all the friends that have accompanied me through my PhD program, for being close every time, no matter how physically far we may happen to be from each other. Thanks to all my friends in the USA for having made my experience abroad awesome. A big thank you goes to my parents, Luisa and Massimo, to my brother Mattia and my grandmother Maria, for supporting me and for being close every time. Finally, I have to thank Fabrizio, for his love and constant support, for all the late nights and early mornings, I owe you everything.*

*Thank you,*

*Lucia*

## References

- <sup>1</sup> Lerner, A. B.; Case, J. D.; Takahashi, Y.; Lee, T. H.; Mori, W. *J. Am. Chem. Soc.*, **1958**, 80, 2587.
- <sup>2</sup> Klein, D. C.; Coon, S. L.; Roseboom, P. H.; Weller, J. L.; Bernard, M.; Gastel, J. A.; Zatz, M.; Iuvone, P.; Rodeiguez, I. R.; Begay, V.; Falcon, G. M.; Cahill, V. M.; Cassone, V. M.; Baler, R. *Rec. Prog. Horm. Res.*, **1997**, 52, 307.
- <sup>3</sup> Reiter, R. *J. Endocr. Rev.*, **1991**, 12, 151.
- <sup>4</sup> Xie, Z.; Chen, F.; Li, W. A.; Geng, X.; Li, C.; Meng, X.; Feng, Y.; Liu, W.; Yu, F. *Neurol Res.*, **2017**, 6, 559.
- <sup>5</sup> Hardeland, R.; Cardinali, D. P.; Srinivasan, V.; Spence, D. W.; Brown, G. M.; Pandi-Perumal, S. R. *Prog. Neurobiol.*, **2011**, 93, 350.
- <sup>6</sup> Li, Y.; Li, S.; Zhou, Y.; Meng, X.; Zhang, J. J.; Xu, D. P.; Li, H. B. *Oncotarget*, **2017**, 8, 39896.
- <sup>7</sup> Fourtillan, J. B.; Brisson, A. M.; Gobin, P.; Ingrand, I.; Decourt, J. P.; Girault, J. *Biopharm. Drug Dispos.*, **2000**, 21, 15.
- <sup>8</sup> Markantonis, S. L.; Tsakalozou, E.; Paraskeva, A.; Staikou, C.; Fassoulaki, A. *J Clin Pharmacol.*, **2008**, 48, 240.
- <sup>9</sup> Jockers, R.; Delagrang, P.; Dubocovich, M. L.; Markus, R. P.; Renault, N.; Tosini, G.; Cecon, E.; Zlotos, D. P. *Br. J. Pharmacol.*, **2016**, 173, 2702.
- <sup>10</sup> Vriend, J.; Reiter, R. *J. Mol. Cell. Endocrinol.*, **2015**, 401, 213.
- <sup>11</sup> Liu, J.; Clough, S. J.; Hutchinson, A. J.; Adamah-Biassi, E. B.; Popovska-Gorevski, M.; Dubocovich, M. L. *Annu. Rev. Pharmacol. Toxicol.*, **2016**, 56, 361.
- <sup>12</sup> Mailliet, F.; Ferry, G.; Vella, F.; Berger, S.; Cogé, F.; Chromarat, P.; Mallet, C.; Guénin, S. P.; Guillaumet, G.; Viaud-Massuard, M. C.; Yous, S.; Delagrang, P.; Boutin, J. A. *Biochem. Pharmacol.*, **2005**, 71, 74.
- <sup>13</sup> Reppert, S. M.; Weaver, D. R.; Godson, C. *Trends Pharmacol. Sci.*, **1996**, 17, 100.
- <sup>14</sup> Lacoste, B.; Angeloni, D.; Dominquez-Lopez, S.; Calderoni, S.; Mauro, A.; Frascini, F.; Descarries, L.; Gobbi, G. *J. Pineal Res.*, **2015**, 58, 397.
- <sup>15</sup> Jockers, R.; Maurice, P.; Boutin, J. A.; Delagrang, P.; *Br. J. Pharmacol.*, **2008**, 154, 1182.
- <sup>16</sup> Zlotos, D. P.; Jockers, R.; Cecon, E.; Rivara, S.; Witt-Enderby, P. A. *J. Med. Chem.*, **2014**, 57, 3161.
- <sup>17</sup> Katon K.; Hirai, K.; Nishiyama, K.; Uchikawa, O.; Fukatsu, K.; Ohkawa, S.; Kawamata, Y.; Hinuma, S.; Miyamoto, M. *Neuropharmacol.*, **2005**, 48, 301.
- <sup>18</sup> Hardeland, R. *Curr. Opin. Investig. Drugs*, **2009**, 10, 691.
- <sup>19</sup> De Bodinat, C.; Guardiola-Lemaitre, B.; Mocaër, E.; Renard, P.; Muñoz, C.; Millan, M. J. *Nat. Rev. Drug Discov.*, **2010**, 9, 628.
- <sup>20</sup> Descamps-Francois, C.; Yous, S.; Chavatte, P.; Audinot, V.; Bonnaud, A.; Boutin, J. A.; Delagrang, P.; Bennejean, C.; Renard, P.; Lesieur, D. *J. Med. Chem.*, **2003**, 46, 1127.
- <sup>21</sup> Spadoni, G.; Bedini, A.; Orlando, P.; Lucarini, S.; Tarzia, G.; Mor, M.; Rivara, S.; Lucini, V.; Pannacci, M.; Scaglione, F. *Bioorg. Med. Chem.*, **2011**, 19, 4910.
- <sup>22</sup> Markl, C.; Clafshenkel, W. P.; Attia, M. I.; Sethi, S.; Witt-Enderby, P. A.; Zlotos, D. A. *Arch. Pharm.*, **2011**, 344, 666.
- <sup>23</sup> Rivara, S.; Pala, D.; Lodola, A.; Mor, M.; Lucini, V.; Dugnani, S.; Scaglione, F.; Bedini, A.; Lucarini, S.; Tarzia, G.; Spadoni, G. *ChemMedChem*, **2012**, 7, 1954.
- <sup>24</sup> Pala, D.; Lodola, A.; Bedini, A.; Spadoni, G.; Rivara, S. *Int J Mol Sci.*, **2013**, 4, 8093.
- <sup>25</sup> Spadoni, G.; Bedini, A.; Lucarini, S.; Mari, M.; Caignard, D. H.; Boutin, J. A.; Delagrang, P.; Lucini, V.; Scaglione, F.; Lodola, A.; Zanardi, F.; Pala, D.; Mor, M.; Rivara, S. *J. Med. Chem.*, **2015**, 58, 7512.
- <sup>26</sup> Sridharan, V.; Suryavanshi, P. A.; Menéndez, J. C. *Chem. Rev.*, **2011**, 111, 7157.
- <sup>27</sup> B. E. Evans; K. E. Rittle; M. G. Bock; R. M. DiPardo; R. M. Freidinger; W. L. Whitter; G. F. Lundell; D. F. Veber; P. S. Anderson; R. S. L. Chang; V. J. Lotti; D. J. Cerino; T. B. Chen; P. J. Kling; K. A. Kunkel; J. P. Springer, J. Hirshfield. *J. Med. Chem.*, **1988**, 31, 2235.
- <sup>28</sup> [www.cambridgemedchemconsulting.com](http://www.cambridgemedchemconsulting.com)
- <sup>29</sup> Landagaray, E.; Ettaoussi, M.; Leclerc, V.; Traoré, B.; Perez, V.; Nosjean, O.; Boutin, J. A.; Caignard, D.-H.; Delagrang, P.; Berthelot, P.; Yous, S. *Bioorg. Med. Chem.*, **2014**, 22, 986.
- <sup>30</sup> Bedini, A.; Lucarini, S.; Spadoni, G.; Tarzia, G.; Scaglione, F.; Dugnani, S.; Pannacci, M.; Lucini, V.; Carmi, C.; Pala, D.; Rivara, S.; Mor, M. *J. Med. Chem.*, **2011**, 54, 8362.
- <sup>31</sup> Xie, J. H.; Liu, S.; Huo, X. H.; Cheng, X.; Duan, H. F.; Fan, B. M.; Wang, L. X.; Zhou, Q. L. *J. Org. Chem.*, **2005**, 70, 2967.
- <sup>32</sup> Guo, P.; Joo, J. M.; Rakshit, S.; Sames, D. C.-H. *J. Am. Chem. Soc.*, **2011**, 133, 16338.
- <sup>33</sup> Wikstrom, H. V.; Carlsson, P. A. E.; Andersson, B. R.; Bengt, R.; Svensson, K. A. I.; Elebring, S. T.; Stjernlof, N. P.; Romero, A. G.; Haadsma, S. R.; Lin, C. H.; Ennis, M. D. *PCT Int. Appl.*, WO9111435A1, **1991**
- <sup>34</sup> Rivara, S.; Mor, M.; Silva, C.; Zuliani, V.; Vacondio, F.; Spadoni, G.; Bedini, A.; Tarzia, G.; Lucini, V.; Pannacci, M.; Frascini, F.; Plazzi, P. V. *J. Med. Chem.*, **2003**, 46, 1429.
- <sup>35</sup> Savelieff, M. G.; Nam, G.; Kang, J.; Lee, H. J.; Lee, M.; Lim, M. H. *Chem. Rev.*, **2019**, 119, 1221.

- <sup>36</sup> Sansone, R. A.; Sansone, L. A. *Innov. Clin. Neurosci.*, **2011**, 8, 10.
- <sup>37</sup> Rodríguez-Franco, M. I.; Fernández-Bachiller, M. I.; Pérez, C.; Hernández-Ledesma, B.; Bartolomé, B. *J. Med. Chem.*, **2006**, 49, 459.
- <sup>38</sup> López-Iglesias, B.; Pérez, C.; Morales-García, J.A.; Alonso-Gil, S.; Pérez-Castillo, A.; Romero, A.; López, M.G.; Villarroya, M.; Conde, S.; Rodríguez-Franco, M.I. *J. Med. Chem.*, **2014**, 57, 3773
- <sup>39</sup> Chojnacki, J. E.; Liu, K.; Yan, X.; Toldo, S.; Selden, T.; Estrada, M.; Rodríguez-Franco, M. I.; Halquist, M. S.; Ye, D.; Zhang, S. *ACS Chem. Neurosci.*, **2014**, 5, 690
- <sup>40</sup> Piomelli, D. *Nat. Rev. Neurosci.*, **2003**, 4, 873.
- <sup>41</sup> Croke, A.; Colligris, B.; Pintor, J. *Curr. Med. Chem.*, **2012**, 19, 3508.
- <sup>42</sup> Porcella, A.; Maxia, C.; Gessa, G. L.; Pani, L. *Eur. J. Neurosci.*, **2001**, 13, 409.
- <sup>43</sup> Slusar, J. E.; Cairns, E. A.; Szczesniak, A-M.; Bradshaw, H. B.; Di Polo, A.; Kelly, M. E. M. *Neuropharmac.*, **2013**, 72, 116.
- <sup>44</sup> Wang, X.; Sirianni, A.; Pei, Z.; Cormier, K.; Smith, K.; Jiang, J.; Zhou, S.; Wang, H.; Zhao, R.; Yano, H.; Kim, J. E.; Li, V.; Kristal, B. S.; Ferrante, R. J.; Friedlander, R. M. *J. Neurosci.*, **2011**, 31, 14496.
- <sup>45</sup> Alarma-Estrany, P.; Pintor, J. *Pharmacol. Ther.*, **2007**, 113, 507.
- <sup>46</sup> Martínez-Águila, A.; Fonseca, B.; Pérez de Lara, M. J.; Pintor, J. *J. Pharmacol. Exp. Ther.*, **2016**, 357, 293.
- <sup>47</sup> Alarma-Estrany, P.; Croke, A.; Mediero, A.; Peláez, T.; Pintor, J. *J. Pineal Res.*, **2008**, 45, 468.
- <sup>48</sup> Serle, J. B.; Wang, R. F.; Peterson, W. M.; Plourde, R.; Yerxa, B. R. *J. Glaucoma*, **2004**, 13, 385.
- <sup>49</sup> Samples, J. R.; Krause, G.; Lewy, A. J. *Curr. Eye Res.*, **1988**, 7, 649.
- <sup>50</sup> Ismail, S. A.; Mowafi, H. A. *Anesth. Analg.*, **2009**, 108, 1146.
- <sup>51</sup> Croke, A.; Huete-Toral, F.; Martínez-Águila, A.; Martín-Gil, A.; Pintor, J. *J. Pharmacol. Exp. Ther.*, **2013**, 346, 138.
- <sup>52</sup> Martínez-Águila, A.; Fonseca, B.; Pérez de Lara, M. J.; Pintor, J. *J. Pharmacol. Exp. Ther.*, **2016**, 357, 293.
- <sup>53</sup> Hepler, R. S.; Frank, I. R. *JAMA*, **1971**, 217, 1392.
- <sup>54</sup> Panahi, Y.; Manayi, A.; Nikan, M.; Vazirian, M. *Biomed. Pharmacother.*, **2017**, 86, 620.
- <sup>55</sup> Rivara, S.; Lodola, A.; Mor, M.; Bedini, A.; Spadoni, G.; Lucini, V.; Panacci, M.; Frascini, F.; Scaglione, F.; Ochoa-Sanchez, R.; Gobbi, G.; Tarzia, G. *J. Med. Chem.*, **2007**, 50, 6618.
- <sup>56</sup> Tarzia, G.; Duranti, A.; Tontini, A.; Piersanti, G.; Mor, M.; Rivara, S.; Plazzi, P. V.; Park, C.; Kathuria, S.; Piomelli, D. *J. Med. Chem.*, **2003**, 46, 2352.
- <sup>57</sup> Mor, M.; Rivara, S.; Lodola, A.; Plazzi, P. V.; Tarzia, G.; Duranti, A.; Piersanti, G.; Kathuria, S.; Piomelli, D. *J. Med. Chem.*, **2004**, 47, 4998.
- <sup>58</sup> Clapper, J. R.; Vacondio, F.; King, A. R.; Duranti, A.; Tontini, A.; Silva, C.; Sanchini, S.; Taria, G.; Mor, M.; Piomelli, D. *ChemMedChem*, **2009**, 4, 1505.
- <sup>59</sup> Ahn, K.; Johnson, D. S.; Fitzgerald, L. R.; Liimatta, M.; Arendse, A.; Stevenson, T.; Lund, E. T.; Nugent, R. A.; Nomanbhoy, T. K.; Alexander, J. P.; Cravatt, B. F. *Biochemistry*, **2007**, 46, 13019.
- <sup>60</sup> Johnson, D. S.; Ahn, K.; Kesten, S.; Lazerwith, S. E.; Song, Y.; Morris, M.; Fay, L.; Gregory, T.; Stiff, C.; Dunbar, J. B. Jr.; Liimatta, M.; Beidler, D.; Smith, S.; Nomanbhoy, T. K.; Cravatt, B. F. *Bioorg. Med. Chem. Lett.*, **2009**, 19, 2865.
- <sup>61</sup> Johnson, D. S.; Stiff, C.; Lazerwith, S. E.; Kesten, S. R.; Fay, L. K.; Morris, M.; Beidler, D.; Liimatta, M. B.; Smith, S. E.; Dudley, D. T.; Sadagopan, N.; Bhattachar, S. N.; Kesten, S. J.; Nomanbhoy, T. K.; Cravatt, B. F.; Ahn, K. *ACS Med. Chem. Lett.*, **2011**, 2, 91.
- <sup>62</sup> Alexander, J. P.; Cravatt, B. F. *Chem. Biol.*, **2005**, 12, 1179.
- <sup>63</sup> Boger, D. L.; Sato, H.; Lerner, A. E.; Hedrick, M. P.; Fecik, R. A.; Miyauchi, H.; Wilkie, G. D.; Austin, B. J.; Patricelli, M. P.; Cravatt, B. F. *Proc. Natl. Acad. Sci. USA*, **2000**, 97, 5044.
- <sup>64</sup> Otrubova, K.; Ezzili, C.; Boger, D. L. *Bioorg. Med. Chem. Lett.*, **2011**, 21, 4674.
- <sup>65</sup> Otrubova, K.; Boger, D. L. *ACS Chem. Neurosci.*, **2012**, 3, 340.
- <sup>66</sup> Otrubova, K.; Brown, M.; Mc-Cormick, M. S.; Han, G. W.; O'Neal, S. T.; Cravatt, B. F.; Stevens, R. C.; Lichtman, A. H.; Boger, D. L. *J. Am. Chem. Soc.*, **2013**, 135, 6289.
- <sup>67</sup> Otrubova, K.; Cravatt, B. F.; Boger, D. L. *J. Med. Chem.*, **2014**, 57, 1079.
- <sup>68</sup> Feledziak, M.; Lambert, D. M.; Marchand-Brynaert, J.; Muccioli, G. G. *Recent Pat. CNS Drug Discov.*, **2012**, 7, 49.
- <sup>69</sup> Kathuria, S.; Gaetani, S.; Fegley, D.; Valino, F.; Duranti, A.; Tontini, A.; Mor, M.; Tariza, G.; La Rana, G.; Calignano, A.; Giustino, A.; Tattoli, M.; Palmery, M.; Cuomo, V.; Piomelli, D. *Nat. Med.*, **2002**, 9, 76.
- <sup>70</sup> Tarzia, G.; Duranti, A.; Gatti, G.; Piersanti, G.; Tontini, A.; Rivara, S.; Lodola, A.; Plazzi, P. V.; Mor, M.; Kathuria, S.; Piomelli, D. *ChemMedChem*, **2006**, 1, 130
- <sup>71</sup> Mor, M.; Lodola, A.; Rivara, S.; Vacondio, F.; Duranti, A.; Tontini, A.; Sanchini, S.; Piersanti, G.; Clapper, J. R.; King, A. R.; Tarzia, G.; Piomelli, D.; *J. Med. Chem.*, **2008**, 51, 3487.
- <sup>72</sup> Vacondio, F.; Silva, C.; Lodola, A.; Fioni, A.; Rivara, S.; Duranti, A.; Tontini, A.; Sanchini, S.; Clapper, J. R.; Piomelli, D.; Mor, M.; Tarzia, G. *ChemMedChem*, **2009**, 4, 1495.



- <sup>73</sup> Clapper, J. R.; Moreno-Sanz, G.; Russo, R.; Guijarro, A.; Vacondio, F.; Duranti, A.; Sanchini, S.; Sciolino, N. R.; Spradley, J. M.; Hohmann, A. G.; Calignano, A.; Mor, M.; Tarzia, G.; Piomelli, D. *Nat. Neurosci.*, **2010**, 13, 1265.
- <sup>74</sup> Vacondio, F.; Silva, C.; Lodola, A.; Carmi, C.; Rivara, S.; Duranti, A.; Tontini, A.; Sanchini, J. R.; Clapper, J. R.; Piomelli, D.; Tarzia, G.; Mor, M. *Eur. J. Med. Chem.*, **2011**, 46, 4466.
- <sup>75</sup> Piomelli, D.; Tarzia, G.; Duranti, A.; Tontini, A.; Mor, M.; Compton, T. R.; Dasse, O.; Monaghan, E. P.; Parrott, J. A.; Putman, D. *CNS Drug Rev.*, **2006**, 12, 21.
- <sup>76</sup> Basavarajappa, B. S. *Protein Pept. Lett.*, **2007**, 14, 237.
- <sup>77</sup> Palermo, G.; Campomanes, P.; Cavalli, A.; Rothlisberger, U.; De Vivo, M. *J. Phys. Chem. B.*, **2015**, 119, 789.
- <sup>78</sup> Lodola, A.; Mor, M.; Hermann, J. C.; Tarzia, G.; Piomelli, D.; Mulholland, A. J. *Chem. Commun.*, **2005**, 4399.
- <sup>79</sup> Lodola, A.; Mor, M.; Zurek, J.; Tarzia, G.; Piomelli, D.; Harvey, J. N.; Mulholland, A. J. *Biophys. J.*, **2007**, 92, L20.
- <sup>80</sup> Chudyk, E. I.; Dyguda-Kazimierowicz, E.; Langner, K. M.; Sokalski, W. A.; Lodola, A.; Mor, M.; Siriralik, J.; Mulholland, J. *J. Phys. Chem. B.*, **2013**, 117, 6656.
- <sup>81</sup> Lodola, A.; Capoferri, L.; Rivara, S.; Tarzia, G.; Piomelli, D.; Mulholland, J.; Mor, M. *J. Med. Chem.*, **2013**, 56, 2500.
- <sup>82</sup> Mileni, M.; Kamtekar, S.; Wood, D. C.; Benson, T. E.; Cravatt, B. F.; Stevens, R. C. *J. Mol. Biol.*, **2010**, 400, 743.
- <sup>83</sup> Righi, M.; Bedini, A.; Piersanti, G.; Romagnoli, F.; Spadoni, G. *J. Org. Chem.*, **2011**, 76, 704.
- <sup>84</sup> Cheng, Y.; Prusoff, W. H. *Biochem. Pharmacol.*, **1973**, 22, 3099.
- <sup>85</sup> Alcantara-Contreras, S.; Baba, K.; Tosini, G. *Neurosci. Lett.*, **2011**, 494, 61.
- <sup>86</sup> Rivara, S.; Pala, D.; Lodola, A.; Mor, M.; Lucini, V.; Dugnani, S.; Scaglione, F.; Bedini, A.; Lucarini, S.; Tarzia, G.; Spadoni, G. *ChemMedChem*, **2012**, 7, 1954.
- <sup>87</sup> Makriyannis, A.; Nikas Spyridon, P.; Alapafuja Shakiru, O.; Shukla Vidyanand, G. *PCT Int. Appl., WO2008013963*, **2008**.
- <sup>88</sup> Masseroni, D.; Mosca, S.; Mower, P. M.; Blackmond, D. G.; Rebek, J. *Angew. Chem. Int. Ed.*, **2016**, 55, 8290.
- <sup>89</sup> DeSimone, A.; Russo, D.; Ruda, G. F.; Micoli, A.; Ferraro, M.; Di Martino, R. M. C.; Ottonello, G.; Summa, M.; Armirotti, A.; Bandiera, T.; Cavalli, A.; Bottegoni, G. *J. Med. Chem.*, **2017**, 60, 2287.
- <sup>90</sup> Stupp, R.; Mason, W.; van den Bent, M. J.; Weller, M.; Fisher, B. M.; Taphoorn, M. J. B.; Belanger, K.; Brandes, A. A.; Marosi, C.; Bogdahn, U.; Curschmann, J.; Janzer, R. C.; Ludwin, S. K.; Gorlia, T.; Allgeier, A.; Lacombe, D.; Cairncross, G.; Eisenhauer, E.; Mirimanoff, R. O. *N. Engl. J. Med.*, **2005**, 352, 987.
- <sup>91</sup> Kleihues, P.; Louis, D. N.; Scheithauer, B. W.; Rorke, L. B.; Reifenberger, G.; Burger, P. C.; Cavenee, W. K. *J. Neuropathol. Exp. Neurol.*, **2002**, 61, 215.
- <sup>92</sup> Avgeropoulos, N. G.; Batchelor, T. T. *Oncologist*, **1999**, 4, 209.
- <sup>93</sup> Stupp, R.; Hegi, M. E.; Mason, W. P.; Van den Bent, M. J.; Taphoorn, M. J.; Janzer, R. C.; Ludwin, S. K.; Allgeier, A.; Fisher, B.; Belanger, K.; Hau, P.; Brandes, A. A.; Gijtenbeek, J.; Marosi, C.; Vecht, C. J.; Mokhtari, K.; Wesseling, P.; Villa, S.; Eisenhauer, E.; Gorlia, T.; Weller, M.; Lacombe, D.; Cairncross, J. G.; Mirimanoff, R. O. *Lancet Oncol.*, **2009**, 10, 459.
- <sup>94</sup> Stevens, M. F. G.; Hickman, J. A.; Stone, R.; Gibson, N. W.; Baig, G. U.; Lunt, E.; Newton, C. G. *J. Med. Chem.*, **1984**, 27, 196.
- <sup>95</sup> Newlands, E. S.; Blackledge, G.; Slack, J. A.; Goddard, C.; Brindley, C. J.; Holden, L.; Stevens, M. F. G. *Cancer Treat. Rep.*, **1985**, 69, 801.
- <sup>96</sup> Zhang, J.; Stevens, M. F. G.; Bradshaw, T. D. *Curr. Mol. Pharmacol.*, **2012**, 5, 102.
- <sup>97</sup> O'Reilly, S. M.; Newlands, E. S.; Glaser, M. G.; Brampton, M.; Rice-Edwards, J. M.; Illingworth, R. D.; Richards, P. G.; Kennard, C.; Colquhoun, I. R.; Lewis, P.; and Stevens, M. F. G. *Eur. J. Cancer*, **1993**, 29A, 940.
- <sup>98</sup> Bower, M.; Newlands, E. S.; Bleehen, N. M.; Brada, M.; Begent, R. J. H.; Calvert, H.; Colquhoun, I.; Lewis, P.; and Brampton, M. H. *Cancer Chemother. Pharmacol.*, **1997**, 40, 484.
- <sup>99</sup> Paulsen, F.; Hoffmann, W.; Becker, G.; Belka, C.; Weinmann, M.; Classen, J.; Kortmann, R. D.; and Bamberg, M. *J. Cancer Res. Clin. Oncol.*, **1999**, 125, 411.
- <sup>100</sup> Estlin, E. J.; Lashford, L.; Ablett, S.; Price, L.; Gowing, R.; Gholkar, A.; Kohler, J.; Lewis, I. J.; Morland, B.; Pinkerton, C. R.; Stevens, M. C. G.; Mott, M.; Stevens, R.; Newell, D. R.; Walker, D.; Dicks-Mireaux, C.; McDowell, H.; Reidenberg, P.; Statkevich, P.; Marco, A.; Batra, V.; Dugan, M.; Pearson, A. D. *J. Br. J. Cancer*, **1998**, 78, 652.
- <sup>101</sup> Reifenberger, G.; Wirsching, H.-G.; Knobbe-Thomsen, C. B.; Weller, M. *Nat. Rev. Clin. Oncol.*, **2017**, 14, 434.
- <sup>102</sup> Karran, P.; Macpherson, P.; Ceccotti, S.; Dogliotti, E.; Griffin, S.; Bignami, M. *J. Biol. Chem.*, **1993**, 268, 15878.
- <sup>103</sup> Ceccotti, S.; Aquilina, G.; Macpherson, P.; Yamada, M.; Karran, P.; Bignami, M. *Curr. Biol.*, **1996**, 6, 1528.
- <sup>104</sup> Margison, G. P.; Santibanez Koref, M. F.; Povey, A. C. *Mutagenesis*, **2002**, 17, 483.

- <sup>105</sup> Tisdale, M. J. *Biochem. Pharmacol.*, **1987**, 36, 457.
- <sup>106</sup> Blanc, J. L.; Wager, M.; Guilhot, J.; Kusy, S.; Bataille, B.; Chantereau, T.; Lapierre, F.; Larsen, C.J.; Karayan-Tapon, L. *J. Neurooncol.*, **2004**, 68, 275283.
- <sup>107</sup> Stupp, R.; Hegi, M. E.; Van den Bent, M. J.; Mason, W. P.; Weller, M.; Mirimanoff, R. O.; Cairncross, J. G.; *Oncologist*, **2006**, 11, 165180.
- <sup>108</sup> Moody, C. L.; Wheelhouse, R. T. *Pharmaceuticals*, **2014**, 7, 797.
- <sup>109</sup> Lund, E.; Newton, C. G.; Smith, C.; Stevens, G. P.; Stevens, M. F. G.; Straw, G. S.; R.; Walsh, R. J. A.; Warren, P. J.; Fizames, C.; Lavelle, F.; Langdon, S. P.; Vickers, L. M. *J. Med. Chem.*, **1987**, 30, 357.
- <sup>110</sup> Stevens, M. F. G. *Second generation azolotetrazinones*, Harrap, K. R.; Connors, T. A. Editors; *New avenues in developmental cancer chemotherapy*, **1987**, 8, 335.
- <sup>111</sup> Lunt, E.; Newton, C. G.; Smith, C.; Stevens, G. P.; Stevens, M. F. G.; Straw, C. G.; Walsh, R. J. A.; Warren, P. J.; Fizames, C.; Lavelle, F.; Langdon, S. P.; Vickers, L. M. *J. Med. Chem.*, **1987**, 30, 357.
- <sup>112</sup> Clark, A. S.; Deans, B.; Stevens, M. F. G.; Tisdale, M. J.; Wheelhouse, R. T.; Denny, B. J.; Hartley, J. A. *J. Med. Chem.*, **1995**, 38, 1493.
- <sup>113</sup> Stevens, M. F. G. *Cancer Drug Design and Discovery*, 2<sup>nd</sup> Ed, Neidle, S. Editor. *Temozolomide: from cytotoxic to Molecularly targeted agent*, **2014**, 5, 145.
- <sup>114</sup> Denny, B. J.; Wheelhouse, R. T.; Stevens, M. F.; Tsang, L. L.; Slack, J. *Biochemistry*, **1994**, 33, 9045.
- <sup>115</sup> Lowe, P. R.; Sansom, C. E.; Schwalbe, C. H.; Stevens, M. F. G.; Clark, A. S. *J. Med. Chem.*, **1992**, 35, 3377.
- <sup>116</sup> Suppasansatorn, P.; Wang, G.; Conway, B. R.; Wang, W.; Wang, Y. *Cancer Lett.*, **2006**, 244, 42.
- <sup>117</sup> Liu, D.; Yang, J. G.; Cheng, J.; Zhao, L. X. *Molecules*, **2010**, 15, 9427.
- <sup>118</sup> Hummersone, M. G.; Stevens, M. F. G.; Cousin, D. *PCT Int. Appl., WO 2010149968*, **2010**.
- <sup>119</sup> Stevens, M. F. G.; Hickman, J. A.; Stone, R.; Gibson, N. W.; Baig, G. U.; Lunt, E.; Newton, C. G. *J. Med. Chem.*, **1984**, 27, 196.
- <sup>120</sup> Ege, G.; Gilbert, K. *Tetrahedron Lett.*, **1979**, 20, 4253.
- <sup>121</sup> Shealy, Y. F.; Struck, R. F.; Holum, L. B.; Montgomery, J. A. *J. Org. Chem.*, **1961**, 26, 2396.
- <sup>122</sup> Shechter, H.; Magee, W. L.; Rao, C. B.; Glinka, J.; Hui, H.; Amick, T. J.; Fiscus, D.; Kakodkar, S.; Nair, M. *J. Org. Chem.*, **1987**, 52, 5538.
- <sup>123</sup> Reifenberger, G.; Wirsching, H.-G.; Knobbe-Thomsen, C. B.; Weller, M. *Nat. Rev. Clin. Oncol.*, **2017**, 14, 434.
- <sup>124</sup> Zhang, J.; Stevens, M. F. G.; Bradshaw, T. D. *Curr. Mol. Pharmacol.*, **2012**, 5, 102.
- <sup>125</sup> Ostermann, S.; Csajka, C.; Buclin, T.; Leyvraz, S.; Lejeune, F.; Decosterd, L. A.; Stupp, R. *Clin. Cancer Res.*, **2004**, 10, 3728.
- <sup>126</sup> Portnow, J.; Badie, B.; Chen, M.; Liu, A.; Blanchard, S.; Synold, T. W. *Clin. Cancer Res.*, **2009**, 15, 7092.
- <sup>127</sup> Bleehen, N. M.; Newlands, E. S.; Lee, S. M.; Thatcher, N.; Selby, P.; Calvert, A. H.; Rustin, G. J. S.; Brampton, M.; Stevens, M. F. G. *J. Clin. Oncol.*, **1995**, 13, 910.
- <sup>128</sup> Newlands, E. S.; Blackledge, G. R.; Slack, J. A.; Rustin, G. J.; Smith, D. B.; Stuart, N. S.; Quarterman, C. P.; Hoffman, R.; Stevens, M. F.; Brampton, M. H.; et al. *Br. J. Cancer*, **1992**, 65 (2), 287.
- <sup>129</sup> O'Reilly, S. M.; Newlands, E. S.; Glaser, M. G.; Brampton, M.; Rice-Edwards, J. M.; Illingworth, R. D.; Richards, P. G.; Kennard, C.; Colquhoun, I. R.; Lewis, P.; Stevens, M. F. G. *Eur. J. Cancer*, **1993**, 29A, 940.
- <sup>130</sup> Norinder, U.; Haerberlein, M. *Adv. Drug. Deliv. Rev.*, **2002**, 54, 291.
- <sup>131</sup> Wager, T. T.; Hou, X.; Verhoest, P. R.; Villalobos, A. *ACS Chem. Neurosci.*, **2010**, 1, 435.
- <sup>132</sup> Wager, T. T.; Hou, X.; Verhoest, P. R.; Villalobos, A. *ACS Chem. Neurosci.*, **2016**, 7, 767.
- <sup>133</sup> West, D. C.; Qin, Y.; Peterson, Q. P.; Thomas, D. L.; Palchauthuri, R.; Morrison, K. C.; Lucas, P. W.; Palmer, A. E.; Fan, T. M.; Hergenrother, P. J. *Mol. Pharm.*, **2012**, 9, 1425.
- <sup>134</sup> Tian, S.; Wang, J.; Li, Y.; Li, D.; Xu, L.; Hou, T. *Adv. Drug Deliv. Rev.*, **2015**, 86, 2.
- <sup>135</sup> Daina, A.; Zoete, V. *ChemMedChem*, **2016**, 11, 1117.
- <sup>136</sup> Horspool, K. R.; Stevens, M. F. G.; Baig, G. U.; Newton, C. G.; Lunt, E.; Walsh, R. J. A.; Pedgrift, B. L.; Lavelle, F.; Fizames, C. *J. Med. Chem.*, **1990**, 33, 1393.
- <sup>137</sup> Evans, D. A.; Carter, P. H.; Dinsmore, C. J.; Barrow, J. C.; Katz, J. L.; Kung, D. W. *Tetrahedron Lett.*, **1997**, 38, 4535.
- <sup>138</sup> Langnel, D. A. F.; Arrowsmith, J.; Stevens, M. F. G. *ARKIVOC*, **2000**, iii, 421.
- <sup>139</sup> Stevens, M. A.; Giner-Sorolla, A.; Smith, H. W.; Bosworth Brown, G. *J. Org. Chem.*, **1962**, 27, 567.
- <sup>140</sup> Doucet, H.; *Eur. J. Org. Chem.*, **2008**, 2013.
- <sup>141</sup> Horspool, K. R.; Stevens, M. F. G.; Baig, G. U.; Newton, C. G.; Lunt, E.; Walsh, R. J. A.; Pedgrift, B. L.; Lavelle, F.; Fizames, C. *J. Med. Chem.*, **1990**, 33, 1393.
- <sup>142</sup> Hansch, C.; Leo, A.; Taft, R. W. *Chem. Rev.*, **1991**, 91, 165.
- <sup>143</sup> Scaringi, C.; De Sanctis, V.; Minniti, G.; Enrici, R. M. *Onkologie*, **2013**, 36, 444.
- <sup>144</sup> Binder, Z. A.; Wilson, K. M.; Salmasi, V.; Orr, B. A.; Eberhart, C. G.; Siu, I. M.; Lim, M.; Weingart, J. D. *PLoS One*, **2016**, 11, e0150271.

- 
- <sup>145</sup> Cheng, Y.; Sk, U. H.; Zhang, Y.; Ren, X.; Zhang, L.; Huber-Keener, K. J.; Sun, Y. W.; Liao, J.; Amin, S.; Sharma, A. K.; Yang, J. M. *PLoS One*, **2012**, 7 (4), e35104.
- <sup>146</sup> Arrowsmith, J.; Jennings, S. A.; Clark, A. S.; Stevens, M. F. G. *J. Med. Chem.*, **2002**, 45, 5458.
- <sup>147</sup> Wang, Y.; Conway, B.; Suppasansatorn, P. *PCT USA Appl.*, US20060047117, **2006**.
- <sup>148</sup> Marasco, C. J.; Pera, P. J.; Spiess, A. J.; Bernacki, R.; Sufrin, J. R. *Molecules*, **2005**, 10, 1015.
- <sup>149</sup> Jiao, Y. G.; Yu, H. T. *Synlett*, **2001**, 73.
- <sup>150</sup> West, D. C.; Qin, Y.; Peterson, Q. P.; Thomas, D. L.; Palchaudhuri, R.; Morrison, K. C.; Lucas, P. W.; Palmer, A. E.; Fan, T. M.; Hergenrother, P. *J. Mol. Pharm.*, **2012**, 9, 1425.